APPLICATION OF RANDOM MATRIX THEORY IN QUANTUM CHROMODYNAMICS

A thesis Submitted
in Partial Fulfilment of the Requirements
for the Degree of

MASTER OF SCIENCE

by

RENU RAMAN SAHU

to the

School of Physical Sciences

National Institute of Science Education and Research

Bhubaneswar

Date June 6, 2020

DECLARATION

I hereby declare that I am the sole author of this thesis in partial fulfillment of the requirements for a postgraduate degree from National Institute of Science Education and Research (NISER). I authorize NISER to lend this thesis to other institutions or individuals for the purpose of scholarly research.

Signature of the Student

Date:

The thesis work reported in the thesis entitled ..... was carried out under my supervision, in the school of ..... at NISER, Bhubaneswar, India.

Signature of the thesis supervisor

School:

Date:

ACKNOWLEDGEMENTS

I am grateful to Dr. Subhasis Basak for the useful discussions. It was his vision to research on the application of random matrix theory to QCD. Without his guidance this work could not have been possible. Also, I thank Dr. Dipankar Chakrabarty and Mr. Ankur Singha for some insightful discussions.

ABSTRACT

With an introduction to the random matrix theory (RMT), the application of random matrices to describe the spectrum of Wilson fermions and staggered fermions is demonstrated. It is shown that the eigenvalues of random matrices from gaussian ensembles are confined in a single interval of the real line and the eigenvalues repel each other. For large-N dimensional Gaussian random matrices, it is shown by using the Coulomb gas technique, that the eigenvalues tend to be distributed by a semi-circular distribution function. From the joint probability density of the eigenvalues, the normal modes of fluctuation of the eigenvalues about their mean position were calculated. In the application part, the spectrum of Wilson fermion was obtained for a two-color case, by replacing the gauge fields by random matrices from the Gaussian orthogonal ensemble (GOE). The unfolding procedure was demonstrated for the case of GOE eigenvalues. For the staggered fermion case, which respects chiral symmetry, the chiral random matrix ensemble was used. In this case, the eigenvalues obtained from RMT and those obtained from lattice quantum chromo-dynamics (lattice QCD) were first unfolded, and then they were compared to show that they match atleast in some regime.

Contents

List of Figures

Chapter 1

Introduction

The applications of Random Matrices in physics gained prominence in several branches of physics after the pioneering work Eugene P. Wigner to explain the statistics of nuclear level spacings in 1950 [1]. The nuclear energy levels are the eigen values of a complicated Hamiltonian. Wigner replaced the Hamiltonian by a suitable Random Matrix with certain symmetry properties exhibited by the system and obtained the correct statistics of the nuclear energy levels. Thus, the detailed information of the system is wiped out by this replacement, but the information about the quantities pertaining to the symmetry of the system is preserved. Such quantities are not specific to the system under consideration, but to the entire class of systems which possess the same symmetry properties. Such quantites are called the universal quantities. While applying Random Matrix Theory to certain system, we trade off the detailed dynamics of the system to get the information about it's universal quantites. The basic idea of RMT is to replace a quantity by an ensemble average over random Hamiltonian matrices. The underlying philosophy of Random Matrix Thory in the words of Dyson [2], "What is here required is a new kind of statistical mechanics, in which we renounce exact knowledge not of the state of the system but of the system itself. We picture a complex nucleus as a "black box" in which a large number of particles are interacting according to unknown laws. The problem then is to define in a mathematically precise way an ensemble of systems in which all possible laws of interaction are equally possible." It was J.J.M. Verbaarschot who conceived the idea of using random matrix theory in Quantum Chromodynamics having analysed the universality in the Dirac spectra [3] [4].

In this thesis, we shall focus on the application of the random matrix theory(RMT) in Quantum Chromodynamics(QCD). In particular we shall be interested in the Dirac spectrum obtained using RMT. In the first chapter we introduce the basic concepts of probability theory based on which we shall develop the random

matrix theory and ensembles of random matrices. We shall be particularly interested in Gaussian Orthogonal Ensemble (GOE) and Gaussian Unitary Ensemble (GUE) for the physical applications. In the second chapter, we discuss how the eigen values of the random matrices from these ensembles behave and interact among each other. Given these interactions among the eigen values, we discuss their distribution in chapter three. Besides discussing the mathematical aspects of random matrices, we shall develop some physical insight into the properties of eigen values of random matrices. In particular, we look at the eigen values of large N-dimensional random matrices, and obtain the distribution by using a physically motivated method known as the coulomb gas technique in the fourth chapter. In the fifth chapter we study the study the fluctuations of the eigen values about their mean location and determine different normal modes. The normal modes contain the information about the spectrum of the ensemble.

We then focus on the application of the random matrices from chapter six. Quantum Chromodynamics is an extremely difficult problem to handle analytically in the non-perturbative regime. That is why one uses the computational method to approach the problem. One popular approach is lattice QCD in which the fermionic fields are put on a lattice. Once put on a lattice, there are several choices of schemes of discretisation each leading to the same continuum limit. Moreover, naively discretising the fermionic field in d-dimensional spacetime leads to appearace of 2^d spurious states which are unphysical. This is known as the fermion doubling problem. A theorem due to H. B. Nielsen and M. Ninomiya, also called the no-go theorem for the fermions require that the action for fermions on a lattice with periodic boundary conditions has to give up one of the properties amongst chiral symmetry, locality, translational invariance and hermiticity in order to remove the unphysical fermionic states [5]. One of discretisation schemes due to Wilson removes the doublers by trading off the chiral symmetry. Another scheme of discretisation due to Kogut and Susskind is that of staggered fermion, which preserves the chiral symmetry but the resulting lagrangian is non-local.

The spectrum of Wilson fermions has been determined through the application

of random matrices. In the sixth chapter we reproduce and compare the Wilson spectrum with the one obtained from the lattice QCD [8]. The study of staggered fermions spectrum is through a different approach which involves more than just replacing the blocks of a matrix with the random ones. Procedure to remove the system dependent effects on the spectrum, called unfolding, is elaborated and demonstrated in the seventh chapter. This is important because the results obtained through the random matrix theory are not system specific. Before concluding in the final chapter, we discuss how to obtain the spectrum of the staggered fermions from RMT, and how do we compare the results so obtained with those obtained from lattice QCD.

Chapter 2

Random Matrices

The spectra of both finite-dimensional and infinite-dimensional Gaussian Random Matrices have been studied. The physical interpretation of Coulomb gas was given to the eigenvalues of the Gaussian Orthogonal Ensemble using the formalism of statistical mechanics. The normal modes of oscillation of the eigenvalues of Gaussian Random Matrices were determined for the finite dimension.

2.1 Random Variables

A random variable is a function that can map the set of outcomes of a random experiment or phenomena to a real number. Given the sample space, a random variable can take any value depending on the subset of the sample space considered. For our purposes, it suffices to think of a random variable as a number that can take either discrete values (eg. outcomes of a coin toss or a die) or continuous values (eg. temperature of a city). For our purposes, we say that a random variable is discrete if two distinct possible values that the random variable can take cannot be arbitrarily closed to each other. On the other hand, in the case of continuous random variables, two distinct random values can arbitrarily close to each other. The discussion henceforth shall be restricted to continuous random variables.

The probability of an event E will be denoted by $P(E)$. For example, probability of the event $X \in (a, b)$ will be denoted by $P(a < X < b)$. The probability of the event $X > a$ will be denoted as $P(X > a)$. The probability density function for the random variable X is defined as $p_X(x)$ satisfying the following two conditions

$$\text{i) } p_X(s) \geq 0 \forall x$$

$$\text{ii) } \int_{-\infty}^{\infty} p_X(x)dx = 1$$

The definition of probability density enables us to define the probability of events concerning X taking values in certain ranges. For example,

$$P(a < X < b) = \int_a^b p_X(x)dx$$

One can interpret $p_X(x)dx$ as $P(x < X < x+dx)$, the probability of X taking values in the interval of length dx at x. We shall denote this probability as $P_X(X = x)$.

$$P_X(X = x) = p_X(x)dx$$

Now suppose we have a random vector $\mathbf{X}$ of n-dimension. It simply means a list of n random variables.

$$\mathbf{X} = (X_1, X_2, \dots X_i, \dots X_n)$$

The joint probability density function for the random vector $\mathbf{X}$ satisfies the following two conditions

$$p_{\mathbf{X}}(x_1, x_2 \dots x_n) \geq 0 \tag{2.1}$$

$$\int_\sigma p_{\mathbf{X}}(x_1, x_2 \dots x_n)dx_1dx_2 \dots dx_n = 1 \tag{2.2}$$

where $\sigma = \{\mathbf{x} : p_{\mathbf{X}}(\mathbf{x}) > 0\}$. The probability of $\mathbf{X}$ taking the value in a volume $dx_1 \dots dx_n$ at $(x_1, x_2 \dots x_n)$ is $p_{\mathbf{X}}(x_1, x_2 \dots, x_n)dx_1 \dots dx_n$.

The marginal probability density of the random variable X_i is defined as

$$p_{X_i}(x) = \int_{x_1} \dots \int_{x_{i-1}} \int_{x_{i+1}} \dots \int_{x_n} p_{\mathbf{X}}(x_1, x_2, \dots x_n)dx_1 \dots dx_{i-1}dx_{i+1} \dots dx_n \tag{2.3}$$

The concept of independence is of extreme physical importance. For example the results of two different experiments for a particular(single) physical quantity can be taken as two random variables. If the experimental conditions of one does not affect those of the other, it is legitimate to assume that the two random variables are independent. Mathematically, the notion of independence is rigorously defined. For the purposes of this study, we restrict ourselves to the case of continuous random variables. Two random variables X_1 and X_2 with joint probability density function $p_{X_1,X_2}(x_1, x_2)$ are said to be independent if the joint density function factorize into two functions $p_{X_1}(x_1)$ and $p_{X_2}(x_2)$ such that

$$p_{X_1,X_2}(x_1, x_2) = p_{X_1}(x_1)p_{X_2}(x_2)$$

For n- independent random variables $X_1 \dots X_n$, the joint probability distribution is

$$p_{\mathbf{X}}(\mathbf{x}) = \prod_{i=1}^{n} p_{X_i}(x_i)$$

Two random variables X_1 and X_2 are said to be identical if the functional forms of their density function are the same. That is $p_{X_1}(x) = p_{X_2}(x)$. With this, the probability density function of $\mathbf{X}$ for identical and independent (denoted as iid) random variables $(X_1, \ldots X_2)$ is given by

$$p_{\mathbf{X}}(\mathbf{x}) = \prod_{i=1}^{n} p_{X_1}(x_i) = \prod_{i=1}^{n} p(x_i) \tag{2.4}$$

Henceforth, the subscript X_i will be dropped wherever it is understood from the context that iid random variables are used.

2.2 The Gaussian Distribution

A random variable X is said be be a Gaussian(or normal) random variable with mean μ and variance σ^2, if the probability density function is given by

$$p(x) = \frac{1}{\sqrt{2\pi\sigma^2}} \exp\left(\frac{-(x-\mu)^2}{2\sigma^2}\right) \tag{2.5}$$

The random variable following normal distribution with above density function will be denoted as $X \sim N(\mu, \sigma^2)$.

The standard normal distribution is the one with vanishing mean and unit variance. That is, $X \sim N(0, 1)$ if X is a standard normal RV.

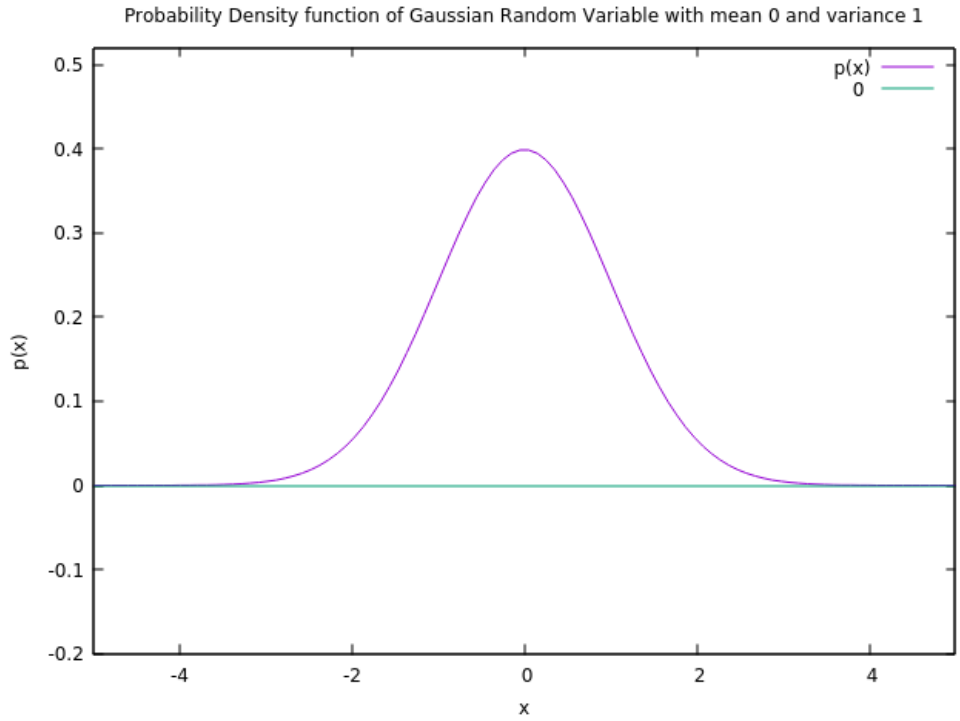

Figure 2.1: The probability density function of $X \sim N(0, 1)$. It is more likely that the random variable following this distribution takes a value near 0 when an instance is drawn. The probability of the random variable taking values far from the origin is vanishingly small.

The density function reveals that the probability of the random variable taking values at 0 is the highest. The probability of the random variable taking values farther away from zero reduces rapidly.

The linear combination of independent Normal random variables is again a normal random variable (RV). Consider two random variables $X_1 \sim N(\mu_1, \sigma_1^2)$ and $X_2 \sim N(\mu_2, \sigma_2^2)$. Then the random variable Y which is the sum of variables X_1 and X_2 follows a normal distribution

$$Y = aX_1 + bX_2 \sim N(a\mu_1 + b\mu_2, a^2\sigma_1^2 + b^2\sigma_2^2) \tag{2.6}$$

where a and b are real numbers.

With these concepts, we can introduce random matrices. First, we shall consider a matrix with elements drawn from a standard normal distribution. Then we shall consider the matrix with complex-values elements whose real and imaginary parts are standard normal random variables.

2.3 Ensembles of Random Matrices

As mentioned earlier, a matrix with some or all of its elements as a random variable is known as a random variable [9]. We shall restrict ourselves with those random matrices, for which we are assured that the eigenvalues would be real. This is important from the perspective of potential physical applications.

In quantum mechanics, there are operators for every physical observable. And the laws of quantum mechanics dictate that the possible result of an experiment measuring the physical observable are the eigen values of the corresponding operator. Since the result of an experiment has to be a real number, the operator has to be such that its eigenvalue is a real number.

Consider a random matrix with it's elements taken from $N(0,1)$. Following is an instance of the matrix.

$$H = \begin{bmatrix} -0.5708 & -2.244 & -1.444 & -0.9136 & -0.01092 & -0.3367 & 0.1253 & 0.09694 \\ 0.9554 & 0.893 & 1.336 & 1.816 & 1.835 & 2.065 & -1.689 & -0.8769 \\ 0.07244 & 1.779 & -0.3666 & 0.2214 & -0.8142 & -0.09503 & 0.6673 & 0.04657 \\ -0.1066 & -0.1712 & 0.8709 & 0.8872 & 0.7368 & -0.8329 & 0.51 & -1.122 \\ -0.1889 & 0.4364 & -0.3897 & 1.502 & -1.1 & -0.2492 & -0.8297 & -0.6318 \\ -1.63 & -2.124 & 0.7587 & 2.651 & -1.683 & -1.495 & 1.318 & 0.2169 \\ 1.541 & -0.3213 & -0.3116 & -1.57 & 0.8771 & 1.512 & -0.002632 & -0.1869 \\ -0.2185 & -0.2872 & 0.592 & 0.0943 & -0.411 & 0.3054 & 1.191 & -0.4767 \end{bmatrix}$$

The problem with such matrix is that the eigen-values might have non-zero imaginary part. For example, the above instance of random matrix has the following eigen values

$$\begin{bmatrix} (-1.468, +2.958) \\ (-1.468, -2.958) \\ (+2.950, +0.000) \\ (+0.894, +1.231) \\ (+0.894, -1.231) \\ (-2.504, +0.000) \\ (-0.764, +0.121) \\ (-0.764, -0.121) \end{bmatrix}$$

Since we want to obtain real eigen values, we symmetrise the above random matrix.

$$H_s = \frac{H + H^T}{2}$$

where H^T is the transpose of H.

$$H_s = \begin{bmatrix} -0.5708 & -0.6445 & -0.686 & -0.5101 & -0.09992 & -0.9831 & 0.8334 & -0.06077 \\ -0.6445 & 0.893 & 1.558 & 0.8226 & 1.136 & -0.02937 & -1.005 & -0.5821 \\ -0.686 & 1.558 & -0.3666 & 0.5461 & -0.602 & 0.3318 & 0.1779 & 0.3193 \\ -0.5101 & 0.8226 & 0.5461 & 0.8872 & 1.12 & 0.9089 & -0.5299 & -0.5138 \\ -0.09992 & 1.136 & -0.602 & 1.12 & -1.1 & -0.9661 & 0.02372 & -0.5214 \\ -0.9831 & -0.02937 & 0.3318 & 0.9089 & -0.9661 & -1.495 & 1.415 & 0.2612 \\ 0.8334 & -1.005 & 0.1779 & -0.5299 & 0.02372 & 1.415 & -0.002632 & 0.502 \\ -0.06077 & -0.5821 & 0.3193 & -0.5138 & -0.5214 & 0.2612 & 0.502 & -0.4767 \end{bmatrix}$$

The eigenvalues of the above matrix are

$$\begin{bmatrix} 3.6629 \\ -3.7785 \\ -2.0955 \\ 1.4499 \\ 0.7169 \\ -0.0815 \\ -1.1863 \\ -0.9191 \end{bmatrix}$$

A real symmetric matrix always has real eigenvalues. This matrix is an example of an instance of an ensemble of matrices called Gaussian Orthogonal Ensemble(GOE).

In the light of above example, we can list out the properties of random matrices from Gaussian Orthogonal Ensemble. Consider the matrix elements of H. The matrix element at the i-th row and $j-$th column, $(H)_{ij}$, is a standard normal random variable. $(H)_{ij} \sim N(0,1)$. So the probability density function of the random variable $(H)_{ij}$ is

$$p_{(H)_{ij}}(H_{ij}) = \frac{1}{\sqrt{2\pi}} \exp\left(\frac{H_{ij}^2}{2}\right) \tag{2.7}$$

The joint probability density function of the matrix elements of H is

$$p[H] = \prod_{i=1}^{N}\prod_{j=1}^{N} \frac{1}{\sqrt{2\pi}} \exp\left(\frac{H_{ij}^2}{2}\right) = \frac{1}{(2\pi)^{N/2}} \exp\left(-\frac{\sum_{i,j=1}^{N} H_{ij}^2}{2}\right) \tag{2.8}$$

When H is symmetrise d to obtain H_s, The diagonal elements remain the same. Hence, $(H_s)_{ii} = H_{ii}$. The probability density function of diagonal elements of $(H_s)_{ii} \sim N(0,1)$. But the off-diagonal elements are a linear combination of standard normal random variables.

$$(H_s)_{ij} = \frac{H_{ij} + H_{ji}}{2} \tag{2.9}$$

Using eqn. (2.6), the pdf of off-diagonal matrix elements is given by

$$(H_s)_{ij} \sim N(0, 1/2) \tag{2.10}$$

The jpdf of the $N(N-1)/2$ matrix elements in the upper triangle of the matrix is

$$\prod_{i=1, i<j}^{N} \frac{1}{\sqrt{\pi}} \exp\{(-(H_s)_{ij}^2)\}$$

The jpdf of the $N(N+1)$ matrix elements of the Gaussian orthonormal ensemble is

$$p\left((H_s)_{11}, \ldots, (H_s)_{NN}\right) = \prod_{i=1}^{N} \left[\exp\left(-(H_s)_{ii}^2/2\right)/\sqrt{2\pi}\right] \prod_{i<j} \left[\exp\left(-(H_s)_{ij}^2\right)/\sqrt{\pi}\right]$$

Matrices with complex-valued elements, whose real and imaginary parts are taken from Gaussian distribution are the random matrices from **Gaussian Unitary Ensemble**. To obtain real eigenvalues we need to hermitize the operator. There is another ensemble called the **Gaussian Symplectic Ensemble** in which the matrix elements are quarternions.

2.4 Characteristics of Gaussian Random Matrices

For our purpose of study, we shall deal with the square matrices with real eigenvalues. In the above examples, I saw quite a few examples of random matrices. The two important characteristics which make the Gaussian Random Matrices special are as follows:

1. Independent Entries: The entries of the Gaussian Random Matrix are independent of each other.

$$p[H] \propto \prod_{i=1}^{N} f_i\left(H_{ii}\right) \prod_{i<j} f_{ij}\left(H_{ij}\right) \tag{2.11}$$

   where f_i and f_{ij} are the probability density functions of diagonal and off-diagonal matrix elements.

2. Rotational Invariance: If we do a similarity transformation

$$H' = UHU^{-1} \tag{2.12}$$

   the jpdf of the transformed matrix elements has the same functional form as that of original matrix H. To be precise, if

$$p[H] dH_{11} \cdots dH_{NN} = p\left[H'\right] dH'_{11} \cdots dH'_{NN}$$

One can also prove conversely, that if an ensemble has above two properties, i.e. independence of matrix elements as well as rotational invariance, the ensemble has to be a Gaussian Ensemble.

Chapter 3

Random Matrix Spectra

In this chapter, we shall investigate the eigenvalues of random matrices. First, we shall show that the eigenvalues of a 2×2 GOE matrix repel each other. For a comparative study, we also ask if i.i.d. random variables are attractive or repulsive. It turns out that the i.i.d. random variables attract each other.

3.1 Level repulsion in a 2×2 GOE matrix

Consider a 2×2 GOE matrix $H_S = \begin{pmatrix} x_1 & x_3 \\ x_3 & x_2 \end{pmatrix}$, where $x_1, x_2 \sim N(0,1)$ and $x_3 \sim N(0, 1/2)$. Since it is a real symmetric matrix, it has real eigen values, say, λ_1, λ_2 and are given by

$$\lambda_{1,2} = \left(x_1 + x_2 \pm \sqrt{(x_1 - x_2)^2 + 4x_3^2} \right) /2 \tag{3.1}$$

Let is define the random variable $s = \lambda_1 - \lambda_2$. In terms of matrix elements x_1, x_2 and x_3

$$s = \sqrt{(x_1 - x_2)^2 + 4x_3^2} \tag{3.2}$$

The probability density function of s is

$$p(s) = \int_{-\infty}^{\infty} dx_1 dx_2 dx_3 \frac{e^{-\frac{1}{2}x_1^2}}{\sqrt{2\pi}} \frac{e^{-\frac{1}{2}x_2^2}}{\sqrt{2\pi}} \frac{e^{-x_3^2}}{\sqrt{\pi}} \delta(s - \sqrt{(x_1 - x_2)^2 + 4x_3^2}) \tag{3.3}$$

To solve the above integral we do the following change of variable

$$x_1 = \frac{r\cos\theta + \psi}{2} \tag{3.4}$$

$$x_2 = \frac{\psi - r\cos\theta}{2} \tag{3.5}$$

$$x_3 = \frac{r\sin\theta}{2} \tag{3.6}$$

The jacobian for the transformation is given by

$$J = \det \begin{pmatrix} \frac{\partial x_1}{\partial r} & \frac{\partial x_1}{\partial \theta} & \frac{\partial x_1}{\partial \psi} \\ \frac{\partial x_2}{\partial r} & \frac{\partial x_2}{\partial \theta} & \frac{\partial x_2}{\partial \psi} \\ \frac{\partial x_3}{\partial r} & \frac{\partial x_3}{\partial \theta} & \frac{\partial x_3}{\partial \psi} \end{pmatrix} = \det \begin{pmatrix} \cos\theta/2 & -r\sin\theta/2 & 1/2 \\ -\cos\theta/2 & r\sin\theta/2 & 1/2 \\ \sin\theta/2 & r\cos\theta/2 & 0 \end{pmatrix} = -r/4 \tag{3.7}$$

With this change of variable the pdf $p(s)$ becomes

$$\begin{aligned} p(s) =& \frac{1}{8\pi^{3/2}} \int_0^\infty dr r\delta(s-r) \int_0^{2\pi} d\theta \int_{-\infty}^{\infty} d\psi e^{-\frac{1}{2}\left[\left(\frac{r\cos\theta+\Psi}{2}\right)^2+\left(\frac{-r\cos\theta+\psi}{2}\right)^2+\frac{r^2\sin^2\theta}{2}\right]} \\ =& \frac{\sqrt{4\pi}s}{8\pi^{3/2}} \int_0^{2\pi} d\theta e^{-\frac{1}{2}\left[\frac{s^2\cos^2\theta}{2}+\frac{s^2\sin^2\theta}{2}\right]} \\ =& \frac{s}{2} e^{-s^2/4} \end{aligned}$$

The plot of the probability density function is given by the following plot.

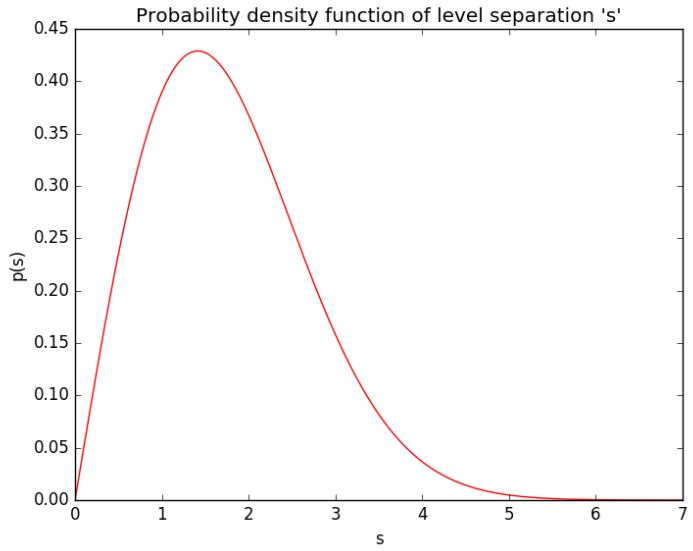

Figure 3.1: This is the probability density of the separation between the two eigen values of a 2×2 gaussian orthogonal ensemble. Note that the probability that the separation between the eigenvalues vanishes goes to zero, which implies a repulsion between them. On the other hand the probability of large separation is also vanishingly small, which implies that the eigen values are confined.

Note that the probability density vanishes at $s = 0$. This means that the two eigenvalues λ_1 and λ_2 tend to repel each other and hence the probability of them coming nearer is small. Also $p(s) \to 0$ as $s \to \infty$. Thus at large separations, the eigenvalues tend to get attracted.

3.2 Spacing between i.i.d. real random variables

In this section we shall study the gaps between i.i.d. real random variables. Consider N i.i.d. real random variables $X_1, X_2 \ldots X_n$ drawn from parent distribution $p_X(x)$. Let σ be the support of $p_X(x)$ and the cumulative distribution function be $F_X(x)$. Given N i.i.d. random variables, we want to find the probability density of s, where s is the gap between two consecutive instances of random variables.

As a pre-requisite to above problem, we need to compute the conditional probability density function, $p_N(s|X_j = x)$(for some j fixed), that given one of the random variable takes the value around x, there is another random variable around $x + s$ and no random variables in between. In other words we want to determine if there exists a gap of size 's'. We claim that

$$p_N\left(s|X_j = x\right) = p_X(x+s)[1 - (F(x+s) - F(x))]^{N-2} \tag{3.8}$$

This is because of the following reason. One of the random already sits at x. Now we have $N-1$ variables. Out of these $N-1$ variables, one should sit at $x+s$ with probability $p_X(x+s)dx$. The probability of any other variable to take values on the left of x, which happens with probability $F(x)$, or on the right of $x+s$, which happens with probability $1 - F(x+s)$ but not in between is

$$1 - [F(x+s) - F(x)] = 1 + F(x) - F(x+s)$$

and there are $N-2$ of such variables.

The probability of obtaining a gap s is irrespective of which random variable is taking x. So, the probability of getting a gap s, given that any of the random variable takes the value near x is

$$\begin{aligned} P_N\left(s|\bigcup_{i=1}^{N}(X_i = x)\right) &= \sum_{i=1}^{N} P_N\left(s|X_i = x\right) P\left(X_i = x\right) \\ &\qquad \text{Using the fact that } X_i\text{s are i.i.d.} \\ &= NP_N\left(s|X_1 = x\right) P_X\left(X_1 = x\right) \end{aligned} \tag{3.9}$$

Now, to obtain the probability density of s, we integrate over x by using $P_X(X_1 = x) = p_X(x)dx$. So,

$$P_N(s) = \int NP_N\left(s|X_1 = N\right) p_X\left(X_1 = x\right) dx \tag{3.10}$$

Now, introducing the probability density function $P_N(s) = p_N(s)ds$, we have

$$p_N(s)ds = ds \quad N\int p_N\left(s|X_1 = x\right) \quad p_X\left(X_1 = x\right) dx \tag{3.11}$$

which implies

$$p_N(s) = N\int p_N\left(s|X_1 = x\right) p_X\left(X_1 = x\right) dx \tag{3.12}$$

Now, we need to verify that eqn. (3.12) is a valid probability density function. Since the integrand is a factor of probability densities, it is non-negative and hence $p_N(s) \geq 0 \forall s$.All we need to verify is its normalization, which has been done in appendix (A.1).

There are N random variables $X_1 \dots X_n$ each with a density function $p_X(x)$. Consider a particular instance of the random variables. The number of random variables at x in an infinitesimal length dx would be $Np_X(x)dx$. Assuming N to be sufficiently large that there are significantly large number of instances of random variables in this small interval. The average spacing between the values of the random variables at x is $dx/Np_X(x)dx \sim 1/Np_X(x)$. Thus it is useful to perform a local change of variable $s = \hat{s}/Np_X(x)$. Let us observe the large-N behavior of $\hat{s} = Nsp_X(x)$. As discussed above s is the separation between the random variables and goes as $1/Np_X(x)$. Therefore $Nsp_X(x) \sim O(1)$ or $\hat{s} \sim 1$.

Using eqn. (3.8), the probability density of gap $\hat{s}/Np_X(x)$, given that a particular random variable X_j takes a value near x is

$$p_N\left(s = \frac{\hat{s}}{Np_X(x)} | X_j = x\right) = p_X\left(x + \hat{s}/Np_X(x)\right)\left[1 + F(x) - F\left(x + \hat{s}/Np_X(x)\right)\right]^{N-2} \tag{3.13}$$

Since $s \sim O(1)$, $\hat{s}/Np_X(x) \to 0$ as $N \to \infty$. In this limit, Taylor expansion of $F(x + \hat{s}/Np_X(x))$ gives

$$\begin{aligned} F(x + \hat{s}/Np_X(x)) \approx & F(x) + p_X(x)\frac{\hat{s}}{Np_X(x)} \\ = & F(x) + \frac{\hat{s}}{N} \end{aligned}$$

Using these in RHS of eqn. (3.13) we obtain

$$p_X(x + \hat{s}/Np_X(x))\left[1 - \frac{\hat{s}}{N}\right]^{N-2}$$

In the limit $N \to \infty$ the above equation becomes

$$p_N\left(s = \frac{\hat{s}}{Np_X(x)} | X_j = x\right) = \lim_{N\to\infty} p_X(x)\left[1 - \frac{\hat{s}}{N}\right]^{N-2} = p_X(x)e^{\hat{s}} \tag{3.14}$$

Let the probability density function for $\hat{s}$ be $\hat{p}_N(\hat{s})$. By change of the variables, we find that the probability density of $\hat{s}$ is related to that of s as follows

$$\hat{p}_N(\hat{s}) = p_N\left(s = \frac{\hat{s}}{Np_X(x)}\right)\frac{ds}{d\hat{s}} \tag{3.15}$$

Now taking the limit $N \to \infty$

$$\lim_{N\to\infty} \hat{p}_N(\hat{s}) := \lim_{N\to\infty} p_N\left(s = \frac{\hat{s}}{Np_X(x)}\right)\frac{ds}{d\hat{s}} \tag{3.16}$$

Using

$$\frac{ds}{d\hat{s}} = \frac{1}{Np_X(x)}$$

along with eqn. (3.12) and (3.14), we obtain

$$\begin{aligned}\lim_{N\to\infty} \hat{p}_N(\hat{s}) =& N\int p_N\left(s = \frac{\hat{s}}{Np_X(x)}|X_1 = x\right)p_X(x)\frac{1}{Np_X(x)}dx \\ =& \int p_X(x)e^{-\hat{s}}dx = e^{-\hat{s}}\end{aligned}$$

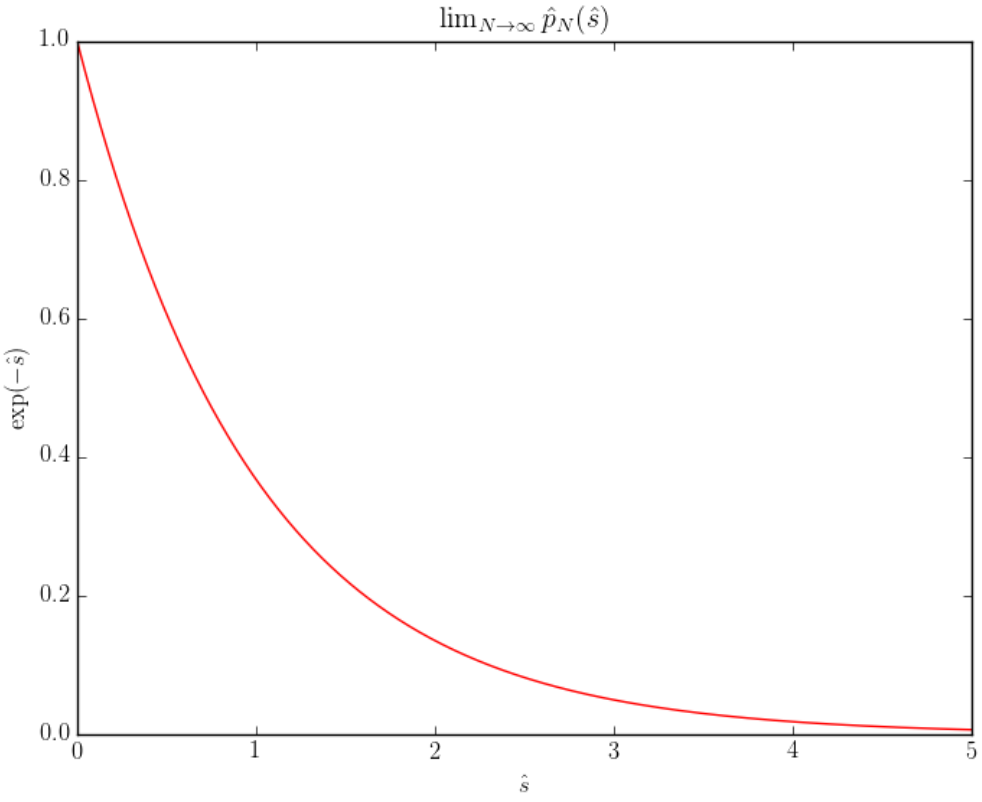

Figure 3.2: The probability density of scaled-spacing, $\hat{s}$, between identical and independent random variables. This shows that the probability that two such random variables are closed to each other is more, implying the attraction between them.

The above plot reveals that the probability density attains maximum at $s = 0$. Thus the iid random variables tend to reduce the gap between them to 0. We can conclude from this behavior that the i.i.d. random variables attract, unlike the repelling eigenvalues of the Gaussian Orthogonal Ensemble.

3.3 The jpdf of eigenvalues of Gaussian Matrices.

Consider an $N \times N$ Gaussian random matrix. We get N eigen-values which are again a random variables. The joint probability density function of the eigen random variables is given by [7]

$$p\left(x_1, \ldots, x_N\right) = \frac{1}{\mathcal{Z}_{N,\beta}} e^{-\frac{1}{2}\sum_{i=1}^{N} x_i^2} \prod_{j<k} |x_j - x_k|^{\beta} \tag{3.17}$$

where

$$\mathcal{Z}_{N,\beta} = (2\pi)^{N/2} \prod_{j=1}^{N} \frac{\Gamma(1 + j\beta/2)}{\Gamma(1 + \beta/2)} \tag{3.18}$$

which normalizes the jpdf. β is the number of real variables needed to specify one entry of the matrix. It is also called Dyson index. For example, in case of Gaussian orthogonal ensemble the matrix elements are real numbers. So only one real entry is required for each matrix element, which makes $\beta = 1$. In case of Gaussian Unitary Ensemble whose matrix elements are complex numbers, two real entries are required for a given matrix element. Thus, $\beta = 2$ in this case.

The factor $\exp\left(-\frac{1}{2}\sum_{i=1}^{N} x_i^2\right)$ reduces the probability of the random variables taking values too far away for 0. Thus, this factor works as a confinement for the random variables. On the other hand, the factor $\prod_{j<k} |x_j - x_k|^{\beta}$ does not allow two random variables to take values too close to each other. This factor thus acts as repulsion between the eigenvalues. The spectrum of the Gaussian random matrix is thus an interplay of the confining potential and the repulsive factor.

Since we have an expression for the probability density function of the separation between eigen values of 2×2 GOE random matrix, we should derive the same using eqn. (3.17). This can be done by calculating

$$p(s) = \int_{-\infty}^{\infty} dx_1 dx_2 p_{X_1 X_2}(x_1, x_2) \delta(s - |x_1 - x_2|) \tag{3.19}$$

It turns out that evaluating this integral(see appendix (A.2)) gives $p(s) = \dfrac{s e^{-s^2/4}}{2}$, which the same expression obtained earlier.

3.4 Remarks

From the above results, we conclude that the eigenvalues of random matrices are suitable for modeling a system in which there are a confining potential and a repulsive term. What needs to be addressed next is the functional form of confining potential and the repulsive term. Then we shall ask if such a potential exists in some physical situation or not. To see the nature of potential we shall investigate the spectrum in the case where $N \to \infty$, that is there are a large number of eigenvalues. In other words, we shall look at a very-large random matrix and then investigate the nature of confining potential and repulsion between the eigenvalues.

Chapter 4

Large N behavior of Gaussian Random Matrix Spectra

In previous sections, we discussed the finite N-behavior of Gaussian Random matrices. We saw the existence of the potential which confines the eigenvalues in a region near 0. There also exists a factor for repulsion. It is natural to ask what happens when a large number of such eigenvalues are there. More precisely, we would like to know the distribution of the eigenvalues in the presence of such a potential and repulsion factor when a large number of them are there.

Suppose we have T matrices of dimension $N \times N$. The large N spectrum of the ensemble of matrices will be given by the histogram of the $T \times N$ eigenvalues. This is the technique we shall apply to determine the distribution computationally.

On the other hand, given the joint pdf of N eigen values, the way to compute the shape of the histogram of the eigen values is to determine the marginal density function $p(x)$ given by

$$p(x) = \int \cdots \int dx_2 \cdots dx_N p\left(x, x_2, \ldots, x_N\right) \tag{4.1}$$

To see why this is so, let us introduce a counting function $n(x)$ such that $\int_a^b n(x')dx'$ gives the fraction of eigen values in between a and b. The following definition of $n(x)$ does this job.

$$n(x) := \frac{1}{N} \sum_{i=1}^{N} \delta(x - x_i) \tag{4.2}$$

Since for different random matrices $n(x)$ will be different because $x_i s$ will be different. Thus, $n(x)$ is a random function.

The function $n(x)$ when averaged with the joint density function $p(x_1, \ldots, x_N)$ we obtain the marginal distribution $p(x)$(see appendix (A.4)). Thus,

$$\langle n(x) \rangle = \int \ldots \int d\mathbf{x} \quad p\left(x_1, \ldots, x_N\right) \frac{1}{N} \sum_{i=1}^{N} \delta\left(x - x_i\right) = p(x)$$

The quantity $\langle n(c) \rangle$ is also called the average spectral density.

Now we consider the average spectral density when the jpdf for Gaussian ensemble (3.17) is used. The spectral density $p(x)$ is rescaled as follows

$$\lim_{N\to\infty} \sqrt{\beta N} p(\sqrt{\beta N} x) = p_{\mathrm{SC}}(x) \tag{4.3}$$

to get rid of N in the large-N limit. According to Wigner's semicircle law

$$p_{SC}(x) = \frac{1}{\pi}\sqrt{2 - x^2} \tag{4.4}$$

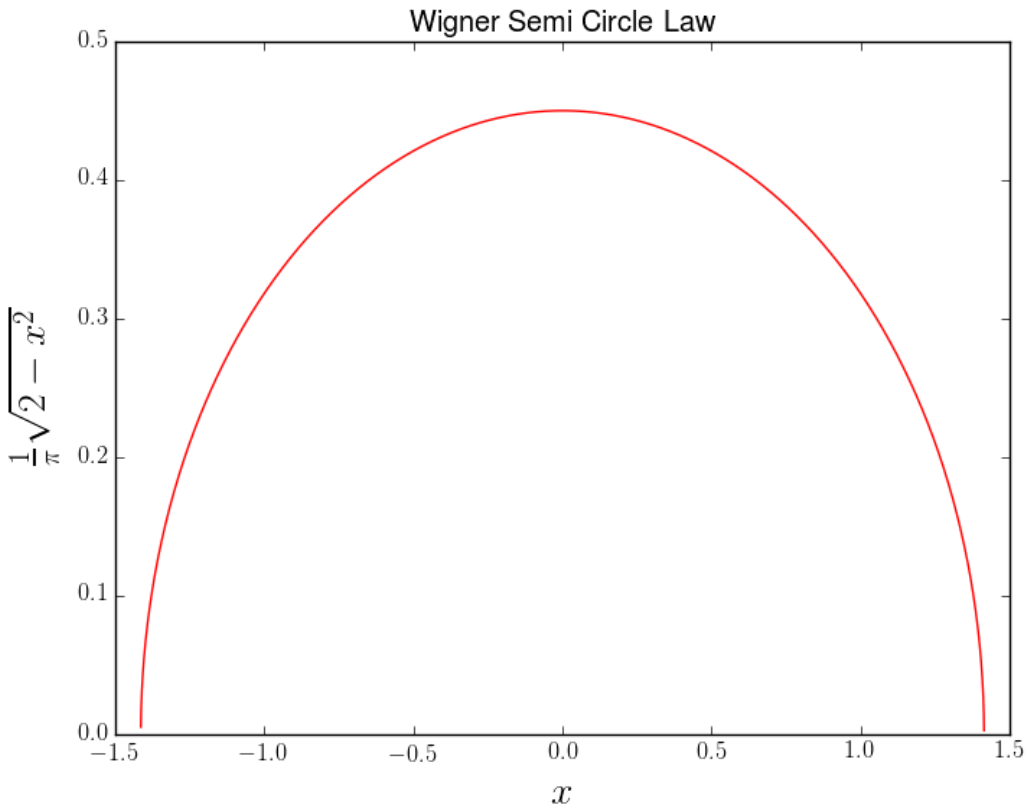

Figure 4.1: Wigner semicircle law is the distribution of the eigenvalues of Gaussian ensembles after appropriate rescaling. The distribution is a semicircle with origin at its centre.

In the following section, we shall verify this computationally for Gaussian Orthogonal Ensemble(GOE) and the Gaussian Unitary Ensemble(GUE).

4.1 Computational Results

The distribution of the eigenvalues in the limit $N \to \infty$ can be computationally determined. T random matrices of order $N \times N$ were generated, and the histogram

of $N \times T$ eigenvalues was plotted. For this computational purpose, we chose $T = 500$ and $N = 200$.

Figure (4.2) and (4.3) is the histogram of the eigenvalues. The blue histogram is that of GOE, and the green one is of GUE. Here, we make the following observation. The edges of the spectral density differ in the case of GOE and GUE. From the figure, it is clear that the spectral edges of the GOE are near ± 20, whereas in the case of GUE the spectral edges are near ± 28. The spectral edges are related to the Dyson index β, and are given by $\pm\sqrt{2\beta N}$. For GOE, $\beta = 1$, and the spectral edges using the formula is $\sqrt{2 \times 1 \times 200} = 20$, which is observed computationally. For GUE, $\beta = 2$, which makes the magnitude of spectral edge $\sqrt{2 \times 2 \times 200} \approx 28.2843$. This reveals that the spectral edges increase with the dimension N of the random matrix as $\sqrt{N}$.

To verify the Wigner semicircle law we need to re-scale the distribution and check for the spectral edges which should be $\pm\sqrt{2} \approx 1.414$. Note that this is easily observed in figure (4.4) and (4.5). Thus, the simulation verifies the Wigner Semi Circle law.

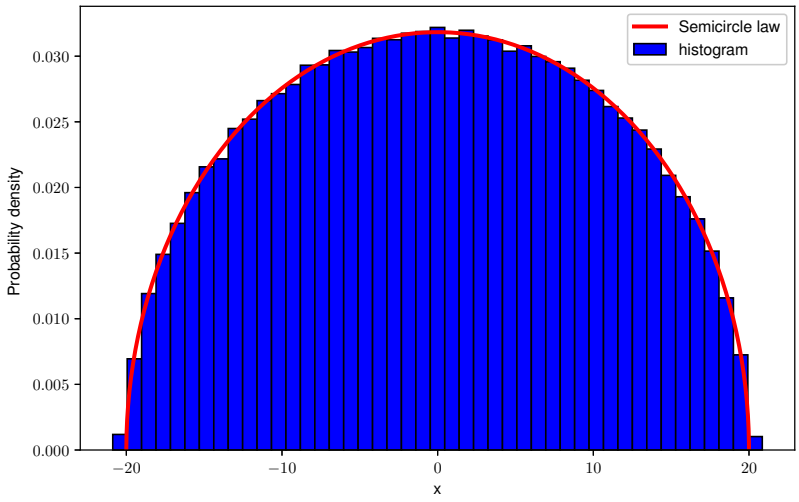

Figure 4.2: The histogram of eigen values of 500 GOE random matrices of dimension 200×200. Note that the distribution is semicircular. The Dyson index $\beta = 1$ in this case.

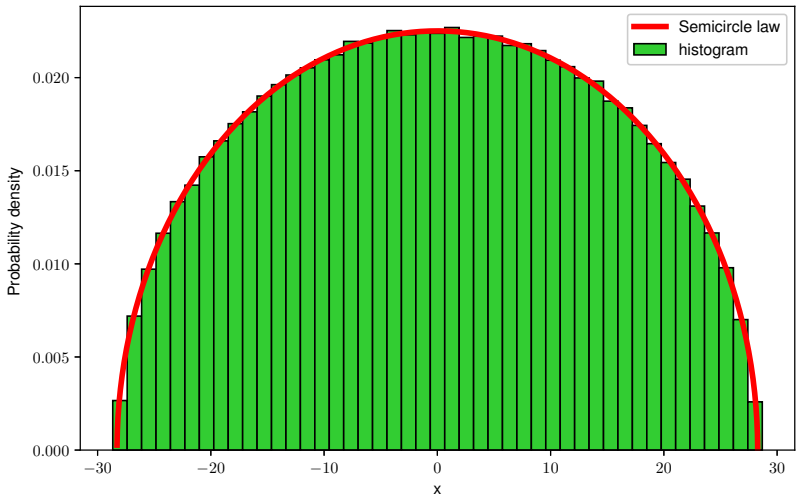

Figure 4.3: The histogram of eigen values of 500 GUE random matrices of dimension 200×200.In this case too, the distribution is semicircular. The radius of the semicircle differs from that in case of GOE (see fig. (4.2)) because the Dyson index is $\beta = 2$ in this case.

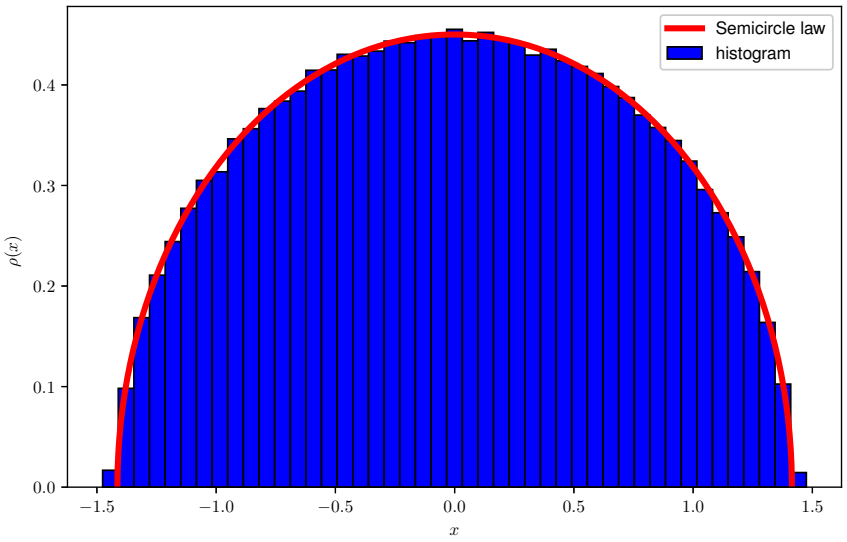

Figure 4.4: The scaled histogram of eigen values of 500 GOE random matrices of dimension 200×200. The distribution now matches with Wigner semicircle law, a semicircular distribution with radius $\sqrt{2}$ and origin as center.

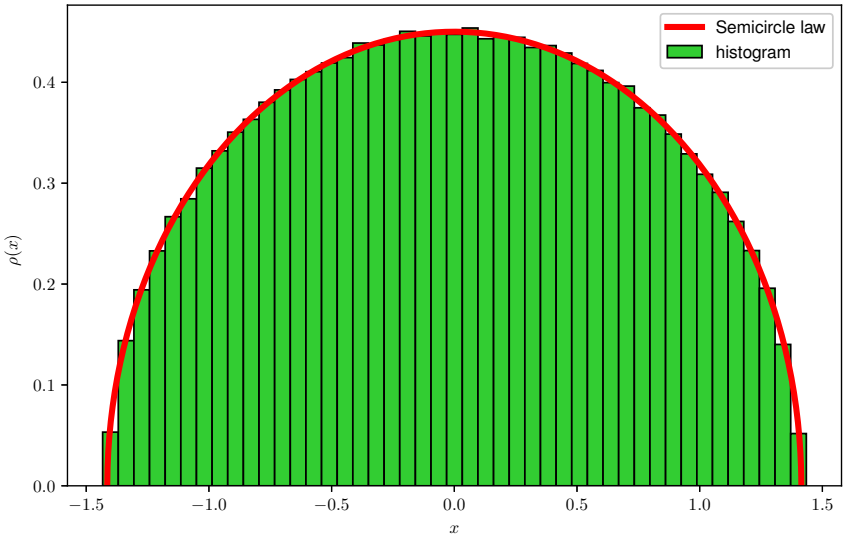

Figure 4.5: The scaled histogram of eigen values of 500 GUE random matrices of dimension 200×200. Again, we obtain the semicircular distribution with radius $\sqrt{2}$ and origin as center.

4.2 Coulomb Gas Technique

Having verified the large-N behavior of the eigenvalues of Gaussian ensembles computationally, let us now determine the semicircle law using some analytic means. In this section, we shall set up a statistical mechanics formalism to determine the Wigner's semicircle law. Wigner had used this technique to determine the semi-circle law.

First, let us have a broad view of the idea to approach the problem. We shall manipulate the expression of the jpdf of eigenvalues to a form that can be interpreted as the partition function in the formalism of statistical mechanics. We shall then identify the free energy from the expression and then minimize it to obtain the equilibrium configuration. We expect that at the equilibrium the distribution of the eigenvalues will follow Wigner semi-circle law.

4.2.1 Confining Potential and the Repulsion Factor

Consider the jpdf (3.17) and let us write the normalization condition after rescaling $x_i \to x_i\sqrt{\beta N}$. With this the normalization constant becomes

$$\mathcal{Z}_{N,\beta} = C_{N,\beta} \int_{\mathbb{R}^N} \prod_{j=1}^{N} dx_j e^{-\frac{\beta}{2} N \sum_{i=1}^{N} x_i^2} \prod_{j<k} |x_j - x_k|^\beta = C_{N,\beta} \int_{\mathbb{R}^N}^{N} \prod_{j=1}^{N} dx_j e^{-\beta N^2 \mathcal{V}[\mathbf{x}]} \tag{4.5}$$

where $C_{N,\beta} = (\sqrt{\beta N})^{N+\beta N(N-1)/2}$ and $\mathcal{V}[\mathbf{x}]$ is given by

$$\mathcal{V}[\boldsymbol{x}] = \frac{1}{2N} \sum_i x_i^2 - \frac{1}{2N^2} \sum_{i \neq j} \ln |x_i - x_j| \tag{4.6}$$

Note that the first term of the potential is a quadratic potential just like the harmonic oscillator potential. The second term is the repulsive term which goes as logarithm of the distance between the eigenvalues.

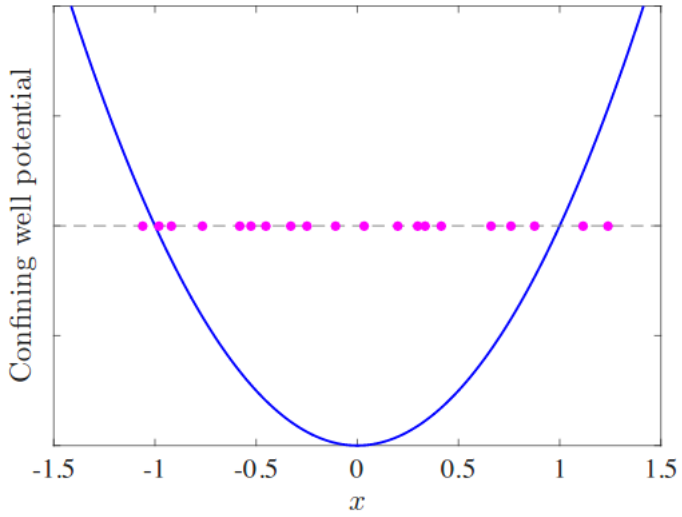

Figure 4.6: The confining potential is quadratic in nature and ensures that the support of distribution of the eigen-values to be a single interval.

The integrand $\exp(-\beta N^2 \mathcal{V}[\mathbf{x}])$ allows us to interpret the eigenvalues as a thermodynamic gas of particles with positions $x_1, \ldots, x_N$ and confined in the quadratic potential. Each eigenvalue x_i repels every other eigenvalue whose magnitude goes as the logarithm of the distance from it. The logarithmic repulsion was seen in electrodynamics as repulsion between two line charge densities. It is useful to imagine that the system is a collection of such line charges, say aligned along z-axis. When viewed on the xy plane it would look like a collection of points on one of the axis, say

x. Since the repulsion is due to coulombic, it is apt to call the system of eigenvalues as coulomb gas.

Since there is no kinetic term, the gas is static. The factor βN^2 acts as a simultaneous zero temperature limit $\beta \to \infty$ and thermodynamic limit $N \to \infty$. To obtain the equilibrium configuration we need to minimize the free energy

$$\mathcal{F} = -\frac{1}{\beta} \ln \mathcal{Z}_{N,\beta}$$

It is mathematically simpler to determine the equilibrium configuration in the thermodynamic limit as it gives us the liberty to use the saddle point approximation.

4.2.2 The Equilibrium Distribution of the Coulomb Gas Particles

We shall first do the coarse-graining to go to a continuum limit. Then by taking the thermodynamic limit, we shall do a saddle point integration. The main goal is to find a distribution that will minimize the free energy. Note that the support of the distribution is also a part of the problem.

We shall take the limit $N \to \infty$ and change the discrete set $\{x_1, \ldots, x_N\}$ into a continuum. To do so, we introduce a counting function $n(x)$ as defined earlier with properties $\int n(x)dx = 1$ and $n(x) \geq 0$ for all x. For finite N it is given by eqn. (4.2). For continuum of eigen values we expect $n(x)$ to be a smooth function. This function can be used to convert discrete variables to continuum as follows. Eqn. (4.2) can be enforced in terms of the following functional integral

$$1 = \int \mathcal{D}[n(x)]\delta\left[n(x) - \frac{1}{N}\sum_{i=1}^{N}\delta\left(x - x_i\right)\right] \tag{4.7}$$

Imposing this condition by representing the functional form of unity inside the integral and interchanging the order of integral, we have the functional integral eqn. (4.5) as

$$\mathcal{Z}_{N,\beta} = C_{N,\beta}\int \mathcal{D}[n(x)] \int_{\mathbb{R}^N}\prod_{j=1}^{N} dx_j e^{-\beta N^2 \mathcal{V}[\mathbf{x}]} \underbrace{\int_{\mathbb{R}^N}\prod_{j=1}^{N} dx_j \delta\left[n(x) - \frac{1}{N}\sum_{i=1}^{N}\delta\left(x - x_i\right)\right]}_{I_N[n(x)]} \tag{4.8}$$

Using $n(x)$ to write $\mathcal{V}[(\mathbf{x})]$ in continuum limit(see appendix (A.4)) we have

$$\mathcal{V}[n(x)] = \frac{1}{2}\int_{\mathbb{R}} dx x^2 n(x) - \frac{1}{2}\iint_{\mathbb{R}^2} dx dx' n(x) n(x') \ln|x-x'| + \frac{1}{2N}\int_{\mathbb{R}} dx n(x) \ln \Delta(x) \tag{4.9}$$

Consider the integrand factor of above integral expression of $\mathcal{Z}_{N,\beta}$, $I_N[n(x)]$ as evaluated in appendix (A.5).

$$I_N[n(x)] \sim \exp\left[-N\int dx n(x) \ln n(x)\right]$$

The integrand of above equation is nothing but in the form of Shannon entropy. Thus we can interpret the factor $I_N[n(x)]$ as contribution due to entropy of the system. Using above expression and putting the short distance cutoff as $c/Nn(x)$(see appendix (A.4)), we have the partition function as

$$\mathcal{Z}_{N,\beta} \simeq C_{N,\beta}\int \mathcal{D}[n(x)] e^{-\beta N^2 \mathcal{F}_0[n(x)] + \frac{\beta}{2} N \ln N + \left(\frac{\beta}{2}-1\right) N \mathcal{F}_1[n(x)] - \frac{\beta}{2} N \ln c + o(N)} \tag{4.10}$$

where,

$$\begin{aligned} \mathcal{F}_0[n(x)] &= \frac{1}{2}\int dx x^2 n(x) - \frac{1}{2}\iint dx dx' n(x) n(x') \ln|x-x'| \\ \mathcal{F}_1[n(x)] &= \int dx n(x) \ln n(x) \end{aligned} \tag{4.11}$$

Note that the entropic term $\mathcal{F}_1[n(x)]$ is sub-leading term, whereas the energetic term $\mathcal{F}_0[n(x)]$ is the dominating term. Note that the leading term of eqn. (4.10) is of the order βN^2.

To impose the condition that $n(x)$ are unit normalized we use

$$\delta\left[\int_{\mathbb{R}} dx n(x) - 1\right] = \int_{\mathbb{R}} \frac{dk}{2\pi} e^{ik\left(\int_{\mathbb{R}} dx n(x) - 1\right)} \tag{4.12}$$

Rescaling $ik \to \beta N^2 \kappa$, and ignoring the sub-leading terms we have

$$\mathcal{Z}_{N,\beta} \approx C_{N,\beta}\int \mathcal{D}[n(x)] \int_{\mathbb{R}} d\kappa e^{-\beta N^2 \mathcal{S}[n(x),\kappa] + \mathcal{O}(N)} \tag{4.13}$$

where the action $\mathcal{S}[n(x),\kappa]$ is

$$\mathcal{S}[n(x),\kappa] = \mathcal{F}_0[n(x)] - \kappa\left(\int dx n(x) - 1\right) \tag{4.14}$$

After doing a saddle point integration we obtain

$$\mathcal{Z}_{N,\beta} \approx \exp\left(-\beta N^2 \mathcal{S}\left[n^\star(x), \kappa^\star\right]\right) \tag{4.15}$$

where $n^\star(x)$ and $\kappa^\star$ are the minimizer of action and satisfy the following equations

$$\begin{aligned} 0 &= \frac{\delta}{\delta n(x)}\mathcal{S}[n(x),\kappa]\Big|_{n=k^\star} = \frac{x^2}{2} - \int_{\mathbb{R}} dx' n^\star(x') \ln|x-x'| - \kappa^\star \\ 0 &= \frac{\partial}{\partial\kappa}\mathcal{S}[n(x),\kappa]\Big|_{n=n^\star} \Rightarrow \int_{\mathbb{R}} dx n^\star(x) = 1 \end{aligned} \tag{4.16}$$

Let us rename $\kappa^\star$ as κ for the simplicity of notations. κ is effectively a Lagrange multiplier for imposing the constraint of normalization of $n(x)$.

The intensive free energy

$$f = -\left(1/\beta N^2\right) \ln \mathcal{Z}_{N,\beta}$$

in the limit $N \to \infty$ for the coulomb gas becomes $f = \mathcal{S}\left[n^\star(x),\kappa\right] \equiv \mathcal{F}_0\left[n^\star(x)\right]$, that is the action evaluated at the saddle point density.

All that is required to do now is to solve for $n^\star(x)$ which satisfies

$$\frac{x^2}{2} - \int_{\mathbb{R}} dx' n^*(x') \ln|x-x'| - \kappa = 0 \tag{4.17}$$

As argued earlier, the solution of above equation $n^\star(x)$, will have a single interval as it's support. Let the infimum and supremum of the interval be a and b. Thus $n^\star(x) = n^\star(x,a,b)$. First the solution will be found with a and b as parameters. Then the requirement to minimize the free energy f will fix a and b.

We shall differentiate eqn. (4.17) weakly(see appendix (A.6)) to obtain

$$\Pr \int dx' \frac{n^\star(x')}{x-x'} = x \tag{4.18}$$

On solving eqn. (4.18) (see appendix (A.7)) we obtain

$$n^\star(x) = \frac{1}{\pi\sqrt{(x-a)(b-x)}}\left[1 - x^2 + \frac{1}{2}(a+b)x + \frac{1}{8}(b-a)^2\right] \tag{4.19}$$

We shall now compute the internal free energy

$$f \equiv \mathcal{F}_0\left[n^\star(x)\right] = \frac{1}{2}\int dx x^2 n^\star(x) - \frac{1}{2}\iint dx dx' n^\star(x) n^\star(x') \ln|x-x'| \tag{4.20}$$

To get rid of the double integral we first multiply $n^\star(x)$ with eqn. (4.17) and integrate over x and obtain the following equation

$$\iint dx dx' n^\star(x) n^\star(x') \ln|x-x'| = \frac{1}{2}\int dx n^\star(x) x^2 - \kappa \tag{4.21}$$

Substituting the expression for the double integral in the expression for f and fixing Lagrange multiplier κ by substituting $x = a$ in eqn. (4.17), we obtain

$$f \equiv \mathcal{F}_0 \left[n^\star(x)\right] = \frac{1}{4}\int_a^b dx n^\star(x)x^2 + \frac{a^2}{4} - \frac{1}{2}\int_a^b dx n^\star(x)\ln(x-a) \tag{4.22}$$

Symbolic computational programs were for the following evaluation. The expression for $n^\star(x)$ is substituted in above expression for f to obtain

$$\begin{aligned} f \equiv f(a,b) = \frac{1}{512}\big(&-9a^4 + 4a^3b + 2a^2\left(5b^2+48\right) + 4ab\left(b^2+16\right) \\ &-256\ln(b-a) - 9b^4 + 96b^2 + 512\ln(2)\big) \end{aligned} \tag{4.23}$$

Minimizing f with respect to a and b yields $a = -\sqrt{2}$ and $b = +\sqrt{2}$. With these values of $a = -b = \sqrt{2}$, eqn. (4.19) becomes

$$n^\star(x) \equiv p_{\mathrm{SC}}(x) = \frac{1}{\pi}\sqrt{2-x^2} \tag{4.24}$$

which is the Wigner semi-circle law. Thus we conclude that in the limit $N \to \infty$ the distribution of the coulomb gas particles(the eigen values of Gaussian random matrices), is given by (4.24).

Chapter 5

Normal Modes of Gaussian Random Matrix

Now we focus our attention on the peak of equilibrium distribution. This corresponds to the most probable configuration of the eigenvalues. In the continuum limit, as we saw in the previous chapter, the equilibrium configuration is given by the semi-circle law. Now let us ask what will happen to the eigenvalues if one of them is perturbed slightly about the equilibrium. The free energy at the equilibrium is minimum, therefore the eigenvalues will oscillate about the equilibrium configuration. But since there are N of them, the overall behavior of the oscillation is given by the normal modes of oscillations. The information about the normal modes will be captured in the displacement of each of the eigenvalues [12]. In this chapter, we shall derive these normal modes for finite N.

5.1 Correlation Matrix

The correlation matrix is analogous to the spring constant k of the harmonic oscillator potential $(1/2)kx^2$. Let $\{x_1, \ldots, x_N\}$ the instances of eigenvalues of Gaussian Random Matrix. The matrix elements C_{ij} relate the displacement of X_i and X_j about their respective equilibrium position.

To determine the correlation matrix, let us first find the equilibrium configuration of the X_is. For mathematical convenience we shall work with the jpdf (3.17) with rescaling $x_i \to \sqrt{\beta N} x_i$. With this the jpdf becomes

$$P_{N\beta}\left(x_1, x_2, \ldots, x_N\right) = C_{N\beta} \prod_{1 \le i < j \le N} |x_i - x_j|^\beta \, \mathrm{e}^{-\frac{\beta}{2} N \sum_{i=1}^{N} x_i^2} \tag{5.1}$$

where $C_{N,\beta}$ is the normalisation constant given by

$$C_{N\beta} = \frac{(N\beta)^{N/2+\beta N(N-1)/4}}{(2\pi)^{N/2}} \frac{\Gamma^N(1+\beta/2)}{\prod_{n=1}^{N} \Gamma(1+\beta n/2)}$$

We denote the maximum value of $P_{N\beta}$ by $P^0_{N\beta}$. Taking log of (5.1) and differentiating

yields the equations for equilibrium configuration which are given by

$$\sum_{j\neq i} \frac{1}{x_i - x_j} - N x_i = 0 \tag{5.2}$$

At the vicinity of the equilibrium the logarithm of $P_{N\beta}$ is given by

$$\ln P_{N\beta} = \ln P^0_{N\beta} + \frac{1}{2}\beta \sum_{i,j} \delta x_i C_{ij} \delta x_j \tag{5.3}$$

The matrix elements C_{ij} are given by

$$C_{ij} = \frac{1}{\beta} \frac{\partial^2}{\partial x_i \partial x_j} \ln P_{N\beta} \tag{5.4}$$

which evaluates to

$$\begin{aligned} C_{ii} &= -\sum_{j\neq i} \frac{1}{(x_i - x_j)^2} - N \\ C_{ij} &= \frac{1}{(x_i - x_j)^2} \end{aligned} \tag{5.5}$$

The solution to (5.3) are given by the zeros of the Hermite polynomial H_N(see appendix (A.8)),

$$H_N\left(\sqrt{N} x_i\right) = 0 \tag{5.6}$$

5.2 Normal Modes

Let δy_i be the displacement of X_i about the equilibrium position x_i. Since C is an $N \times N$ matrix there would be N eigen vectors, $\delta y_i^{(k)}$, where $k = 1, 2, \ldots N$ The eigen values λ_k of C satisfy

$$\sum_{j=1}^{N} C_{ij} \delta y_j^{(k)} = \lambda_k \delta y_i^{(k)} \tag{5.7}$$

It turns out that the eigen values λ_k are given by

$$\lambda_k = -kN \tag{5.8}$$

To determine the eigenvectors $\delta y_j^{(k)}$, we need to determine the action of C on the powers x_i. It is given by

$$\textstyle\sum_{j=1}^{N} C_{ij} x_j^k = \sum_{j\neq i} \frac{x_j^k - x_i^k}{(x_j - x_i)^2} - N x_i^k \tag{5.9}$$

Further, the above equation can be manipulated to obtain the following identities.

$$\begin{aligned}\sum_{j=1}^{N} C_{ij}x_j^k &= \sum_{l=0}^{k-2}(l+1)x_i^l \sum_{j\neq i} x_j^{k-l-2} + kx_i^{k-1}\sum_{j\neq i}\frac{1}{x_j - x_i} - Nx_i^k \\ &= \sum_{l=0}^{k-2}(l+1)\sigma_{k-l-2}x_i^l - \frac{1}{2}k(k-1)x_i^{k-2} - (k+1)Nx_i^k\end{aligned}$$

Here, it is assumed that the sums over l vanishes for $k \leq 1$ and

$$\sigma_m \equiv \sum_{j=1}^{N} x_j^m \tag{5.10}$$

The sums σ_m were determined by summing over i in the first equation of (5.9). Doing so yields

$$\sum_{i=1}^{N}\sum_{j=1}^{N} C_{ij}x_j^k = -N\sum_{i=1}^{N} x_i^k = -N\sigma_k \tag{5.11}$$

Using this along with eqn. (5.9), yields the recurrence relation

$$Nk\sigma_k = \sum_{l=0}^{k-2}(l+1)\sigma_{k-l-2}\sigma_l - \frac{1}{2}k(k-1)\sigma_{k-2} \tag{5.12}$$

having determined the values of the sums using above recurrence relation, we can determine the eigen vectors(see appendix (A.9)) We list out the first four eigen vectors which were determined using this technique

$$\begin{aligned}\delta y_i^{(1)} &= \frac{1}{N^{1/2}} \\ \delta y_i^{(2)} &= \left(\frac{2}{N-1}\right)^{1/2} x_i \\ \delta y_i^{(3)} &= \left(\frac{N-1}{N(N-2)}\right)^{1/2}\left(1 - \frac{2N}{N-1}x_i^2\right) \\ \delta y_i^{(4)} &= \left(\frac{2(2N-3)^2}{(N-1)(N-2)(N-3)}\right)^{1/2}\left(x_i - \frac{2N}{2N-3}x_i^3\right)\end{aligned}$$

It is useful to visualize how the eigenvalues oscillate about their equilibrium position. Consider the eigenvector $\delta y_i^{(1)}$. For all i, it is constant. This means that all x_i will move together in unison and that the displacement of each of them would be the same.

Consider the next eigenvector $y_i^{(2)}$. Note that it is an odd function of x_i. We know from the symmetry of $P_{N\beta}$ that half of x_i are less than 0, and the rest is greater than 0. This means that the displacement of $x_i < 0$ will be opposite to that of those greater than 0. Moreover, the magnitude of displacement would be greater

for the ones farther away from 0. Note that all normal modes for which k is odd, are even functions. For these normal modes, the direction of displacement would be the same for all x_i. On the other hand, normal modes for which k is even, are odd functions. For these normal modes, the direction of displacement would be opposite for x_i which are on the left and right of the origin.

Chapter 6

Wilson Fermion Spectrum using Random Matrices.

In this chapter, the application of the random matrix theory is demonstrated to obtain the spectrum of Wilson fermions. This has been done by Hehl et. al. in 1999 [8]. The purpose of this study is to understand how RMT is applied to get the spectrum of Wilson fermions. The spectrum encapsulates some important physics of the system. For example, once the spectrum is determined, one can determine the chiral condensate, the order parameter for the chiral phase transition, through the Bank-Casher relation [14]. It was shown by Verbaarshot that the microscopic spectral properties of the lattice QCD Dirac operator are universal [3]. By microscopic spectral properties, we mean the behavior of the eigenvalues of the Dirac operator at the scale of mean level spacing. We had seen the microscopic fluctuation of the random matrix eigenvalues about their average positions and determined the eigenmodes and eigenvalues in the case of the Gaussian Orthogonal Ensemble.

6.1 Wilson Action

The Euclidean action in lattice SU(2) theory for Wilson Fermions in the fundamental representation is given by

$$\begin{aligned} S_E =& \frac{1}{2\kappa}\sum_n \psi^\dagger(n)\psi(n) \\ & - \frac{1}{2}\sum_{n,\mu}\left[\psi^\dagger(n)\,(r-\gamma_\mu)\,U_\mu(n)\psi(n+\mu) + \psi^\dagger(n+\mu)\,(r+\gamma_\mu)\,U_\mu^\dagger(n)\psi(n)\right] \\ & + \frac{4}{g^2}\sum_P \left\{1 - \frac{1}{4}\,\mathrm{Tr}\left[U_P(n) + U_P^\dagger(n)\right]\right\} \end{aligned} \tag{6.1}$$

where r is the link variable the Wilson parameter and U is the link variable containing the gauge field A_μ. The fermionic field is denoted by ψ. κ is related to the mass of the fermions by $\kappa = (2m+8)^{-1}$ [8] . In these partition functions, one average over all the gauge fields.

In random matrix theory, one replaces the terms containing the gauge fields by random matrices of a particular ensemble and then the integration is performed over the independent entries of the random matrices. The underlying gauge group and the fermion representation determine which random matrix ensemble is to be used. For $SU(2)$ gauge group in the fundamental representation one has to use the Gaussian Orthogonal Ensemble If the gauge group is $SU(N_c)$ for $N_c \geq 3$ and the fermions are in the fundamental representation, then one has to use the Gaussian Unitary Ensemble. On the other hand, if we use the $SU(N_c)$, $N_c \geq 3$ with the adjoint representation of fermionic fields, the Gaussian symplectic ensemble has to be used [13].

Kalkreuter had investigated the operator $\gamma_5(\not{D}+m)$ for massive Wilson fermions in an $SU(2)$ gauge field background, and we want to compare the results from the random matrix theory, we shall use the Gaussian orthogonal ensemble. The Euclidean partition function with two random matrices is given by

$$\mathcal{Z} = \int \mathcal{D}[A,B] \mathrm{e}^{-\Sigma_A A^\dagger A - \Sigma_B B^\dagger B} \int \mathcal{D}\left[\psi^\dagger, \psi\right] \mathrm{e}^{-\psi^\dagger(\not{D}+m)\psi} \tag{6.2}$$

where Σ_A and Σ_B are the parameters that scale the distribution variance. In the following sections we specify the operator $\not{\partial}\ D+m$ in terms of the random matrices A and B. We chose to separate the fermionic fields into left and right handed fermions $\psi_{R,L} = (1 \pm \gamma_5)\psi/2$. Also we separate the even and odd lattice sites and work in the basis $(\psi^{\mathrm{e}}_{\mathrm{R}}, \psi^{\mathrm{e}}_{\mathrm{L}}, \psi^{\mathrm{o}}_{\mathrm{R}}, \psi^{\mathrm{o}}_{\mathrm{L}})$. The operator $\not{D} + m$ will be expresed in this basis and then the blocks of this matrix will be replaced by random matrices.

6.2 The Mass term

The first term in the action is the mass term given by

$$\frac{1}{2\kappa}\sum_n \psi^\dagger(n)\psi(n)$$

Let us decompose the wavefunction using left and right projection operators

$$P_L = \frac{1-\gamma_5}{2}, \qquad P_R = \frac{1+\gamma_5}{2}, \qquad \psi_{L,R} = P_{L,R}\psi$$

Now separating the even and odd lattice sites, the action can be written as

$$\frac{1}{2\kappa}\sum_n \psi^\dagger(n)\psi(n) = \frac{1}{2\kappa}\left[\sum_{even} \psi^\dagger \left(P_L + P_R\right)\psi(n) + \sum_{odd} \psi^\dagger(n)\left(P_L + P_R\right)\psi(n)\right]$$

In the basis $(\psi^{e}_{R}, \psi^{e}_{L}, \psi^{o}_{R}, \psi^{o}_{L})$, the above term can be written as(see appendix (A.10.1))

$$\begin{array}{c} \begin{matrix} \psi^{e\dagger}_{R} & \psi^{e\dagger}_{L} & \psi^{o\dagger}_{R} & \psi^{o\dagger}_{L} \end{matrix} \\ \begin{bmatrix} \frac{1}{2\kappa} & 0 & 0 & 0 \\ 0 & \frac{1}{2\kappa} & 0 & 0 \\ 0 & 0 & \frac{1}{2\kappa} & 0 \\ 0 & 0 & 0 & \frac{1}{2\kappa} \end{bmatrix} \end{array} \begin{matrix} \psi^{e}_{R} \\ \psi^{e}_{L} \\ \psi^{o}_{R} \\ \psi^{o}_{L} \end{matrix} \tag{6.3}$$

6.3 The Interaction term

The interaction term of the action is

$$-\frac{1}{2}\sum_{n}\sum_{\mu}\left[\psi^{\dagger}(n)\left(1-\gamma_{\mu}\right)U_{\mu}(n)\psi(n+\mu)+\psi^{\dagger}(n+\mu)\left(1+\gamma_{n}\right)U^{\dagger}_{\mu}(n)\psi(n)\right]$$

Using $U_{\mu} = 1 + igaA_{\mu}$ and $U^{\dagger} = 1 - igaA^{\dagger}_{\mu}$ the interaction term can be written as (see appendix (A.10.2))

$$\begin{aligned} = -\frac{1}{2}\sum_{n}\sum_{k}[&\psi(n)^{\dagger}\psi(n+\mu)+\psi^{\dagger}(n+\mu)\psi(n) \\ &-\psi^{\dagger}(n)\gamma_{\mu}\psi(n+\mu)+\psi^{\dagger}(n+\mu)\gamma_{\mu}\psi(n) \\ &+\psi^{\dagger}(n)igaA_{\mu}\psi(n+\mu)-\psi^{\dagger}(n+\mu)igaA^{\dagger}_{\mu}\psi(n) \\ &-\psi^{\dagger}(n)iga\gamma_{\mu}A_{\mu}\psi(n+\mu)-\psi^{\dagger}(n+\mu)iga\gamma_{\mu}A^{\dagger}_{\mu}\psi(n)] \end{aligned} \tag{6.4}$$

Writing these expressions in the basis $(\psi^{e}_{R}, \psi^{e}_{L}, \psi^{o}_{R}, \psi^{o}_{L})$ we get (see appendix (A.10.2))

$$\begin{array}{c} \begin{matrix} \psi^{e\dagger}_{R} & \psi^{e\dagger}_{L} & \psi^{o\dagger}_{R} & \psi^{o\dagger}_{L} \end{matrix} \\ \begin{bmatrix} \frac{1}{2\kappa} & 0 & \mathbb{I}+igaA^{\dagger}_{\dot{\mu}} & \gamma_{\dot{\mu}}-\not{A}^{\dagger} \\ 0 & \frac{1}{2\kappa} & \gamma_{\dot{\mu}}-\not{A}^{\dagger} & \mathbb{I}+igaA^{\dagger}_{\dot{\mu}} \\ \mathbb{I}-igaA^{\dagger}_{\dot{\mu}} & -\gamma_{\dot{\mu}}-\not{A}^{\dagger} & \frac{1}{2\kappa} & 0 \\ -\gamma_{\dot{\mu}}-\not{A}^{\dagger} & \mathbb{I}-igaA^{\dagger}_{\dot{\mu}} & 0 & \frac{1}{2\kappa} \end{bmatrix} \end{array} \begin{matrix} \psi^{e}_{R} \\ \psi^{e}_{L} \\ \psi^{o}_{R} \\ \psi^{o}_{L} \end{matrix} \tag{6.5}$$

where the dot '.' over μ is to remind us that it is not a free index.

Blocks with the gauge fields A_{μ} are replaced by a random matrix A from the gaussian orthogonal ensemble (GOE). Blocks that contain the product of gamma

matrices and gauge fields ($\gamma_\mu A_\mu$) are replaced with another random matrix B from GOE [8] . After replacing by the random matrices we get

$$\begin{array}{c} \begin{matrix} \psi_{\mathrm{R}}^{\mathrm{e}\dagger} & \psi_{\mathrm{L}}^{\mathrm{e}\dagger} & \psi_{\mathrm{R}}^{\mathrm{o}\dagger} & \psi_{\mathrm{L}}^{\mathrm{o}\dagger} \end{matrix} \\ \begin{bmatrix} \frac{1}{2\kappa} & 0 & \mathbb{I}-A & B \\ 0 & \frac{1}{2\kappa} & B & \mathbb{I}-A \\ \mathbb{I}-A^\dagger & -B^\dagger & \frac{1}{2\kappa} & 0 \\ -B^\dagger & \mathbb{I}-A^\dagger & 0 & \frac{1}{2\kappa} \end{bmatrix} \end{array} \begin{matrix} \psi_{\mathrm{R}}^{\mathrm{e}} \\ \psi_{\mathrm{L}}^{\mathrm{e}} \\ \psi_{\mathrm{R}}^{\mathrm{o}} \\ \psi_{\mathrm{L}}^{\mathrm{o}} \end{matrix} \tag{6.6}$$

We define this matrix as dirac operator ($\not{D}+m$) in the partition function

$$\not{D}+m \equiv \begin{bmatrix} \frac{1}{2\kappa} & 0 & \mathbb{I}-A & B \\ 0 & \frac{1}{2\kappa} & B & \mathbb{I}-A \\ \mathbb{I}-A^\dagger & -B^\dagger & \frac{1}{2\kappa} & 0 \\ -B^\dagger & \mathbb{I}-A^\dagger & 0 & \frac{1}{2\kappa} \end{bmatrix} \tag{6.7}$$

We now want to diagonalise this and get the spectrum of this matrix.

6.4 The Computational Approach

Dimensionality of the Matrix $\not{D}+m$

The matrix (6.7) is a matrix consisting of blocks of matrices some of which are Random Matrices. The gauge field A_μ belongs to the $SU(2)$ group and hence is a 2×2 matrix. The matrix B is a direct product of gamma matrices (4×4) and the gauge matrix(2×2). Hence, the matrix B is an 8×8 Random Matrix. Putting these matrices in the matrix in eqn. (6.7) we obtain a 32×32 matrix which we shall diagonalize.

Results

Choosing $\Sigma_A = 2/25$, we define a random matrix A by entering the instances from the distribution $Normal(0,\Sigma_A)$ into it's elements. The matrix A is symmetrized to get an instance of GOE. Then we took the direct product of A with the four-dimensional identity matrix. For B, we took the entries from $Normal(0,\Sigma_B)$ with $\Sigma_B = 8/25$ which was then symmetrized to obtain an instance from GOE.

These were put in (6.7) and then was diagonalized it to get the eigenvalues. Now, for a large number of such instances, 1000 in this case, we plot a histogram of the eigen values. The histogram is shown in the following figure.

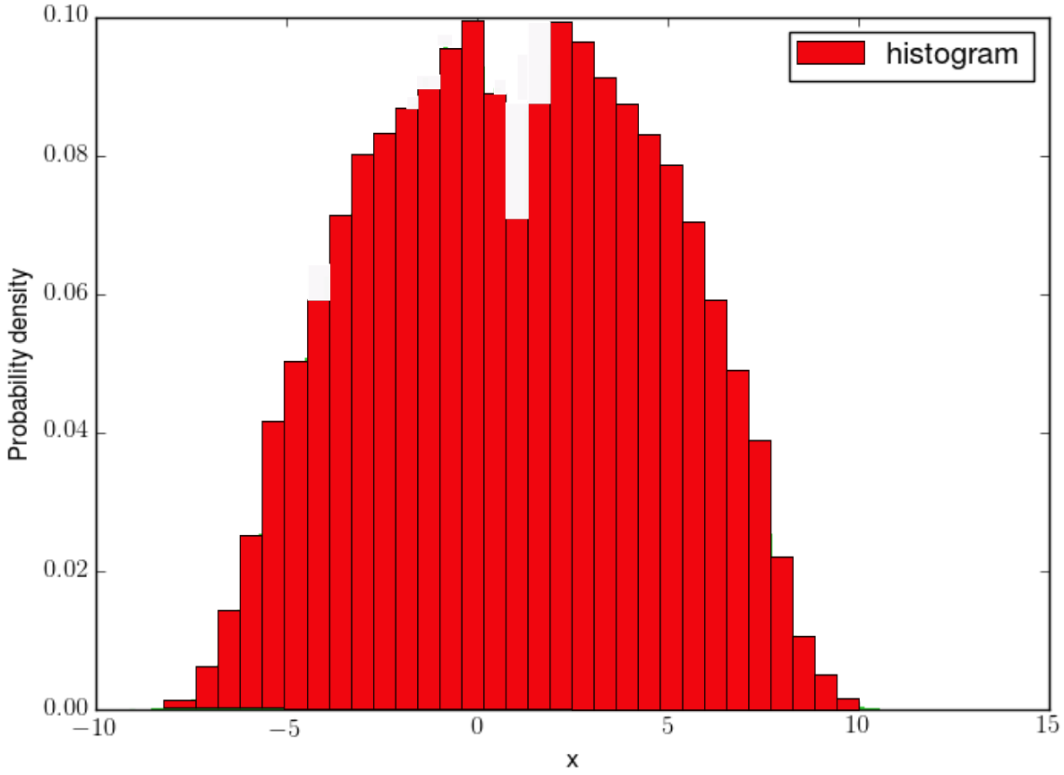

Figure 6.1: The histogram of eigen values of $\not{D} + m$ in terms of gaussian random matrices given by eq. (6.7).

The operator $\not{D} + m$ was multiplied with γ_5 and the basis was changed to $(\psi^{\mathrm{e}}_{\mathrm{R}}, -\psi^{\mathrm{e}}_{\mathrm{L}}, \psi^{\mathrm{o}}_{\mathrm{R}}, \psi^{\mathrm{o}}_{\mathrm{L}})$ to compare with the results of Kalkreuter. In this basis we have eqn. (6.7) as

$$\gamma_5(\not{D} + m) = \begin{pmatrix} 1/2\kappa & 0 & 1-A & B \\ 0 & -1/2\kappa & B & 1-A \\ 1-A^\dagger & B^\dagger & 1/2\kappa & 0 \\ B^\dagger & 1-A^\dagger & 0 & -1/2\kappa \end{pmatrix} \tag{6.8}$$

For different values of κ the spectra was plotted. The nature of spectrum matches qualitatively with that given shown by Kalkreuter [8, 16] .

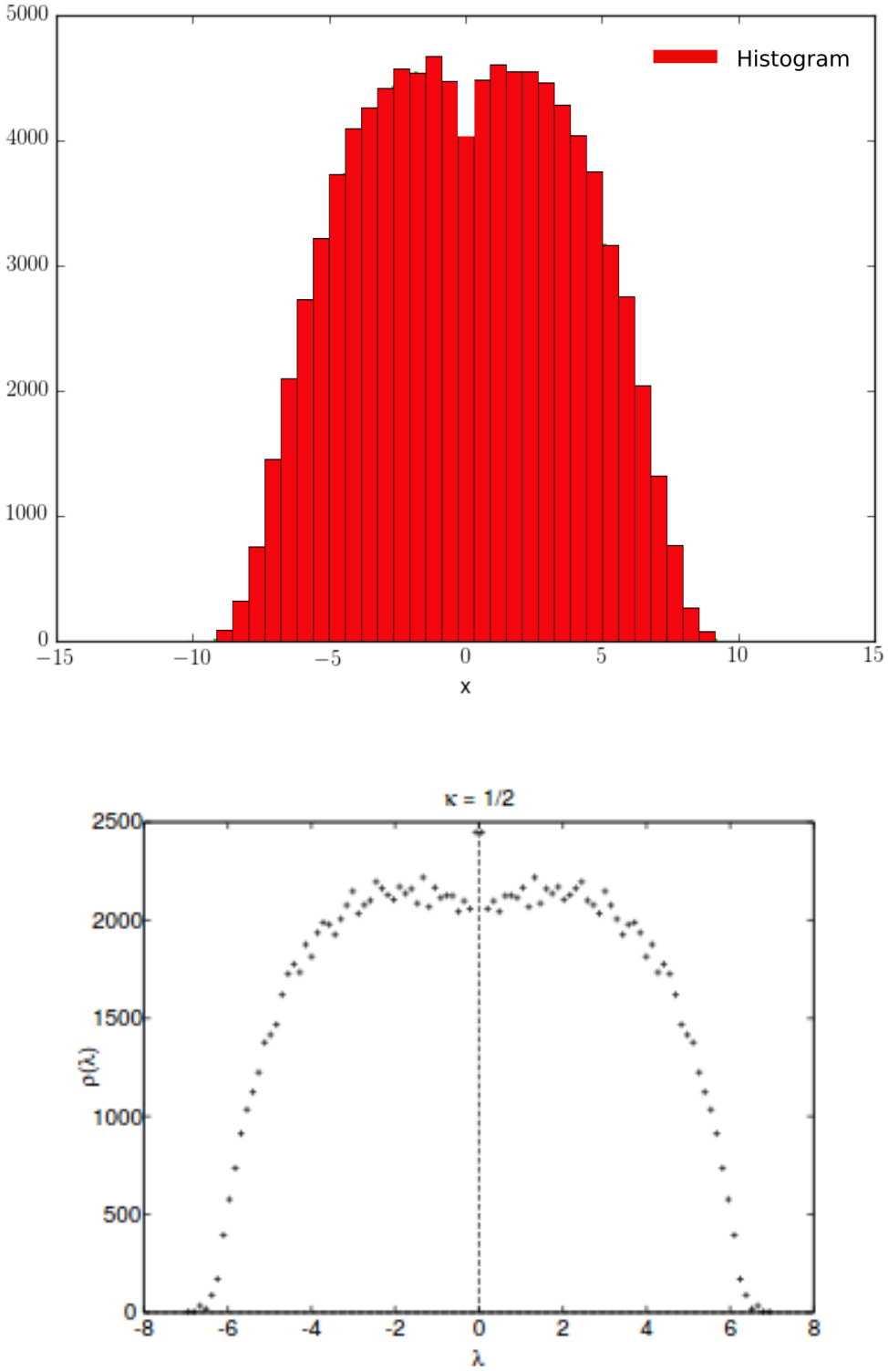

Figure 6.2: The plot on top is the spectrum obtained using RMT by us for $\kappa = 0.5$. The plot below is the one obtained by Hehl [8] et. al. who had shown that this plot matches with that of Kalkreuter. The eigen values are on the x-axis while the y-axis shows the histogram of eigen values of $\gamma_5(\not{D} + m)$

.

Discussion

In this chapter, we saw that the spectrum was obtained by replacing the gauge fields with random matrices. The choice of the ensemble was already fixed by the prescription by Verbaarschot. Since in this case, the gauge group belongs to $SU(2)$ group, which means there are two colors of the quarks, in this case, the relevant ensemble to be used is GOE. We observe that the spectrum obtained by RMT is similar to the one obtained from QCD. Hence we envisage that in order to apply RMT to the minimally doubled fermions we may have to replace some of the blocks of the matrix representation of the corresponding action by the ensemble dictated by the gauge field used and the fermion representation.

Chapter 7

Unfolding and numerical computation of normal modes.

Since random matrix theory (RMT) is supposed to give the results which are not specific to the system under study, the system-specific dependencies need to be removed. As mentioned before, the microscopic fluctuations of Dirac spectra are universal and hence can be modeled by random matrices [3]. We also saw these fluctuations, in the context of Gaussian orthogonal ensemble, by calculating the normal modes. If we have some method to compute the eigenmodes, numerical or computational, we need to rescale so that it can be compared with a physical result. Similarly, we need to rescale and remove the system-specific dependencies from the experimental or physical data (for example, the eigenvalues of a hamiltonian, measured energy spectrum). This is achieved through a procedure called unfolding. Before we compare the theoretical predictions from RMT with the physical theory we need to unfold the respective spectrum [18].

7.1 Unfolding Procedure

Let x denote an eigen value obtained using a certain method, either from experiment or from theory and there are N of them. By unfolding we mean assigning ξ to x using the following transformation.

$$\xi = N(x) \equiv \int_{-\infty}^{x} R_1(x')dx' \tag{7.1}$$

The function $R_1(x)$ follows from the definition of $k-$point spectral correlation functions [18]

$$R_k(x) = \frac{N!}{(N-k)!}\int_{-\infty}^{\infty} dx_2 \ldots \int_{-\infty}^{\infty} dx_N p_{\mathbf{X}}(x, x_2, x_3 \ldots x_N) \tag{7.2}$$

Thus,

$$R_1(x) = Np(x) \tag{7.3}$$

marginal distribution where $p(x)$ is the

$$p(x) = \int_{-\infty}^{\infty} dx_2 \ldots \int_{-\infty}^{\infty} dx_N p_{\mathbf{X}}(x, x_2, \ldots x_N)$$

In the following section, we shall demonstrate how to unfold the Eigen spectrum, in the context of GOE.

7.2 Unfolding GOE spectrum

First an $N \times N$ GOE ensemble of 1000 instances was created with N=100. The normalised histogram (the sum of areas of the bars is unity) of the eigen values so obtained is shown in Fig. (7.1).

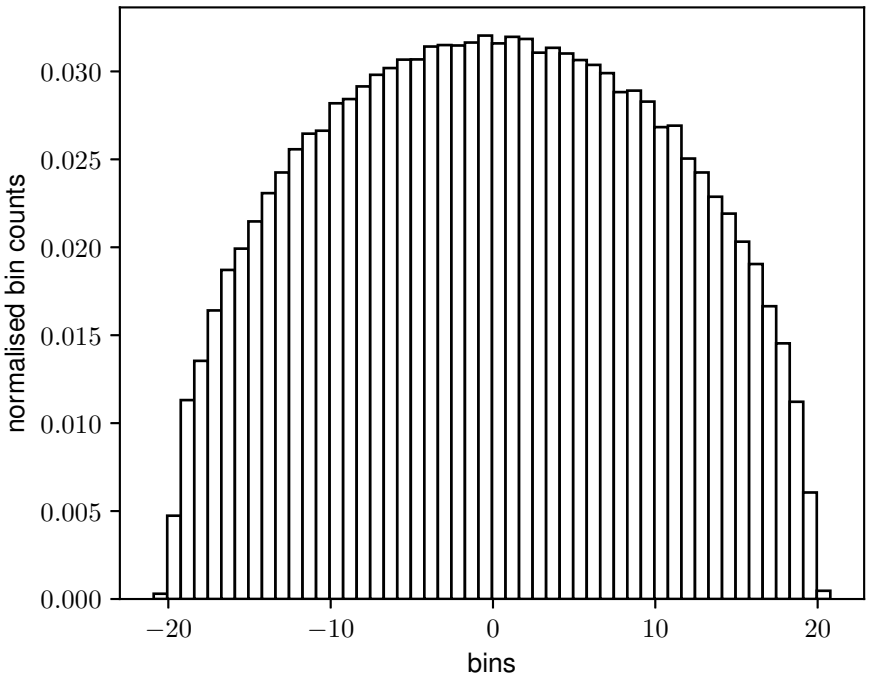

Figure 7.1: This is the histogram of eigenvalues of GOE, for N=100. Note that the distribution is semicircular.

We obtained the bin values and plotted them against the mid-point of the corresponding bin edges (see Fig. (7.2)). In order to find $R_1(x)$ we multiply each points above with $N(= 100)$. The plot so obtained is shown in Fig. (7.3)

We fit these data points with the semi-circle law

$$\tilde{R}_1(x) = A\sqrt{R^2 - x^2} \tag{7.4}$$

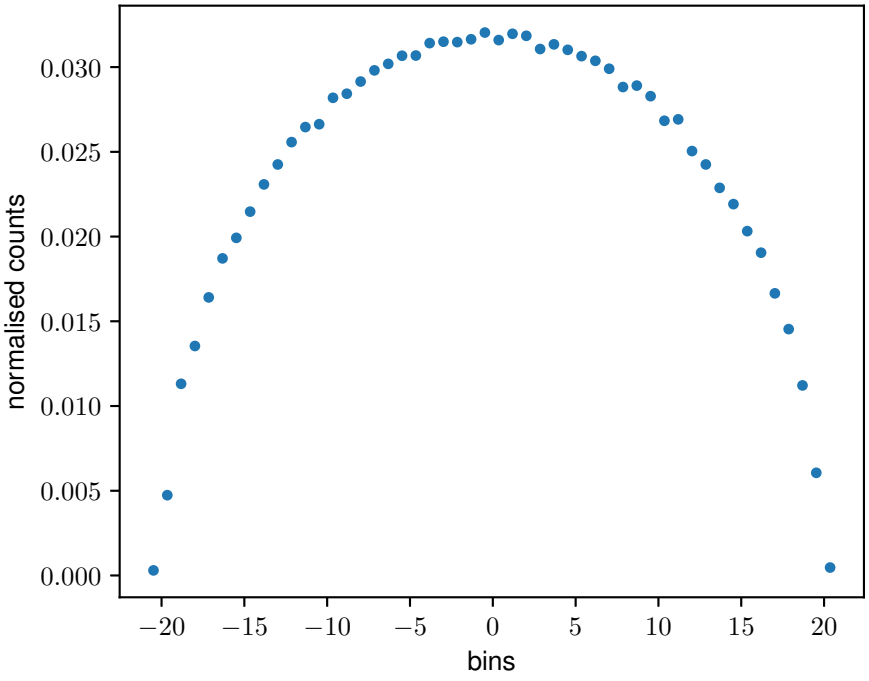

Figure 7.2: The bin-values are plotted against the mid points of the bin-edges. The bin edges are shown in histogram in Fig. (7.1)

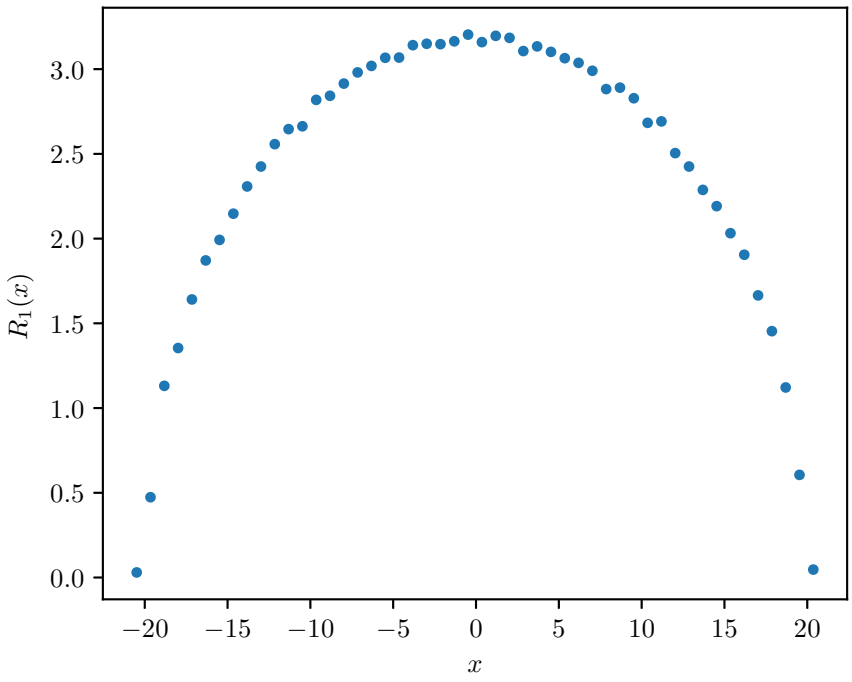

Figure 7.3: The data points $R_1(x)$. This is obtained by multipying the dimension N, (= 100, in this case) of the matrices with the probability density function.

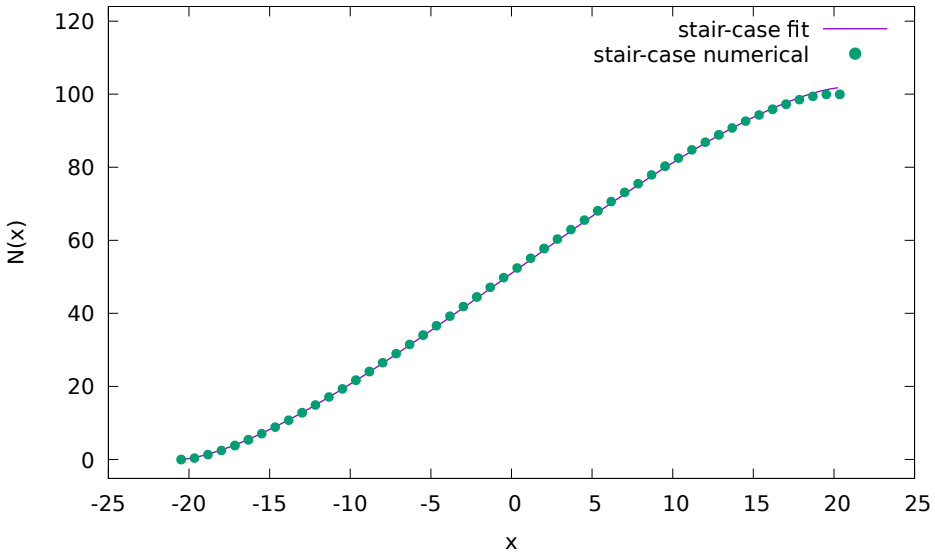

Figure 7.4: The plot of staircase function. The range of the stair case function is $[0, N]$, in this case $N = 100$.

where A and R are the fit parameters. For these data points the fit parameters are as follows (obtained from gnuplot)

$$A = 0.159945 \pm 3.618 \times 10^{-04}$$

$$R = 19.9269 \pm 0.02055$$

These fit parameters will be used as guess parameters when we shall obtain the stair-case function by numerically integrating $R_1(x)$.

The staircase function is the the cumulative distribution function multiplied by the dimension N of the ensemble (see fig. (7.4)). Analytically the expression of staircase function is

$$\tilde{N}(x) = \frac{A}{2}\left(x\sqrt{R^2 - x^2} + R^2 \sin^{-1}\frac{x}{R} + R^2\frac{\pi}{2}\right) \tag{7.5}$$

The fit parameters of the staircase function are

$$\begin{aligned} A &= 0.153886 \pm 0.000877 \\ R &= 20.5276 \pm 0.0639 \end{aligned} \tag{7.6}$$

using these values for A and R we computed the unfolded eigen values. The distribution of the unfolded eigen values are shown in Fig. (7.2)

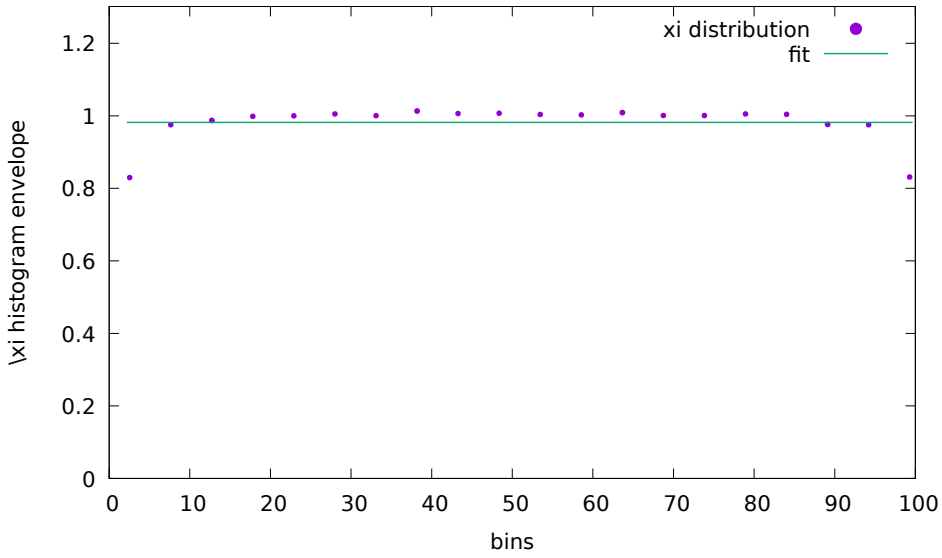

Figure 7.5: The distribution of the unfolded eigen values. After unfolding the distribution becomes uniform. The only information that is retained in the unfolded eigen values is the fluctuation about their averages.

Now suppose we take an instance of the GOE, for N=100, obtain the eigen values and unfold it. From fig. (7.2), we can conclude that on unfolding, the mean spacing between the eigen values becomes unity.

We can see this be considering two consecutive unfolded eigen values

$$\xi_{i+1} - \xi_i = N \int_{x_i}^{x_{i+1}} p(x)dx \approx Np(\bar{x})(x_{i+1} - x_i) \sim 1 \tag{7.7}$$

where $\bar{x} = (x_{i+1} + x_i)/2$. Here we have used the fact that the gap between the eigen values x_i and x_{i+1} is of the order $1/Np(\bar{x})$.

7.3 Computation of Normal Modes for folded and unfolded eigenvalues .

As noted earlier, the information about the microscopic fluctuations in the spectrum is determined by computing the normal modes of the spectrum. In this section, we shall describe the computational procedure adopted to compute the normal modes, both for folded and the unfolded spectrum of GOE.

Let $x_1, x_2 \ldots x_N$ be the eigen values of a $N \times N$ GOE. Let their joint probability density be given by $p_{\mathbf{X}}(x_1, \ldots x_N)$. An important property of this density function is that it is invariant under the exchange $x_i \leftrightarrow x_j$. This invariance allows us to conclude that the distribution of each of the eigen values follows the same marginal

distribution which turns out to be semi-circle law for the correnspondingGaussian Ensemble.

$$p(x) = \int dx_2 dx_3 \dots dx_N p_{\mathbf{X}}(x, x_2 \dots x_N) \tag{7.8}$$

Now, $x_1 \dots x_N$ can be thought of as random variables drawn independently from $p(x)$.

For computing the normal modes we require to compute the eigen values of the matrix D defined by

$$D_{ij} = \langle x_i x_j \rangle - \langle x_i \rangle \langle x_j \rangle \tag{7.9}$$

where $\langle \dots \rangle$ represents the ensemble average. We take 1000 instances of $N \times N$ (with $N = 100$) GOE and order the eigen values, thus imposing the constraint

$$x_1 < x_2 < \dots < x_N$$

Now we compute the matrix $X_{ij} = x_i x_j$. We add X_{ij} for all instances and the divide by N to obtain $\langle x_i x_j \rangle$. To obtain $\langle x_i \rangle$ we take the sum over x_i and then divide by N. Having obtained D, we can diagonalise it and obtain the eigen values and eigen vectors. The eigen values of D for the GOE is shown in the following figure.

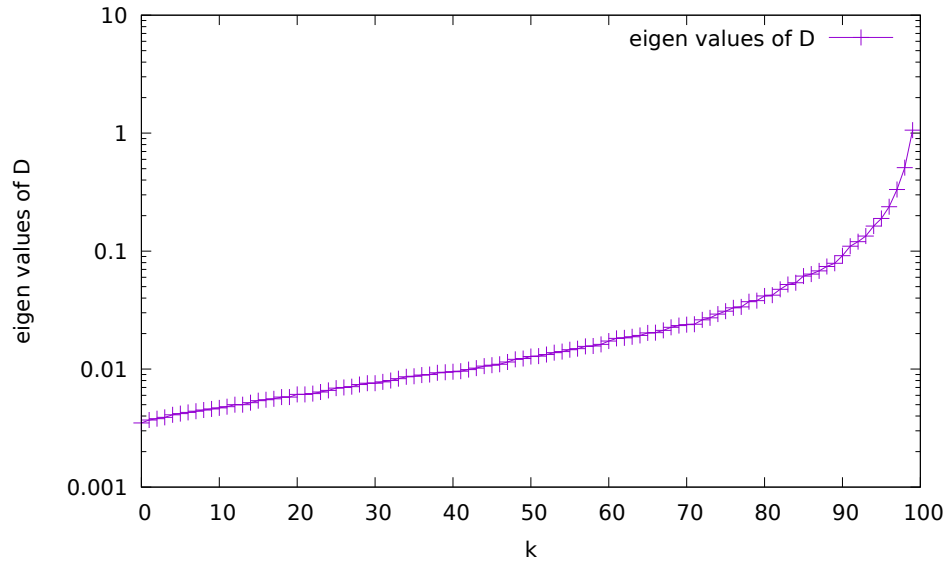

Figure 7.6: The eigen values of matrix D_{ij}.

After unfolding the eigen value spectrum of D is shown below.

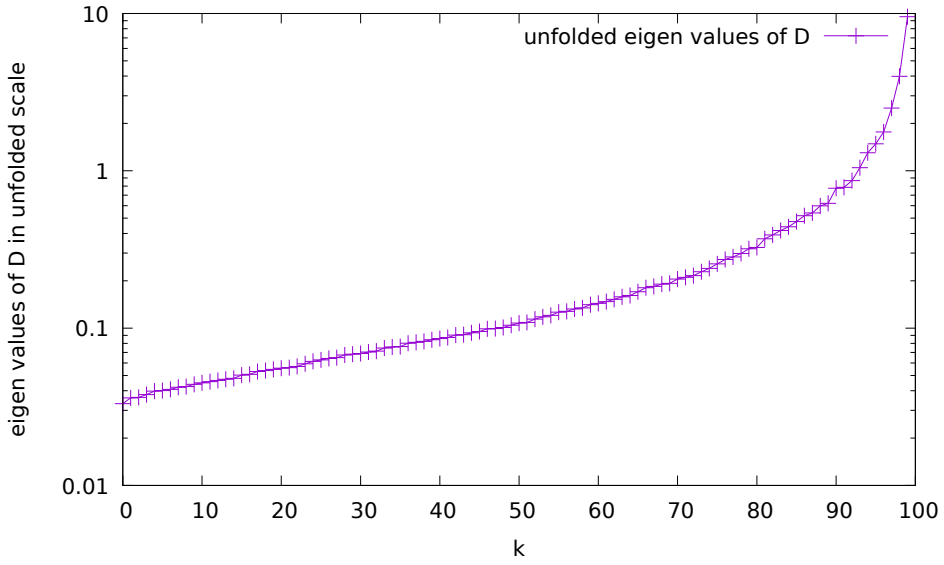

Figure 7.7: The eigen values of matrix D_{ij} in the unfolded scale.

In ref. [18] the author claims that the eigenvalues of C_{ij} obtained through maximizing the joint probability distribution (see chapter (5)) are the reciprocal of the eigenvalues of D, and the eigenvectors of C and D are same, up to the extent that the quadratic approximation is valid. So to obtain the eigenvalues of the matrix C we simply need to take the reciprocal of the eigenvalues of D.

In ref. [11], the author claims that the dispersion relation for GOE is $\omega_k = 1/(Nk)$ in the original scale. After unfolding the dispersion relation becomes $\omega_k = N/(2\sqrt{2}\pi k)$ [17]. The eigen values of C in the original scale is shown in the following figure

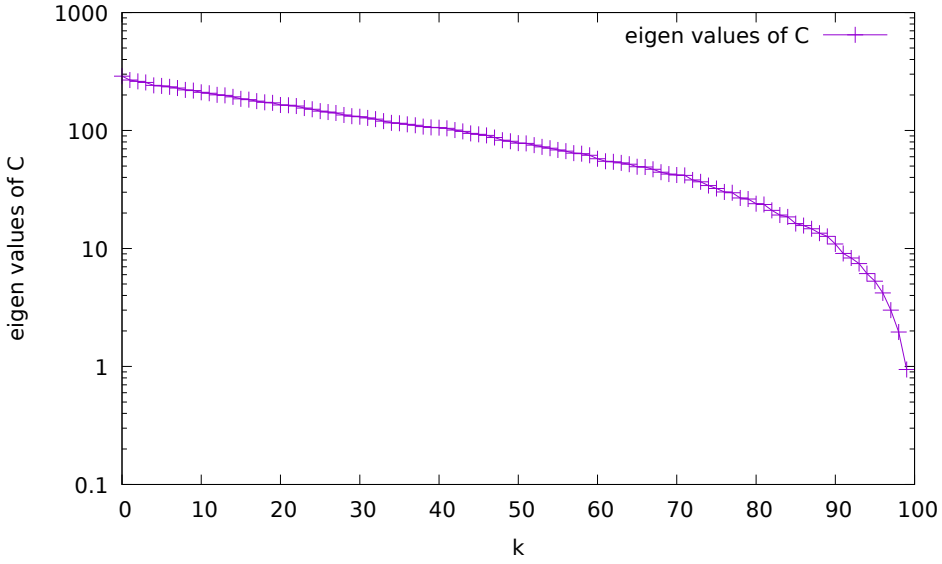

Figure 7.8: The eigen values of C in the original scale.

After unfolding the eigen values of C is shown in the following figure.

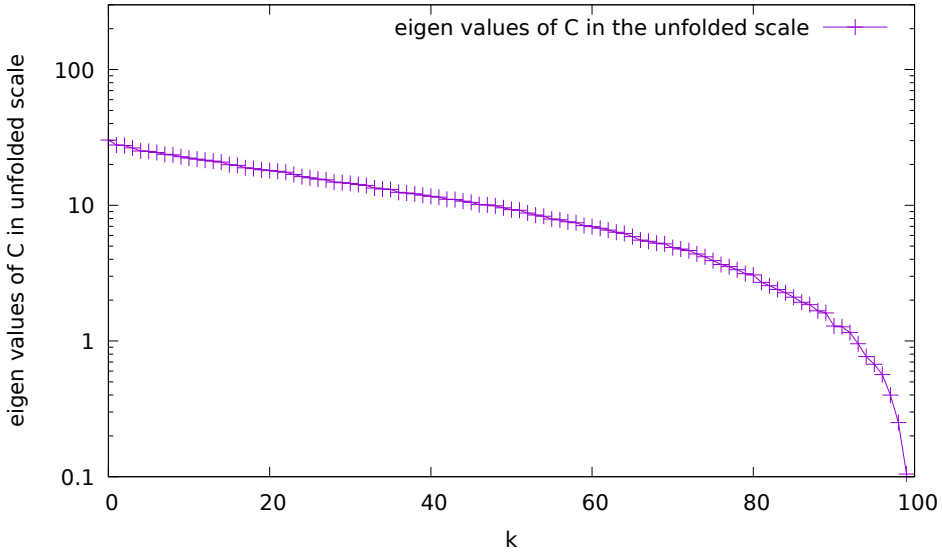

Figure 7.9: The eigen values of C in the unfolded scale.

The plots of the folded and unfolded scale dispersion relation of C in case of GOE agree with the inverse k relationship shown in ref. [11, 17].

We thus got a computational method to compute the eigenvalues of the matrix C for any given ensemble. The spectrum of C in the unfolded scale will be compared with the physical data of the relevant system.

7.4 GOE normal modes.

In the previous section, we saw that the eigenvectors of C and D are same [12]. We show some of the lowest eigenvectors in the unfolded scale. The ground state or the eigenvector corresponding to the lowest eigenvalue is shown below. These modes show the uncorrelated fluctuation modes of the eigenvalues of GOE. For any given instance of GOE, in the unfolded scale, the fluctuation of the eigenvalues about their average can be expressed in terms of these eigenvectors.

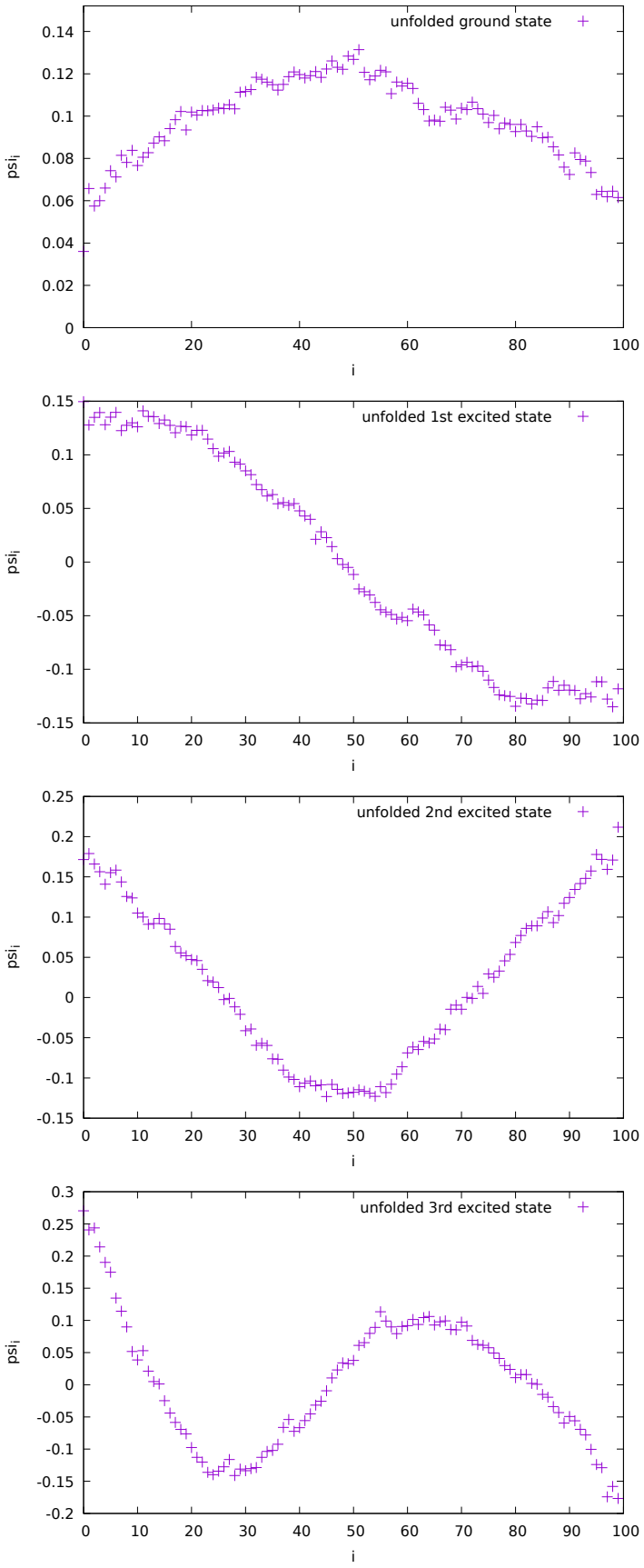

Figure 7.10: The first few eigen vectors of the matrix C. Note that the even states are symmetric about $N/2$ (=50, in this case.)

In this chapter, we learned the unfolding procedure which is important for removing the system-specific dependencies before we can compare the RMT data with that obtained from some other source. We saw how to compute the normal modes of a given ensemble computationally. We shall use this technique to compute the normal modes from RMT which is supposed to be used to compare the data from lattice QCD.

Chapter 8

The chiral random matrix model

Handedness, or chirality, is the projection of spin on the direction of momentum. If the spin ($\vec{s}$) has a positive projection of the momentum($\vec{p}$) direction($\vec{s}\cdot\vec{p}>0$) then we say that the particle is right-handed. On the other hand, the left-handed particles have opposite direction of spin projection onto the momentum direction ($\vec{s}\cdot\vec{p}<0$). The chiral symmetry explicitly broken for massive particles (see appendix (A.12)). Physically this amounts to the fact that one can find an inertial frame in which the chirality of the particle is changed. This is possible because massive particles travel at a speed less than the speed of light. On the other hand, chiral symmetry is a global symmetry of QCD if the particles are massless. This expresses the physical effect that the sign of projection of fermionic spin on its momentum direction cannot be changed if the particle is massless. That is why the limit in which mass becomes vanishingly small is also known as the chiral limit. In the chiral limit, the Dirac operator has a block diagonal structure, because it anti-commutes with γ_5 [11].

$$\not{D} \to \begin{pmatrix} 0 & iT \\ iT^\dagger & 0 \end{pmatrix} \tag{8.1}$$

First, the block T will be replaced by a purely random matrix W with appropriate symmetry properties. The entries of W are purely random, generated according to some probability distribution. For QCD, with gauge groups $SU(N_c)$, with $N_c \geq 3$, the Dirac operator in the fundamental representation has no further symmetries. In this case, the elements of W are taken to be arbitrarily complex. The ensemble formed by $\not{D}$, when it's diagonal block W are replaced by a random matrix with arbitrary complex numbers is called chiral unitary ensemble (chUE). If the probability distribution used for obtaining the entries of W is gaussian, then the ensemble is known as the chiral gaussian unitary ensemble (chGUE). The staggered fermions are described by the chiral Gaussian unitary ensemble for $N_c \geq 3$ [11]. In this chapter, the analysis procedure for obtaining the normal modes of chiral Gaussian Unitary Ensemble (chGUE) is discussed. The dimension of the matrix W is chosen to be

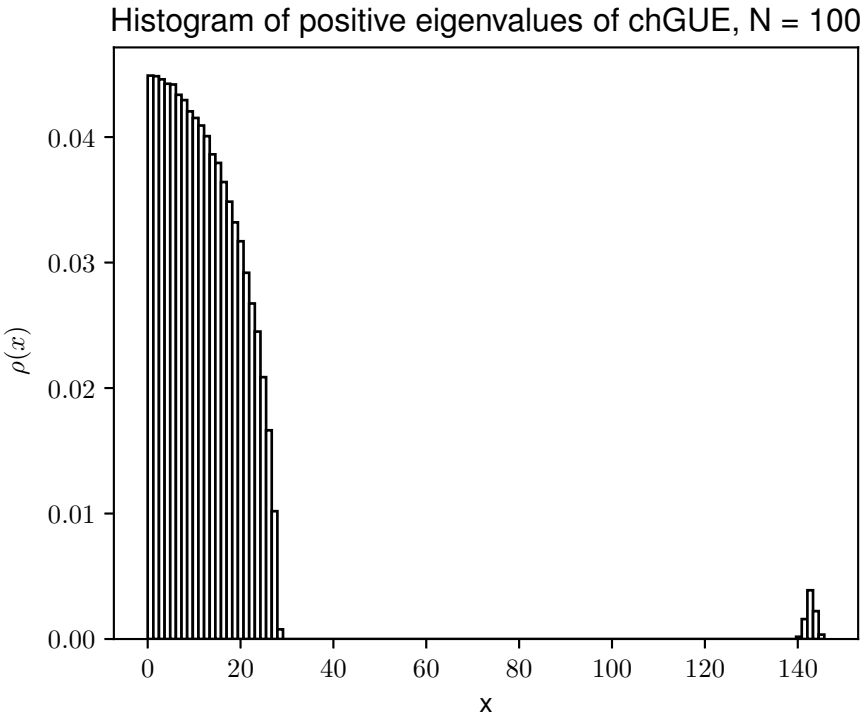

Figure 8.1: The distribution of positive eigenvalues of chGUE. Note that there are two parts of the distibution. While almost all the eigen values are in the semicircular part of the distribution, a vanishingly small number of eigenvalues are located farther away from the origin. In the limit of large N, that is, large dimension of the matrix, the number of eigenvalues farther away are negligible.

$N = 100$.

8.1 The normal modes of ch-GUE

The chiral Gaussian Unitary Ensemble has the structure

$$A = \begin{bmatrix} 0 & W \\ W^\dagger & 0 \end{bmatrix} \tag{8.2}$$

We choose the dimension of W to be $N = 100$.

The probability density of the positive eigen values of A is shown in fig. (8.1) The density function has two parts for large N, one is the semi-circular part and the other is a small hill farther away from the origin (see appendix (A.11)). For the purpose of simulation the density function shown in Fig. (8.1), we took $1000 (= T$, say) such matrices. The total number of positive eigenvalues is then 1000×100, which is 100000. The semicircular part of the density function contains 99000 eigenvalues while the small hill part consists of 1000 eigenvalues. Ignoring the eigenvalues of the small hill part we shall introduce an error of 1%.

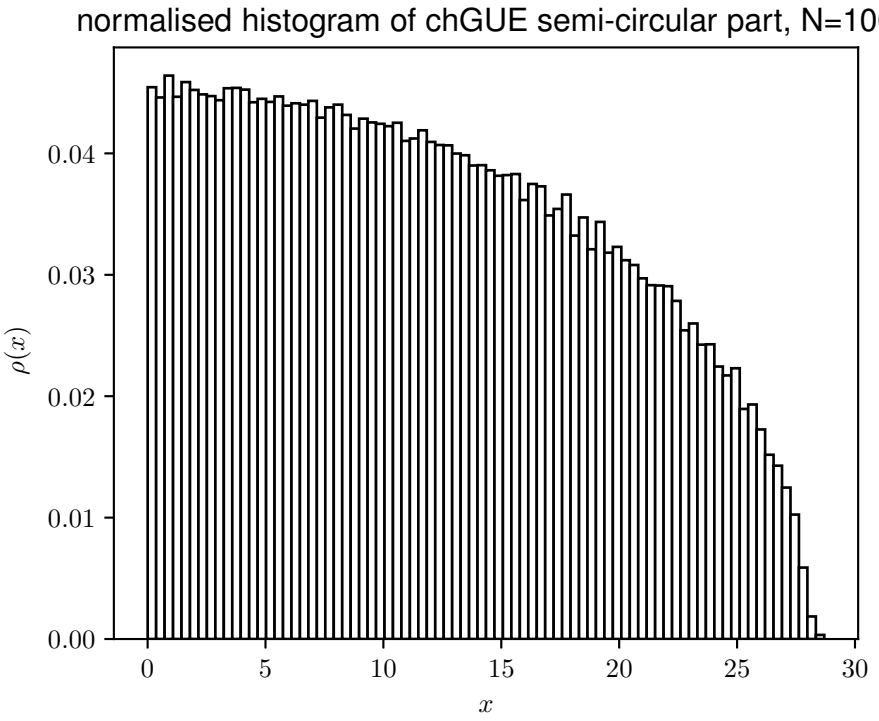

Figure 8.2: The semi-circular part of the density function. In this part the eigenvalues which are farther away from origin outside the semicircular part are neglected.

Now we shall consider the eigen values only in the semicircle. The probability density function of the semi-circular part is shown in Fig. (8.2). From the density function we shall determine the function $R_1(x)$, which is shown in Fig. (8.1). The data points of $R_1(x)$ are fitted with the semicircle Eq. (8.3)

$$R_1(x) = A\sqrt{R^2 - x^2} \tag{8.3}$$

The values of A and R after fitting are

$$\begin{aligned} A &= 0.161143 \pm 0.0004584 \\ R &= 28.1023 \pm 0.03813 \end{aligned} \tag{8.4}$$

Now these parameters will be used as guess values for the parameters of the staircase function $N(x)$ (see Fig. (8.1)). The analytic form of $N(x)$ is

$$N(x) = \frac{A}{2} x\sqrt{R^2 - x^2} + \frac{A}{2} R^2 \sin^{-1}\frac{x}{R} \tag{8.5}$$

The fit parameters A and R are

$$\begin{aligned} A &= 0.165856 \pm 0.0004889 \\ R &= 27.6535 \pm 0.05811 \end{aligned} \tag{8.6}$$

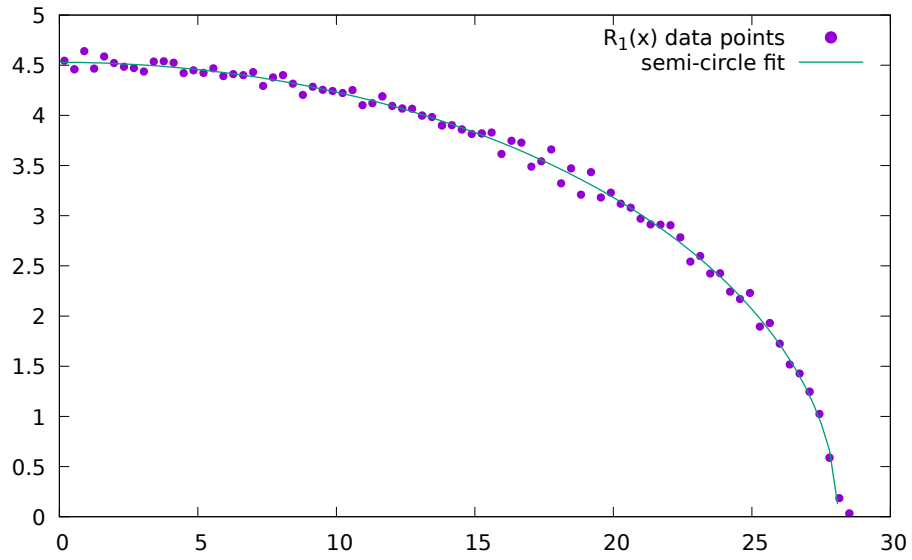

Figure 8.3: Semi-circular fit to the $R_1(x)$ data points.

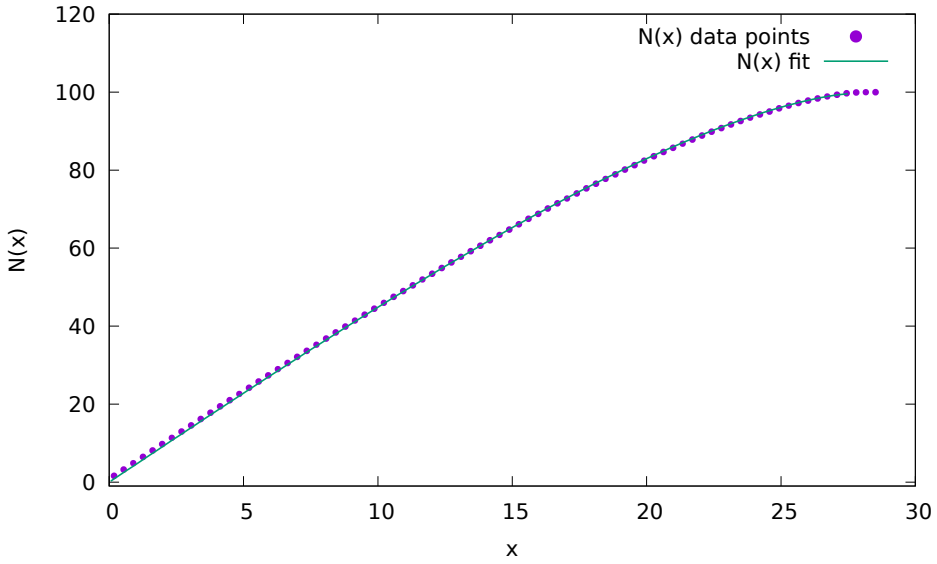

Figure 8.4: The staircase function $N(x)$ fitted with Eq. (8.5)

8.2 Unfolding

Eq. (8.5) was used for unfolding with parameters given by (8.6) for the eigen values $x < R$, while for those greater than R, the corresponding unfolded eigen values were set to the constant N.

$$\xi = \left(\frac{A}{2}x\sqrt{R^2 - x^2} + \frac{A}{2}R^2 \sin^{-1}\frac{x}{R}\right)\Theta(R - x) + N\Theta(x - R) \tag{8.7}$$

8.3 Computing the normal modes.

Let us consider the chiral Gaussian Orthogonal Ensemble (chGUE) with $N \times N$ dimensional matrix W. One would obtain N positive eigenvalues $x_1, x_2 \ldots, x_N$ of the matrix A given by Eq. (8.2). In this section, we obtain the normal modes of the ensemble numerically.

We follow the normal modes computation procedure adopted in Ref. [18]. Let the joint probability density function of $x_1 \ldots x_N$ be $p_N(x_1, x_2, \ldots x_N)$. The matrix C_{ij} is given by

$$C_{ij} = \frac{\partial^2}{\partial x_i \partial x_j} \log p_N(x_1 \ldots x_N) \tag{8.8}$$

evaluated at the point $x_1, \ldots x_N$ which maximises the probability density function. The eigen eigen vectors of C are the normal modes of the ensemble. To compute the normal modes we shall compute the matrix D_{ij} defined by

$$D_{ij} = \langle x_i x_j \rangle - \langle x_i \rangle \langle x_j \rangle \tag{8.9}$$

The eigen values of C are the reciprocals of the eigen values of D, and the eigen vectors of both are the same. [17] The ensemble average $\langle . \rangle$ referes to the averaging with respect to the marginal probability density function

$$p(x) = \int_{-\infty}^{\infty} x_2 \ldots \int_{-\infty}^{\infty} x_N p_N(x, x_2, x_3 \ldots x_N) \tag{8.10}$$

This will be same for all the eigen values because of the invariance of $p_N(x_1 \ldots x_n)$ under the interchange $x_i \leftrightarrow x_j$. For numerical purposes we generate 1000 instances of N dimensional matrices W. For each instance we arrange the eigen values in the ascending order and impose $x_1 < x_2 \ldots x_N$. To compute x_i, we sum over all

the instances of the i^{th} eigen values and divide by the total number of instance to get the corresponding average $\langle x_i \rangle$. Similarly, we compute all the quantities $\langle . \rangle$. The matrix D will be an $N \times N$ symmetrix matrix, and hence it would have N real eigen values. The eigen values of D are arranged in ascending order. Then we compute the reciprocals of the eigen values to get those of C. Now the eigen values of C would be in descending order, by construction, and are plotted against the first N consecutive natural numbers. This is the dispersion relation obtained for the corresponding ensemble. For $N = 100$, the dispersion relation ω_k vs. k is shown in Fig. (8.5). The dispersion relation on the unfolded scale is shown in Fig. (8.6).

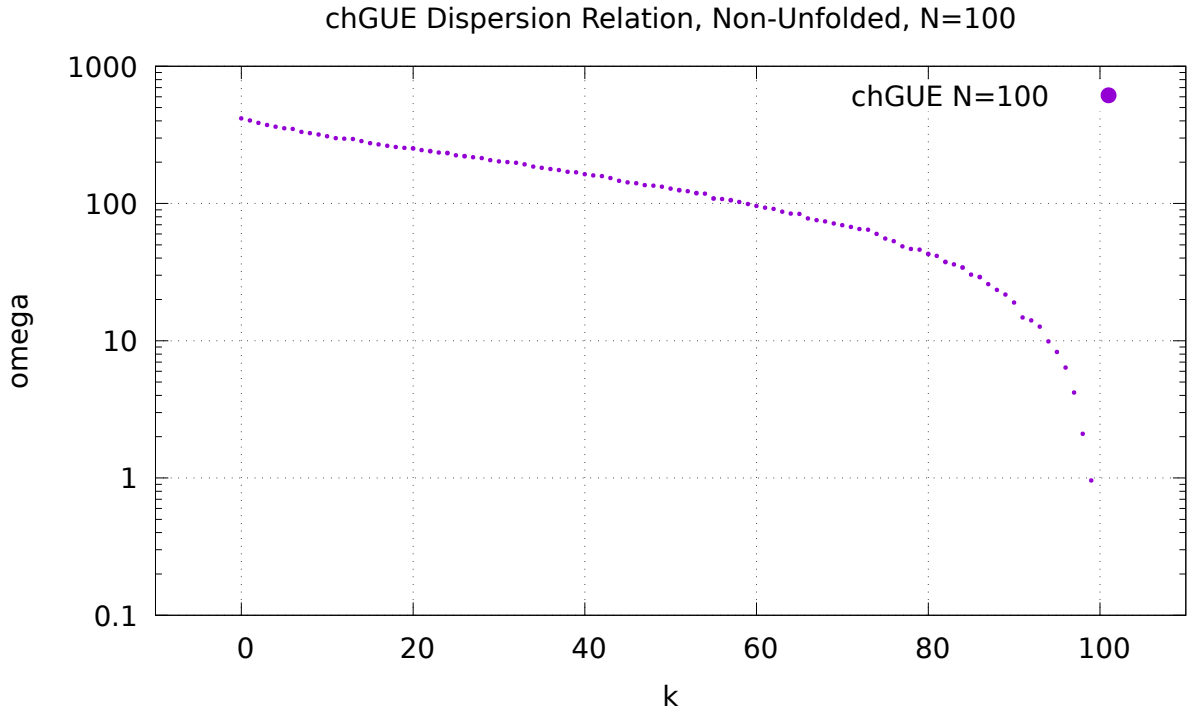

Figure 8.5: The normal modes of chGUE, $N = 100$. in the original scale.

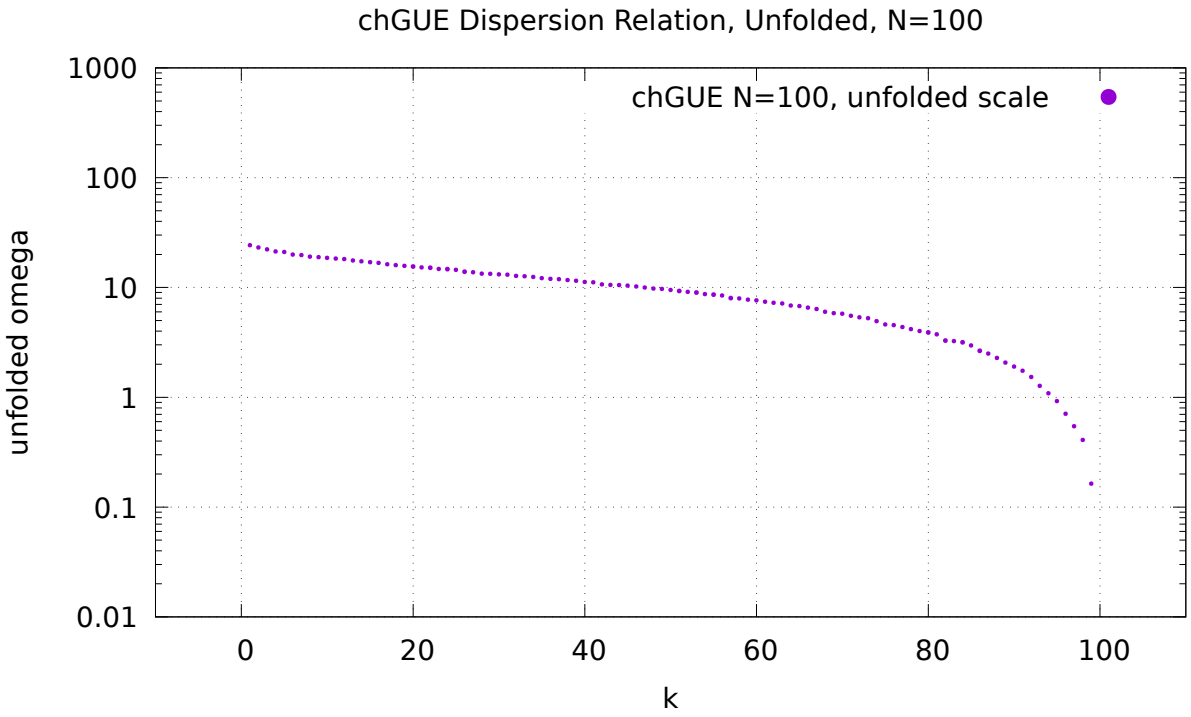

Figure 8.6: The normal modes of chGUE, $N = 100$, in the unfolded scale.

The eigen modes are given by the eigen vectors of D. We plot some of the eigen vectors for lower ω in both folded and unfolded scale as shown in Fig. (8.3).

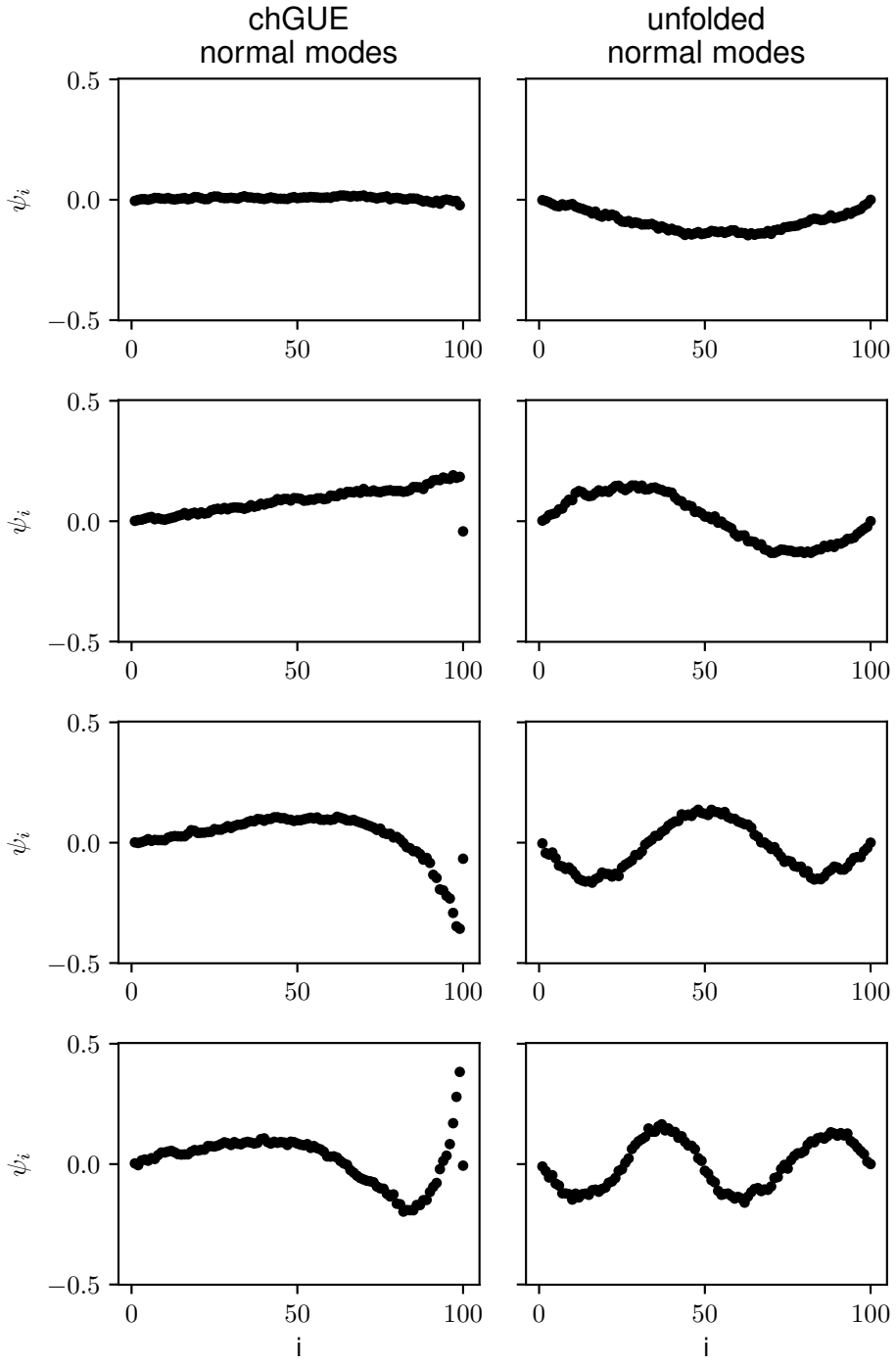

Figure 8.7: The eigen vectors of D for some lower eigen values. The right column of the plots are those in the unfolded-scale.

We note that after unfolding the chGUE eigen modes for the first few modes are similar to that of a vibrating string fixed at both ends.

8.4 Comparing with QCD data.

We showed how to compute the normal modes of chGUE numerically, in both non-unfolded and unfolded scale. Now we have the dispersion relation obtained from the random matrix theory. We have to do now is to compare the QCD data. This exercise will add to the evidence that chRMT describes QCD data, in at least some regime. The QCD data has to be unfolded and then the normal modes have to be compared with that obtained from RMT.

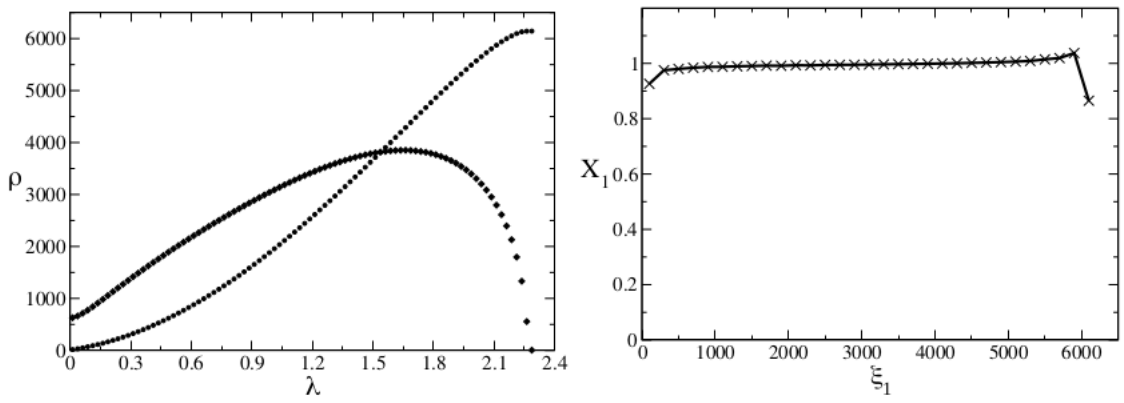

Figure 5.9: QCD lattice data. On the left hand side we plotted the original spectral density (diamonds) and the corresponding stair-case function (circles). On the right hand side we see the corresponding unfolded spectral density. We set $\beta = 5.6$ and $V = 8^4$.

Figure 8.8: This figure is taken from ref. [11]. The left plot shows the distribution of the eigen values of Dirac operator obtained from lattice QCD and the corresponding staircase function. The plot on right shows the distribution of unfolded spectrum.

Fig. (5.9) of ref. [11], shows the plot of $R_1(\lambda)$ for the QCD data and the corresponding staircase function on the left plot. The right plot is that of the unfolded data. For, a given value V, the dimension of the Dirac operator is $N_c V = 3V$. The eigen values of the Dirac operator come in pairs of $\pm\lambda_i$, hence taking only the positive eigen values suffice. So, the number of eigen values for obtaining the above plot is $3V/2$. For $V = 8^4$, $3V/2 = 6144$. Thus density of 6144 data points were determined in the same way demonstrated in chapter (7). This leads to plot of dispersion relation shown in the following plot.

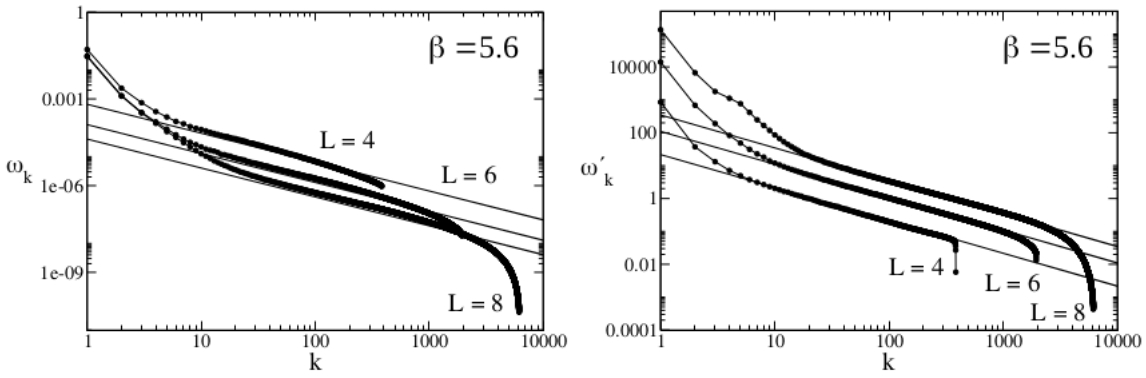

Figure 5.10: Lattice QCD data. We show data for $V = 4^4/6^4/8^4$ and $\beta = 5.6$. Each set contains 7000 configurations. On the left hand side we plotted the dispersion relation of the normal modes of the lattice data and corresponding chRMT prediction (straight lines) on the non unfolded scale. The lowest curve corresponds to highest volume $V = 8^4$. The plot on the right hand side shows the corresponding dispersion relation on the unfolded scale. Here the lowest curve corresponds to the lowest volume $V = 4^4$. Note the good agreement at the intermediate region and the discrepancy for small k.

Figure 8.9: This figure is taken from ref. [11]. This plot is obtained by constructing the matrix D, diagonalizing it, and then taking its reciprocal.

The above plot shows the similarities of the plot of QCD data with that obtained from RMT at least in some regime. What we can conclude from this, is that the spectrum of Dirac operator in the chiral limit can be described by the chiral random matrices. It is the fluctuation of the eigenvalues that are captured by chRMT in terms of the normal modes, and these fluctuations happen to be similar to that of the eigenvalues of Dirac operator.

Chapter 9

Conclusion

We were interested to look for possible applications if random matrix theory in quantum chromodynamics. We studied gaussian ensembles which have the property of rotational invariance and independence of the matrix elements simultaneously. In particular, we looked at the gaussian orthogonal ensemble and gaussian unitary ensemble which has real and complex-valued matrix elements respectively. The eigenvalues of the matrices of these ensembles exhibit their behavior based on two properties. The eigenvalues do not come too close to each other, a property called level-repulsion. In other words, the probability of the eigenvalues being close to each other gets smaller. On the other hand, any two eigenvalues do not go too far from each other. Thus, the eigenvalues are in a confining potential and hence cannot go far apart from each other. This is not the case, had we considered N independent random variables instead of the N eigenvalues of a gaussian ensemble. Interestingly, independent random variables tend to attract each other. Given the two interactions, level-repulsion and confinement, the eigenvalues of large-N dimensional gaussian ensembles tend to get distributed in a semi-circular distribution function. Having known the joint probability distribution function, we found the fluctuation of the eigenvalues about their mean position in the most probable configuration of eigenvalues. The normal modes of the fluctuation and the eigenvalues were determined.

In order to apply the random matrices to a physical system, one needs to identify the symmetries of the system and replace the operators by the random matrices with appropriate symmetries. The random matrices from GOE were used to obtain the spectrum of Wilson fermions, with the assumption that there are two colors ($N_c = 2$). We saw that the spectrum obtained from random matrix theory matches with that obtained from QCD.

The next application was to see how RMT is applied to the fermions respecting

chiral symmetry, in particular to the staggered fermions. The eigenvalues obtained from RMT and from QCD were unfolded. The unfolding procedure removed the system-specific dependencies and retained the information about the fluctuation of the eigenvalues. The fluctuation of the eigenvalues of the Dirac operator contains the information about the dispersion relation, which matched with that obtained from RMT, atleast in some regime.

There is a marked difference between these two applications. In the case of Wilson fermion, the entire spectrum was obtained. We obtained the density of the eigenvalues of the Dirac operator with its blocks replaced by random matrices. In the staggered fermion case, we replaced the Dirac operator in the chiral limit by the random matrices, but we were interested in the normal modes of fluctuation of the eigenvalues. The QCD data was also unfolded before it was compared with the data obtained from RMT. The normal modes obtained from the unfolded data from RMT and QCD matches to some extent.

This motivates us to look for the possible application of RMT for other fermions. Since, according to the no-go theorem, one cannot remove the unphysically doubled fermionic states completely while retaining chiral symmetry, translational symmetry, locality, and hermiticity, the best we can do is to minimize the doubling. We shall investigate the spectrum of minimally doubled fermions and see how RMT can be applied in this case.

References

[1] E. P. Wigner, *Proc. Cam. Phil. Soc.* **47** 790 (1951)

[2] F. J. Dyson, *J. Math. Phys.* **3** 140 (1962)

[3] J.J.M. Verbaarschot, "Universality in Dirac Spectra", (lectures notes, Cambridge 1997)arXiv:hep-th/9710114v1

[4] J.J.M. Verbaarschot, *Nucl. Phys. Proc. Suppl.* **53** 88-94 (1997)

[5] H. B. Nielsen, M. Ninomiya, *Phys. Lett. B* **105** 219-223 (1981)

[6] N.C. Snaith, P.J. Forrester, J.J.M. Verbaarschot, "Developments in Random Matrix Theory" (J.Phys. A36 (2003) R1, Report number: SUNY-NTG-03/03, New York, 2003).

[7] M. L. Metha, Random Matrices, (Academic Press, 3rd Edition, 2004)

[8] Hoger hehl, Andreas Schäfer, *Phys.Rev. D* **59** 117504(1999)

[9] Giacomo Livan, Marcel Novaes, Pierpaolo Vivo, Introduction to Random matrices-Theory and Practice, (Springer International Publishing, 2018)

[10] F. G. Tricomi, Integral Equations (Dover Publications, 1985)

[11] Wolfgang Söldner, thesis, University of Regensburg (2004)

[12] A. Andersen, A.D. Jackson, H.J. Pedersen, *Nuc. Phys. A* **650** 213-223 (1999)

[13] J. Verbaarschot, *Phys. Rev. Lett.* **72** 2531–2533 (1994)

[14] T. Banks, A. Casher, *Nucl. Phys.* **B169**, 103 (1980)

[15] H. J. Rothe, Lattice Gauge Theories (World Scientific, Singapore, 1992).

[16] T. Kalkreuter, *Comput. Phys. Commun.* **95**, 1 (1996)

[17] A.D.Jackson, C.Mejia-Monasterio, T.Rupp, M.Saltzer, T.Wilke, *Nucl.Phys. A* **687** 405-434(2001)

[18] Thomas Guhr, Axel Mueller-Groeling, Hans A. Weidenmueller, **Phys. Rept. 299** 189–425 (1998)

[19] E.P. Wigner, *Ann. Math.* **62** 548 (1955)

Appendix A

A.1 Normalisation of $p_N(s)$

We need to prove $\int_0^\infty p_N(s)ds = 1$. Let us start with LHS.

$$\begin{aligned}&\int_0^\infty p_N(s)ds\\ =&N\int_0^\infty ds\int_\sigma dx p_X(x+s)p_X(x)[1+F(x)-F(x+s)]^{N-2}\end{aligned}$$

Changing the variable $F(x+s)=u$, we obtain $p_X(x+s)ds = du$. At $s=0, u=F(x)$ and at $s\to\infty, u=1$. With this change of variable the above integral becomes

$$\begin{aligned}\int_0^\infty p_N(s)ds =&N\int_\sigma dx\int_{F(x)}^1 p_X(x)(1+F(x)-u)^{N-2}du\\ =&N\int_\sigma dx p_X(x)\quad\frac{[1+F(x)-u]^{N-1}}{(-1)(N-1)}\Big|_{F(x)}^1\\ =&N\int dx p_X(x)\frac{\left([F(x)]^{N-1}-1\right)}{(-1)(N-1)}\end{aligned}$$

Now substituting $F(x)=\nu$, $p_X(x)dx = d\nu$. The property of c.d.f $F(x)$ makes the limit of ν is from 0 to 1. With this,

$$\begin{aligned}=&\frac{-N}{N-1}\int_0^1 d\nu\left(\nu^{N-1}-1\right)\\ =&\frac{N}{N-1}\int_0^1 d\nu\left(1-\nu^{N-1}\right)\\ =&1\end{aligned}$$

Having proved the normalisation, we have shown that $p_N(s)$ is a valid probability density function.

A.2 Derivation of $p(s)$ from the jpdf of eigen values of 2×2 GOE Random Matrix

We need to evaluate

$$p(s)=\int_{-\infty}^\infty\int_{-\infty}^\infty dx_1dx_2p_{X_1X_2}(x_1,x_2)\delta(s-|x_1-x_2|)$$

Let us first find the normalisation factor. Since we are dealing with GOE, $\beta = 1$. $N = 2$ because there are two random variables.

$$\mathcal{Z}_{N,\beta} = \mathcal{Z}_{2,2}$$

Using eqn. 3.18 we have $\mathcal{Z}_{2,2} = 2\sqrt{\pi}$. With this, from eqn. 3.17, we find the probability density function

$$p_{X_1X_2}(x_1, x_2) = \frac{1}{2\sqrt{\pi}}|x_1 - x_2| \exp\left(-\frac{x_1^2 + x_2^2}{2}\right)$$

Using this we obtain

$$p(s) = \int_{-\infty}^{\infty}\int_{-\infty}^{\infty} dx_1 dx_2 \frac{1}{2\sqrt{\pi}}|x_1 - x_2| \exp\left(-\frac{x_1^2 + x_2^2}{2}\right) \delta(s - |x_1 - x_2|)$$

Without loss of generality, assume $x_1 < x_2$. Integrating over x_2 first

$$p(s) = \int_{-\infty}^{\infty} \frac{dx_1 e^{-\frac{1}{2}x_1^2}}{2\sqrt{\pi}} \left[\int_{-\infty}^{x_1} dx_2 e^{-\frac{1}{2}x_2^2} (x_1 - x_2) \left(\delta\left(x - x_1 + x_2\right)\right) + \int_{x_1}^{\infty} dx_2 e^{-\frac{1}{2}x_2^2} (x_2 - x_1) \delta\left(s - x_2 + x_1\right)\right]$$

The first integral vanishes,

$\because s - x_1 + x_2 > 0$ and argument of delta function never vanishes.

$$= \int_{-\infty}^{\infty} \frac{dx_1 e^{-\frac{1}{2}x_1^2}}{2\sqrt{\pi}} \left[s e^{-\frac{1}{2}(x_1+s)^2}\right]$$

$$= \frac{s}{2} e^{-s^2/4}$$

A.3 To show $\langle n(x)\rangle = p(x)$

$$\langle n(x)\rangle = \int \ldots \int d\mathbf{x} \quad p\left(x_1, \ldots, x_N\right) \frac{1}{N} \sum_{i=1}^{N} \delta\left(x - x_i\right)$$

$$= \frac{1}{N}\left[\int d\mathbf{x} \quad p\left(x_1, \ldots, x_N\right) \delta\left(x - x_1\right) + \ldots + \int d\mathbf{x} \quad p\left(x_1, \ldots, x_N\right) \delta\left(x - x_N\right)\right]$$

$$= \frac{1}{N}\left[\int dx_2 \cdots dx_N \quad p\left(x, x_2, \ldots x_N\right) + \ldots + \int dx_1 \cdots dx_{N-1} p\left(x_1 \cdots x_{N-1}, x\right)\right]$$

Since the jpdf is symmetric under the interchange of variables $x_i \leftrightarrow x_j, i \neq j$, we have

$$\langle n(x)\rangle = \frac{1}{N}\left[N \int dx_2 dx_3 \ldots dx_N \quad p(x, x_2, x_3 \ldots, x_N)\right] = p(x)$$

A.4 Converting Sums to Integrals

For transition to the continuum limit it is important to have a method to convert sums to integrals. This can be done using the counting function $n(x)$ as follows. For

discrete values $n(x)$ has the expression as given in eqn. 4.2. With this form of $n(x)$ we have

$$\sum_{i=1}^{N} f\left(x_i\right) = N \int_{\mathbb{R}} n(x) f(x) dx \tag{A.1}$$

and the double sum converts to double integral as

$$\sum_{i,j=1}^{N} g\left(x_i, x_j\right) = N^2 \iint_{\mathbb{R}^2} dx dx' n(x) n\left(x'\right) g\left(x, x'\right) \tag{A.2}$$

Using these conversion, we obtain

$$\frac{1}{2N} \sum_{i=1}^{N} x_i^2 = \frac{1}{2N} \times N \int_{\mathbb{R}} n(x) x^2 dx \tag{A.3}$$

$$\begin{aligned} &\frac{1}{2N^2} \sum_{i \neq j} \ln\left|x_i - x_j\right| = \frac{1}{2N^2} \left[\sum_{i,j} \ln\left|x_i - x_j\right| - \sum_i \ln \Delta\left(x_i\right)\right] = \\ &\frac{1}{2N^2} \times N^2 \iint_{\mathbb{R}^2} dx dx' n(x) n\left(x'\right) \ln\left|x - x'\right| - \frac{1}{2N^2} \times N \int_{\mathbb{R}} dx n(x) \ln \Delta(x) \end{aligned} \tag{A.4}$$

where $\Delta(x)$ is the short distance cutoff. This is introduced to prevent $\ln\left|x_i - x_j\right|$ from diverging.

The short distance cutoff for finite N is of the order $1/Nn(x)$. So, we take

$$\Delta(x) \sim \frac{c}{Nn(x)} \tag{A.5}$$

where $c \sim O(1)$.

A.5 Evaluating $I_N[n(x)]$

We have

$$I_N[n(x)] = \int_{\mathbb{R}^N} \prod_{j=1}^{N} dx_j \delta \left[n(x) - \frac{1}{N} \sum_{i=1}^{N} \delta\left(x - x_i\right)\right]$$

We have the definition of the delta function

$$\delta(x) = \frac{1}{2\pi} \int_{-\infty}^{\infty} dk e^{ikx}$$

In the similar spirit, let us identify

$$\begin{aligned} &\tfrac{dk}{2\pi} \to \mathcal{D}(\hat{n}(x)) \\ &k \to N \textstyle\int \hat{n}(x) dx \\ &x \to n(x) - \tfrac{1}{N} \textstyle\sum_{i=1}^{N} \delta\left(x - x_i\right) \end{aligned} \tag{A.6}$$

With this identification, we have

$$\begin{aligned} &\delta\left[n(x) - \tfrac{1}{N} \textstyle\sum_{i=1}^{N} \delta\left(x - x_i\right)\right] \\ &= \textstyle\int D[\hat{n}(x)] \exp\left[\hat{i} N \int \hat{n}(x) n(x) dx - i \int \hat{n}(x) dx \sum_{i=1}^{N} \delta\left(x - x_i\right)\right] \end{aligned} \tag{A.7}$$

Using this the expression for $I_N[n(x)]$ becomes

$$\begin{aligned} I_N[n(x)] &= \int \mathcal{D}[\hat{n}(x)] \int_{\mathbb{R}^N} \prod_{j=1}^{N} dx_j \exp\left[\mathrm{i}N \int dx n(x)\hat{n}(x) - \mathrm{i} \int dx \hat{n}(x) \sum_{i=1}^{N} \delta\left(x - x_i\right) \right] \\ &= \int \mathcal{D}[\hat{n}(x)] \exp\left[\mathrm{i}N \int dx n(x)\hat{n}(x) \right] \left[\int_{\mathbb{R}} dy e^{-\mathrm{i}\int dx \hat{n}(x)\delta(x-y)} \right]^N \\ &= \int \mathcal{D}[\hat{n}(x)] e^{NS[\hat{n}(x)|n(x)]} \end{aligned}$$

where,

$$S[\hat{n}(x)|n(x)] = \mathrm{i} \int dx n(x)\hat{n}(x) + \ln \int_{\mathbb{R}} dy e^{-\mathrm{i}\hat{n}(y)} \tag{A.8}$$

We then find the critical point of the action $S[\hat{n}](x)|n(x)$

$$0 = \frac{\delta S}{\delta \hat{n}(x)} = \mathrm{i}n(x) - \mathrm{i}\frac{e^{-\mathrm{i}\hat{n}(x)}}{\int_{\mathbb{R}} dy e^{-i\hat{n}(y)}} \tag{A.9}$$

From this, after some manipulation we obtain

$$e^{-i\hat{n}(x)} = n(x) \int_{\mathbb{R}} dy e^{-i\hat{n}(y)} \Rightarrow \hat{i}\hat{n}(x) = -\ln n(x) - \ln \int_{\mathbb{R}} dy e^{-i\hat{n}(y)} \tag{A.10}$$

Now we do a saddle point approximation for $I_N[n(x)]$ an obtain

$$I_N[n(x)] \sim \exp\left[-N \int dx n(x) \ln n(x) \right] \tag{A.11}$$

A.6 Notion of Weak Derivative

Let u be a function in $\mathcal{L}^1([a,b])$, the set of functions which are differentiable almost everywhere in $[a,b]$. We sat that $\nu \in \mathcal{L}^1([a,b])$ is a weak derivative of u if

$$\int_a^b u(x)\varphi'(x)dx = -\int_a^b \nu(x)\varphi(x)dx$$

for all infinitely differentiable functions with $\varphi(a) = \varphi(b) = 0$.

Setting $u(x) = \int dx' n^\star(x') \ln|x - x'|$, we can write

$$\begin{aligned} \int \varphi'(x) \left[\int dx' n^\star(x') \ln|x - x'| \right] dx &= \frac{1}{2} \lim_{\varepsilon \to 0} \int \varphi'(x) \left[\int dx' n^\star(x') \ln\left[(x - x')^2 + \varepsilon^2 \right] \right] dx \\ &= -\frac{1}{2} \int \varphi(x) \left[\int dx' n^\star(x') \frac{2(x - x')}{(x - x')^2 + \varepsilon^2} \right] dx \\ &= -\int \varphi(x) dx \left[\mathrm{Pr} \int dx' \frac{n^\star(x')}{x - x'} \right] \end{aligned}$$

where Pr stands for Cauchy's Principal value.

A.7 Tricomi theorem

Tricomi theorem states that [10]

$$\Pr \int_a^b dx' \frac{f(x')}{x-x'} = g(x) \Rightarrow f(x) = \frac{C - \Pr \int_a^b \frac{dt}{\pi} \frac{\sqrt{(t-a)(b-t)}}{x-t}}{\pi\sqrt{(x-a)(b-x)}} g(t)$$

provided that $[a, b]$ is a single (compact) support and C is an arbitrary constant.

A.8 Calculation of the Most Probable Configuration

Here we prove that the solution to eqn. 5.3 are given by $H_N\left(\sqrt{N}x_i\right) = 0$. The jpdf 3.17 is written as $\exp(-\beta N W)$, where W can be interpreted as free energy of the Coulomb Gas.

$$W = \frac{1}{2}\sum_i^N x_i^2 - \sum_{i \le i < j \le N} \ln|x_i - x_j| \tag{A.12}$$

Let $x_1, x_2 \ldots\ldots x_N$ be the minimum of W

$$0 = -\frac{\partial W}{\partial x_j} \equiv -x_j + \sum_{i(\neq j)} \frac{1}{x_j - x_i} \tag{A.13}$$

consider the polynomial $g(x) = (x-x_1)(x-x_2)\cdots(x-x_N)$

$x_1, x_2 \ldots\ldots x_N$ are zeros of $g(x)$

$$\log g(x) = \sum_{i=1}^N \log|x - x_i| \tag{A.14}$$

Differentiating w.r.t x

$$\frac{1}{g(x)} g'(x) = \sum_{i=1}^N \frac{\partial \log|x-x_i|}{\partial x} = \sum_{i=1}^N \frac{1}{x-x_i} = \sum_{i(\neq j)} \frac{1}{x-x_i} + \frac{1}{x-x_j} \tag{A.15}$$

$$\frac{g'(x)}{g(x)} - \frac{1}{x-x_j} = \sum_{i(\neq j)} \frac{1}{x-x_i} \tag{A.16}$$

$$\frac{(x-x_j)\,g'(x) - g(x)}{g(x)\,(x-x_j)} = \sum_{i(\neq j)} \frac{1}{x-x_i} \tag{A.17}$$

The LHS of above equation takes 0/0 form near $x = x_j$

$$\begin{aligned}\sum_{i(\neq j)} \frac{1}{x_j - x_i} &= \lim_{x \to x_j} \frac{(x - x_j)\, g'(x) - g(x)}{(x - x_j)\, g(x)} \\ &= \lim_{x \to x_j} \frac{g'(x) + (x - x_j)\, g''(x) - g'(x_j)}{(x - x_j)\, g'(x) + g(x)}\end{aligned} \tag{A.18}$$

$$\begin{aligned}&= \lim_{x \to x_j} \frac{(x - x_i) g''(x)}{(x - x_i) g'(x) + g(x)} \\ &= \lim_{x \to x_j} \frac{(x - x_j) g'''(x) + g''(x)}{(x - x_j) g''(x) + g'(x) + g'(x)} \\ &= \frac{g''(x)}{2g'(x_j)}\end{aligned} \tag{A.19}$$

We had

$$0 = -x_j + \frac{g''(x_j)}{2g'(x_j)} \tag{A.20}$$

$$\Rightarrow g''(x_j) - 2x_j g'(x_j) = 0 \tag{A.21}$$

The polynomial $g''(x_j) - 2x_j g'(x_j)$ is a N order polynomial, it has its zeros at $x_1, x_2, ..., x_N$, hence it must be proportional to $g(x)$

$$g''(x) - 2xg'(x) \quad \propto g(x) \tag{A.22}$$

$$g(x) = (x - x_1)(x - x_2) \cdots \quad (x - x_N) \tag{A.23}$$

coefficient of x^N is 1.

$$\begin{aligned}g'(x) = &(x - x_2)(x - x_3) \cdots (x - x_N) \\ &+ (x - x_1)(x - x_3) \cdots (x - x_N) \\ &+ (x - x_1)(x - x_2)(x - x_3) \cdots (x - x_N) \\ &+ (x - x_1) \cdots (x - x_{N-1})\end{aligned} \tag{A.24}$$

coefficient of x^N in $-2xg'(x) = -2N$

For coefficient of both side of the equation to be same

$$g''(x) - 2xg'(x) = -2Ng(x) \tag{A.25}$$

$$\Rightarrow \quad g''(x) - 2xg'(x) + 2Ng(x) = 0 \tag{A.26}$$

This is a Hermite D.E.

A.9 Determination of normal eigen vectors of correlation matrix C

A.9.1 Computing the sums σ_k

We shall use the recursion relation

$$Nk\sigma_k = \sum_{l=0}^{k-2}(l+1)\sigma_{k-l-2}\sigma_l - \frac{1}{2}k(k-1)\sigma_{k-2} \tag{A.27}$$

Let us find σ_2, σ_4 and σ_6 using this equation with $\sigma_0 = N$ and $\sigma_{2k-1} = 0 \forall k \geq 1$.

Putting $k = 2$

$$\begin{aligned} N2\sigma_2 &= \sum_{l=0}^{0}(l+1)\sigma_{2-l-2}\sigma_l - \frac{1}{2}2(2-1)\sigma_0 \\ &= \sigma_{-l}\sigma_l|_{l=0} - \sigma_0 = \sigma_0^2 - \sigma_0 = N(N-1) \end{aligned}$$

This implies

$$\sigma_2 = \frac{N-1}{2} \tag{A.28}$$

Similarly,

$$\begin{aligned} \sigma_4 &= \frac{(N-1)(2N-3)}{4N} \\ \sigma_6 &= \frac{1}{8N^2}(N-1)\left(5N^2+17N+15\right) \end{aligned} \tag{A.29}$$

A.9.2 Computing Eigen Vectors of C

Using eqn. 5.2 we have

$$\sum_{j=1}^{N} C_{ij}x_j^k = \sum_{l=0}^{k-2}(l+1)\sigma_{k-l-2}x_i^l - \frac{1}{2}k(k-1)x_i^{k-2} - (k+1)Nx_i^k$$

For $k = 0$, we get the first eigen vector.

$$\sum_{j=1}^{N} C_{ij}\frac{x_i^0}{\sqrt{N}} = -(1N)\frac{x_i^0}{\sqrt{N}}$$

which after normalisation gives

$$\delta y_i^{(1)} = \frac{1}{\sqrt{N}} \tag{A.30}$$

Let $\delta y_i^{(2)} = Ax_i$. For $k = 1$, we get

$$\sum_{j=1}^{N} C_{ij}x_j^1 = -2Nx_i$$

After normalizing, we obtain

$$A = \frac{1}{\sqrt{\sum_{i=1}^{N} x_i^2}} = \frac{1}{\sqrt{\sigma_2}} = \sqrt{\frac{2}{N-1}}$$

So,

$$\delta y_i^{(2)} = \left(\frac{2}{N-1}\right)^{1/2} x_i \tag{A.31}$$

Let $\delta y_i^{(3)} = P + Qx_i + Rx_i^2$. For $k = 2$,

$$\begin{aligned}\sum_{j=1}^{N} C_{ij} x_j^2 &= \sum_{l=0}^{2-2} (l+1)\sigma_{-l} x_i^l - \frac{1}{2} 2(2-1)x_i^0 - 3Nx_i^2 \\ &= \sigma_0 - 1 - 3Nx_i^2 = (N-1) - 3Nx_i^2\end{aligned}$$

Now the eigen value equation reads

$$\sum_{j=1}^{N} C_{ij} \left[P + Qx_j + Rx_j^2\right] = \lambda \left(P + Qx_i + R{x_i}^2\right)$$

with $R \neq 0$. The LHS of above equation using previous results becomes,

$$\begin{aligned}\sum_{j=1}^{N} C_{ij} \left[P + Qx_j + Rx_j^2\right] &= -PN - 2NQx_i + R\left(N - 1 - 3Nx_i^2\right) \\ &= -PN + R(N-1) - 2NQx_i - 3NRx_i^2\end{aligned}$$

Comparing the coefficients of LHS and RHS we obtain

$$\begin{aligned} R/P &= \frac{\lambda + N}{N-1} \\ -2NQ &= \lambda Q \\ -3NR &= \lambda R \end{aligned}$$

the above three equations along with the normalisation equation

$$\sum_{i=1}^{N} \left(P + Qx_i + Rx_i^2\right)^2 = 1$$

are the four equations required to determine the four variables P, Q, R and λ. Thus, we obtain $\lambda = -3N$. After getting the expression of P, Q and R we obtain

$$\delta y_i^{(3)} = \left(\frac{N-1}{N(N-2)}\right)^{1/2} \left(1 - \frac{2N}{N-1} x_i^2\right) \tag{A.32}$$

Similar technique gives $\delta y_i^{(k)}$, for any k.

A.10 Matrix representation of Wilson fermion

The Euclidean action in lattice SU(2) theory for Wilson Fermions in the fundamental representation is given by (6.1).

A.10.1 Mass term

The first term in the action is the mass term given by

$$\frac{1}{2\kappa}\sum_{n}\psi^{\dagger}(n)\psi(n)$$

Let us decompose the wavefunction using left and right projection operators

$$P_L=\frac{1-\gamma_5}{2},\qquad P_R=\frac{1+\gamma_5}{2},\qquad \psi_{L,R}=P_{L,R}\psi$$

Now separating the even and odd lattice sites, the action can be written as

$$\frac{1}{2\kappa}\sum_{n}\psi^{\dagger}(n)\psi(n)=\frac{1}{2\kappa}\left[\sum_{even}\psi^{\dagger}\left(P_L+P_R\right)\psi(n)+\sum_{odd}\psi^{\dagger}(n)\left(P_L+P_R\right)\psi(n)\right]$$

Using the property of projection operator that $P_{L,R}^2=P_{L,R}$ we have

$$\begin{aligned}
=&\frac{1}{2\kappa}\left[\sum_{\text{even}}\psi^{\dagger}(n)P_LP_L\psi(n)+\sum_{\text{even}}\psi^{+}(n)P_RP_R\psi(n)+\sum_{\text{odd}}\psi^{\dagger}(n)P_LP_L\psi(n)+\sum_{odd}\psi^{\dagger}_{(n)}P_RP_R\psi(n)\right]\\
=&\frac{1}{2\kappa}\left[\sum_{\text{even}}\left(P_L\psi(n)\right)^{\dagger}\left(P_L\psi(n)\right)+\left(P_R\psi(n)\left(P_R\psi(n)\right)\right.+\right.\\
&\qquad\sum_{\text{odd}}\left(P_L\psi(n)\right)^{\dagger}\Big(P_L\psi\left(n\right))+\left(P_R\psi(n)\right)^{\dagger}\left(P_R\psi(n)\right)\Big]\\
=&\frac{1}{2\kappa}\left[\psi_L^{e\dagger}\psi_L^{e}+\psi_R^{e\dagger}\psi_R^{e}+\psi_L^{o\dagger}\psi_L^{o}+\psi_R^{o\dagger}\psi_R^{o}\right]
\end{aligned}$$

In the basis $(\psi_{\mathrm{R}}^{\mathrm{e}},\psi_{\mathrm{L}}^{\mathrm{e}},\psi_{\mathrm{R}}^{\mathrm{o}},\psi_{\mathrm{L}}^{\mathrm{o}})$, the above term can be written as

$$\begin{array}{c}
\begin{array}{cccc}\psi_{\mathrm{R}}^{\mathrm{e}\dagger} & \psi_{\mathrm{L}}^{\mathrm{e}\dagger} & \psi_{\mathrm{R}}^{\mathrm{o}\dagger} & \psi_{\mathrm{L}}^{\mathrm{o}\dagger}\end{array}\\
\begin{bmatrix}\frac{1}{2\kappa} & 0 & 0 & 0\\ 0 & \frac{1}{2\kappa} & 0 & 0\\ 0 & 0 & \frac{1}{2\kappa} & 0\\ 0 & 0 & 0 & \frac{1}{2\kappa}\end{bmatrix}
\begin{array}{c}\psi_{\mathrm{R}}^{\mathrm{e}}\\ \psi_{\mathrm{L}}^{\mathrm{e}}\\ \psi_{\mathrm{R}}^{\mathrm{o}}\\ \psi_{\mathrm{L}}^{\mathrm{o}}\end{array}
\end{array}\tag{A.33}$$

A.10.2 Interaction term

The interaction term of the action is

$$-\frac{1}{2}\sum_{n}\sum_{\mu}\left[\psi^{\dagger}(n)\left(1-\gamma_{\mu}\right)U_{\mu}(n)\psi(n+\mu)+\psi^{\dagger}(n+\mu)\left(1+\gamma_{n}\right)U_{\mu}^{\dagger}(n)\psi(n)\right]$$

Using $U_\mu = 1 + igaA_\mu$ and $U^\dagger = 1 - igaA^\dagger_\mu$ we obtain,

$$
\begin{aligned}
&= -\frac{1}{2}\sum_n\sum_\mu \left[\psi^\dagger_{(n)}\left(1-\gamma_\mu\right)\left(1+igaA_\mu\right)\psi(n+\mu) + \psi^\dagger(n+\mu)\left(1+\gamma_\mu\right)\left(1-igaA^\dagger_\mu\right)\psi(n)\right] \\
&= -\frac{1}{2}\sum_n\sum_\mu \Big[\psi(n)^\dagger\left(1-\gamma_\mu+igaA_\mu - iga\gamma_\mu A_\mu\right)\psi(n+\mu) + \\
&\qquad\qquad \psi^\dagger(n+\mu)\left(1+\gamma_\mu - igaA^\dagger_\mu - iga\gamma_\mu A^\dagger_\mu\right)\psi(n)\Big] \\
&= -\frac{1}{2}\sum_n\sum_\mu \big[\psi^\dagger(n)\psi(n+\mu) + \psi^\dagger(n+\mu)\psi(n) - \psi^\dagger(n)\gamma_\mu\psi(n+\mu) + \psi^\dagger(n+\mu)\gamma_\mu\psi(n) \\
&\qquad + \psi^\dagger(n)igaA_\mu\psi(n+\mu) - \psi^\dagger(n+\mu)igaA^\dagger_\mu\psi(n) - \psi^\dagger(n)iga\gamma_\mu A_\mu\psi(n+\mu) \\
&\qquad -\psi^\dagger(n+\mu)iga\gamma_\mu A^\dagger_\mu\psi(n)\big]
\end{aligned}
$$

The above expression is written as

$$
\begin{aligned}
= -\frac{1}{2}\sum_n\sum_k [&\psi(n)^\dagger\psi(n+\mu) + \psi^\dagger(n+\mu)\psi(n) \\
&- \psi^\dagger(n)\gamma_\mu\psi(n+\mu) + \psi^\dagger(n+\mu)\gamma_\mu\psi(n) \\
&+ \psi^\dagger(n)igaA_\mu\psi(n+\mu) - \psi^\dagger(n+\mu)igaA^\dagger_\mu\psi(n) \\
&-\psi^\dagger(n)iga\gamma_\mu A_\mu\psi(n+\mu) - \psi^\dagger(n+\mu)iga\gamma_\mu A^\dagger_\mu\psi(n)\big]
\end{aligned} \tag{A.34}
$$

Using the property of projection operator that $P_L + P_R = \mathbb{I}$, the first line of above expression is

$$
\left(-\frac{1}{2}\right)\sum_n\sum_\mu \left[\psi^\dagger(n)P_R^2\psi(n+\mu) + \psi^\dagger(n)P_L^2\psi(n+\mu) + \psi^\dagger(n+\mu)P_R^2\psi(n) + \psi^\dagger(n+\mu)P_L^2\psi(n)\right]
$$

Taking n to be even, we get

$$
= -\frac{1}{2}\left(\psi^{e\dagger}_L\psi^o_L + \psi^{e\dagger}_R\psi^o_R + \psi^{o\dagger}_L\psi^e_L + \psi^{o\dagger}_R\psi^e_R\right)
$$

The second line of eqn. A.34 gives

$$
\begin{aligned}
&= -\frac{1}{2}\sum_n\sum_\mu \left[-\psi^\dagger(n)\gamma_\mu\psi(n+\mu) + \psi^\dagger(n+\mu)\gamma_\mu\psi(n)\right] \\
&= -\frac{1}{2}\sum_n\sum_\mu \left[-\psi^\dagger(n)\gamma_\mu\left(P_L^2+P_R^2\right)\psi(n+\mu) + \psi^\dagger(n+\mu)\gamma_\mu\left(P_R^2+P_L^2\right)\psi(n)\right] \\
&= -\frac{1}{2}\sum_n\sum_\mu \big[-\psi^\dagger(n)P_L\gamma_\mu(n+\mu) - \psi^\dagger(n)P_R\gamma_\mu P_L\psi(n+\mu) \\
&\qquad\qquad + \psi^\dagger(n+\mu)P_L\gamma_\mu P_R\psi(n) + \psi^\dagger(n+\mu)P_R\gamma_\mu P_L\psi(n)\big] \\
&\equiv \left(-\frac{1}{2}\right)\left[-\psi^{e\dagger}_L\gamma_{\dot\mu}\psi^o_R - \psi^{e\dagger}_R\gamma_{\dot\mu}\psi^o_L + \psi^{o\dagger}_L\gamma_{\dot\mu}\psi^e_R + \psi^{o\dagger}_L\gamma_{\dot\mu}\psi^e_R\right]
\end{aligned}
$$

The third line of equation A.34 gives

$$
\begin{aligned}
&-\frac{1}{2}\sum_n\sum_\mu\left[\psi^\dagger(n)igaA_\mu\psi(n+\mu)-\psi^\dagger(n+\mu)igaA_\mu^\dagger\psi(n)\right]\\
=&-\frac{1}{2}\sum_n\sum_\mu\left[\psi^\dagger(n)igaA_\mu\left(P_L^2+P_R^2\right)\psi(n+\mu)-\psi^\dagger(n+\mu)igaA_\mu^\dagger\left(P_L^2+P_R^2\right)\psi(n)\right]\\
=&-\frac{1}{2}iga\sum_n\sum_\mu\left[\psi^\dagger(n)P_LA_\mu P_L\psi(n+\mu)+\psi^\dagger(n)P_RA_\mu P_R\psi(n+\mu)\right.\\
&\qquad\left.-\psi^\dagger(n+\mu)P_LA_\mu^\dagger P_L\psi(n)-\psi^\dagger(n+\mu)P_RA_\mu^\dagger P_R\psi(n)\right]\\
=&\frac{-iga}{2}\left[\psi_L^{e\dagger}A_{\dot\mu}\psi_L^o+\psi_R^{e\dagger}A_{\dot\mu}\psi_R^o-\psi_L^{o\dagger}A_\mu\psi_L^e-\psi_R^{o\dagger}A_{\dot\mu}\psi_R^e\right]
\end{aligned}
$$

The fourth line in eqn. A.34 gives

$$
\begin{aligned}
&\left(-\frac{1}{2}\right)\sum_n\sum_\mu\left[-\psi^\dagger(n)iga\gamma_\mu A_\mu\psi(n+\mu)-\psi^\dagger(n+\mu)iga\gamma_\mu A_\mu^\dagger\psi(n)\right]\\
=&-\frac{iga}{2}\sum_n\sum_\mu\left[-\psi^\dagger(n)P_L\gamma_\mu A_\mu P_R\psi(n+\mu)-\psi^\dagger(n)P_R\gamma_\mu A_\mu P_L\psi(\eta+\mu)\right.\\
&\qquad\left.-\psi^\dagger(n+\mu)P_L\gamma_\mu A_\mu^\dagger P_R\psi(n)-\psi^\dagger(n+\mu)P_R\gamma_\mu A_\mu^\dagger P_L\psi(n)\right]\\
=&-\frac{iga}{2}\left[-\psi_L^{e\dagger}\not{A}\,\psi_R^o-\psi_R^{e\dagger}\not{A}\,\psi_L^o-\psi_L^{o\dagger}\not{A}^\dagger\,\psi_R^e-\psi_R^{o\dagger}\not{A}^\dagger\,\psi_L^e\right]
\end{aligned}
$$

Writing all the four expressions for the interaction and the mass term in basis $(\psi_{\mathrm{R}}^{\mathrm{e}},\psi_{\mathrm{L}}^{\mathrm{e}},\psi_{\mathrm{R}}^{\mathrm{o}},\psi_{\mathrm{L}}^{\mathrm{o}})$ we get

$$
\begin{array}{c}
\begin{array}{cccc}\psi_{\mathrm{R}}^{\mathrm{e}\dagger} & \psi_{\mathrm{L}}^{\mathrm{e}\dagger} & \psi_{\mathrm{R}}^{\mathrm{o}\dagger} & \psi_{\mathrm{L}}^{\mathrm{o}\dagger}\end{array}\\
\begin{bmatrix}
\frac{1}{2\kappa} & 0 & \mathbb{I}+igaA_{\dot\mu}^\dagger & \gamma_{\dot\mu}-\not{A}^\dagger\\
0 & \frac{1}{2\kappa} & \gamma_{\dot\mu}-\not{A}^\dagger & \mathbb{I}+igaA_{\dot\mu}^\dagger\\
\mathbb{I}-igaA_{\dot\mu}^\dagger & -\gamma_{\dot\mu}-\not{A}^\dagger & \frac{1}{2\kappa} & 0\\
-\gamma_{\dot\mu}-\not{A}^\dagger & \mathbb{I}-igaA_{\dot\mu}^\dagger & 0 & \frac{1}{2\kappa}
\end{bmatrix}
\begin{matrix}\psi_{\mathrm{R}}^{\mathrm{e}}\\ \psi_{\mathrm{L}}^{\mathrm{e}}\\ \psi_{\mathrm{R}}^{\mathrm{o}}\\ \psi_{\mathrm{L}}^{\mathrm{o}}\end{matrix}
\end{array}
\tag{A.35}
$$

A.11 Analysis of chGUE Distribution

It is important to discuss the density function of the chiral Gaussian Unitary Ensemble(chGUE) because it is after this step we can determine the expression of staircase function required for unfolding procedure.

The ensemble of matrices with the structure

$$
A=\begin{bmatrix}0 & W\\ W^\dagger & 0\end{bmatrix}
\tag{A.36}
$$

where W is a square-matrix with complex entries. Had the entries been real, the ensemble would have been called ch-GOE(chiral Gaussian Orthogonal Ensemble).

Similarly, for quanrternionic matrix elements of W, A is said to be a matrix of chiral Gaussian Symplectic Ensemble(ch-GSE). For the purpose of this report we shall focus on the chGUE ensemble.

A.11.1 An instance of matrix A.

Let us examine an instance of the matrix A. We first construct the matrix W. Let us choose W to be of dimension 2×2. An instance of W looks like

$$W = \begin{bmatrix} 1.452 + i1.299 & 1.880 - i0.301 \\ 1.155 + i0.7913 & -0.4003 - i0.1705 \end{bmatrix}$$

Now using Eq. (A.36)

$$A = \begin{bmatrix} 0 & 0 & 1.452 + i1.299 & 1.880 - i0.301 \\ 0 & 0 & 1.155 + i0.7913 & -0.4003 - i0.1705 \\ 1.452 - i1.299 & 1.155 - i0.7913 & 0 & 0 \\ 1.880 + i0.301 & -0.4003 + i0.1705 & 0 & 0 \end{bmatrix}$$

Note that the matrix A is hermitian, and that it's trace is vanishing. A being hermitian the eigen values are guaranteed to be real. For the vanishing trace it is natural to expect that for every positive eigen value, the corresponding negative value is also an eigen value. The eigen values in this case are

$$\text{Eigen values of } A = \{-2.8619, -1.1750, 1.1750, 2.8619\}$$

It can be proven that the eigen values of A are the square roots of the eigen values of $WW^\dagger$. Thus, the information about the spectrum is contained in the positive eigen values of A.

The probability density function of chGUE is interesting in low dimensions. The semicircle law is obeyed for large N, but for lower dimensions the probability density behave in an interesting way. We shall see how the probability density of chGUE vary with it's dimension N.

We then determine the histogram of these eigen values which is shown below, for differrent dimensions.

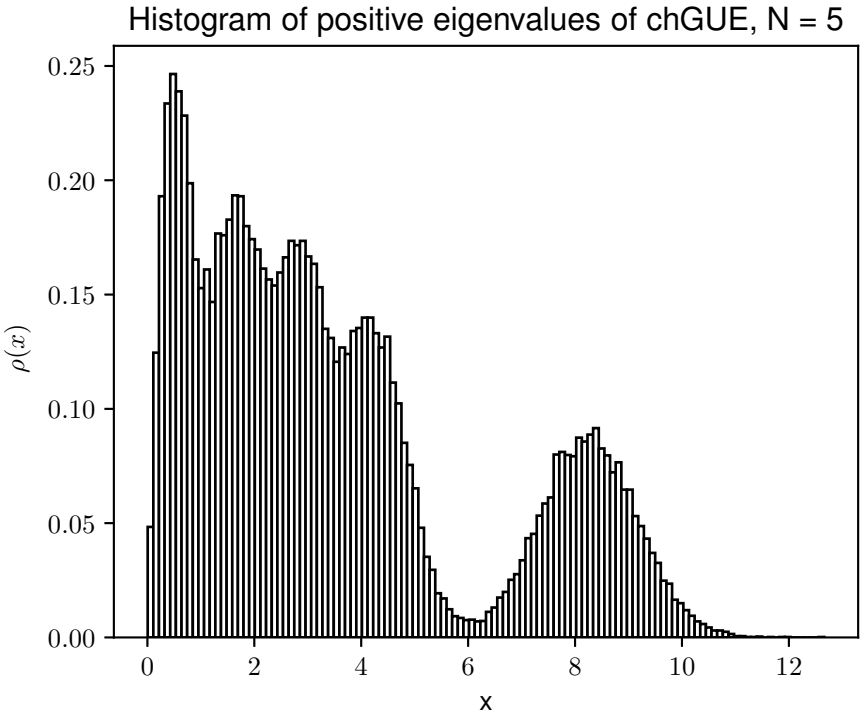

Figure A.1: Histogram of positive eigen values for N=5.

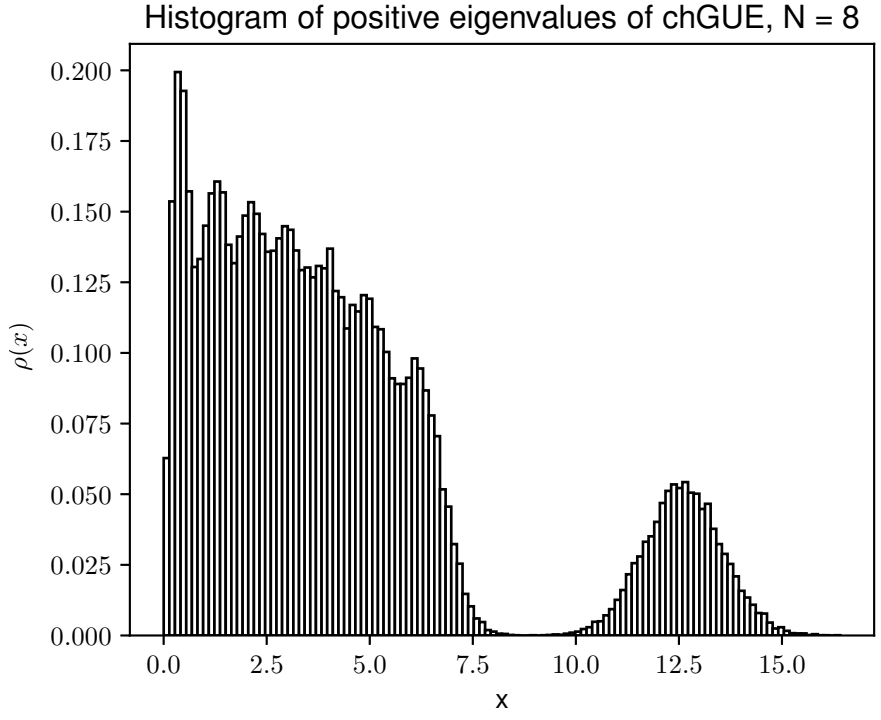

Figure A.2: Histogram of positive eigen values for N=8.

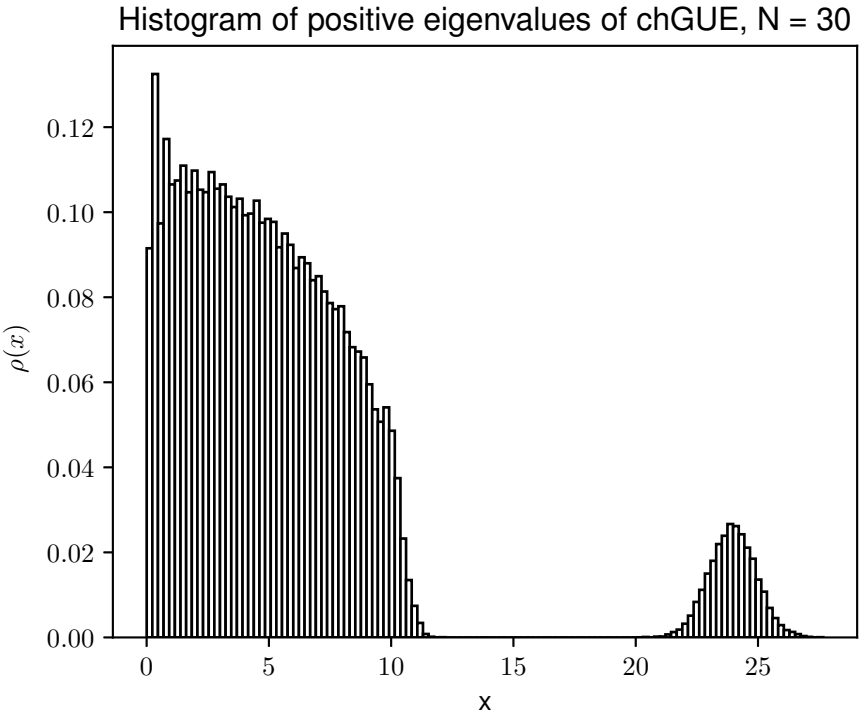

Figure A.3: Histogram of positive eigen values for N=30.

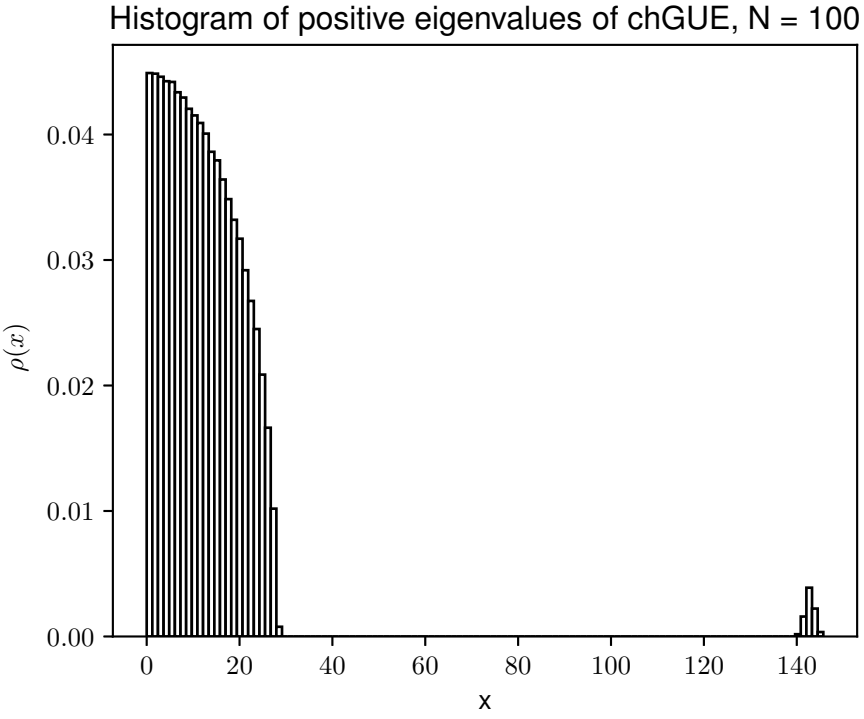

Figure A.4: Histogram of positive eigen values for N=100.

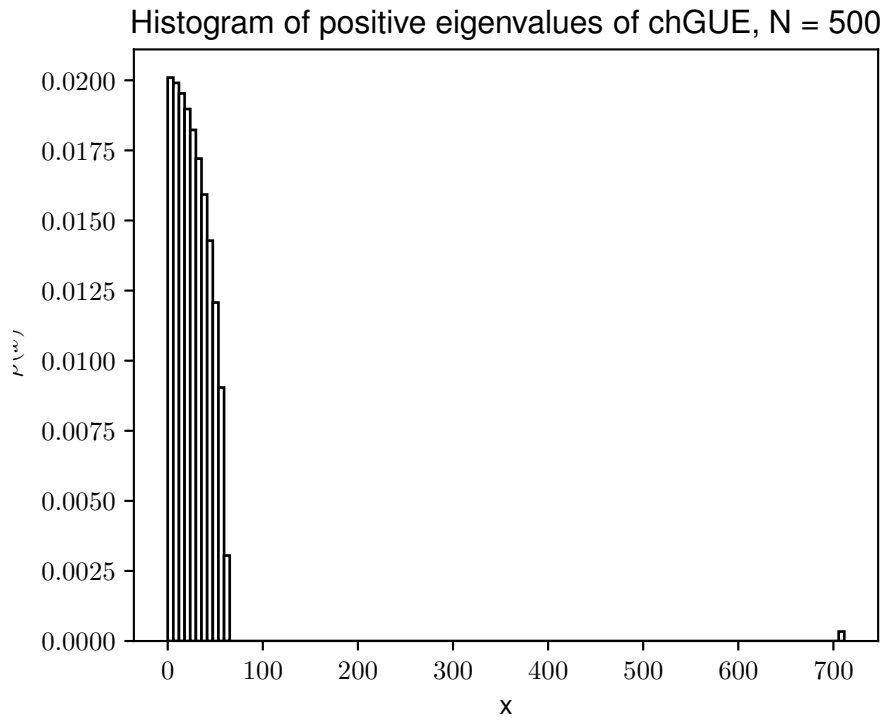

Figure A.5: Histogram of positive eigen values for N=500.

The above figures reveal that small N, the number of peaks of the density function is equal to the dimension of the matrix W, But as N increases only two peaks become significant. With further increase in N, the one near the origin takes a semicircular shape while the one farther gets smaller and goes farther from origin. In the limit $N \to \infty$, the probability density at the later peak vanishes.We shall, henceforth, consider the semicircular part of the probability density to get the stair case function.

A.11.2 Unfolding of chGUE

For the purpose of analysis we shall discard the data points farther away from the semi-circular part of the distribution. Here an error is introduced due to this, which we shall ignore. Now, the histogram of the contains the semicircular part as shown in Fig. (A.6). The envelope of this histogram is shown in Fig. (A.7).

To get the function $R_1(x)$ we multiply the data points shown in Fig. (A.7) with N(here, $N = 500$). Fig. (A.8) shows the data points of $R_1(x)$ which is to be fitted with the semicircle law Eq. (A.37).

$$R_1(x) = A\sqrt{R^2 - x^2} \tag{A.37}$$

After fitting (see Fig. (A.9)) we obtain the parameters

$$A = 0.159558 \pm 9.807 \times 10^{-05}(0.06146\%)$$
$$R = 63.1643 \pm 0.01768(0.02798\%)$$

These parameters also fit the staircase function which was numerically obtained earlier because we have now ignored the small part of the density function which

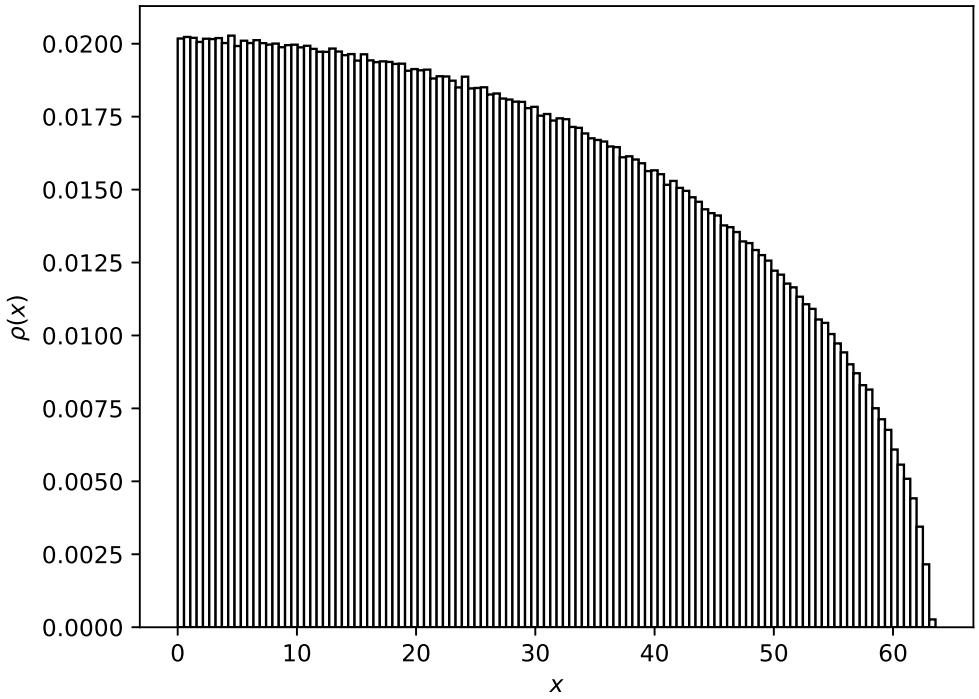

Figure A.6: The semicircular part of histogram in Fig. A.5

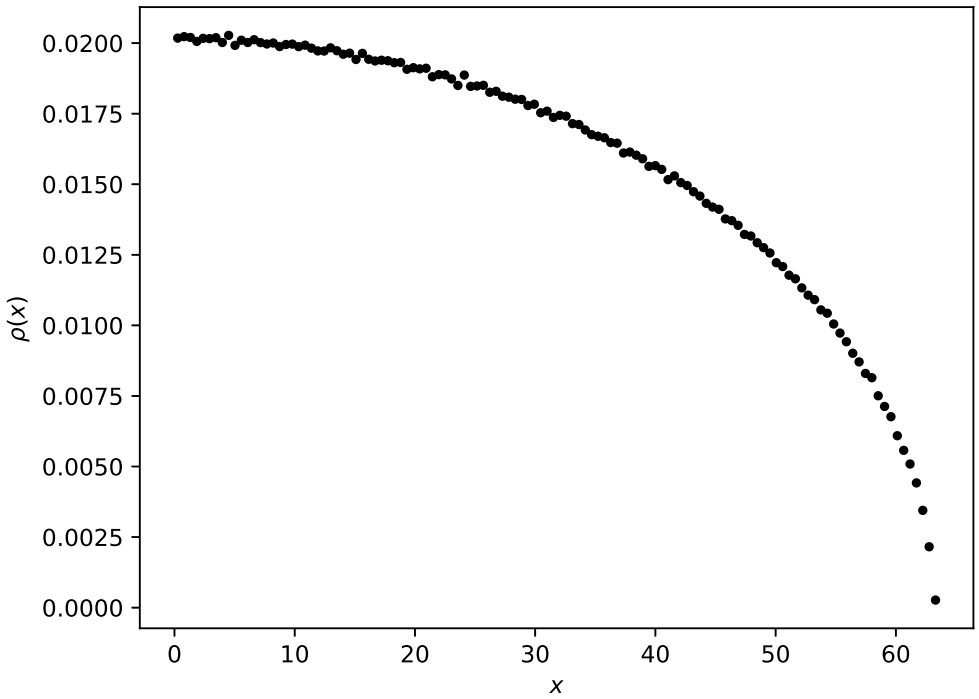

Figure A.7: The envelope of the histogram in Fig. A.6.

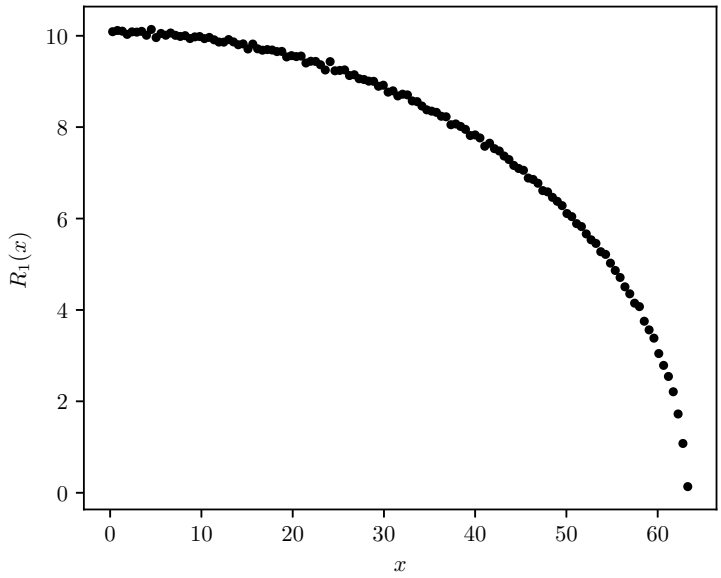

Figure A.8: The envelope of the histogram in Fig. A.6 is multiplied with $N(= 500)$. This is the function $R_1(x)$ which will be used for unfolding.

was farther away from the semi-circular part. Numerically integrating the function $R_1(x)$ we obtain the stair case function $N(x)$ as shown in Fig. (A.10).

$$N(x) = \frac{A}{2} x\sqrt{R^2 - x^2} + \frac{A}{2} R^2 \sin^{-1} \frac{x}{R} \tag{A.38}$$

After unfolding the eigen values of the chGUE ensemble with Eq. (A.38), we obtained the histogram of un folded eigen-values as shwon in Fig. (A.11.2).

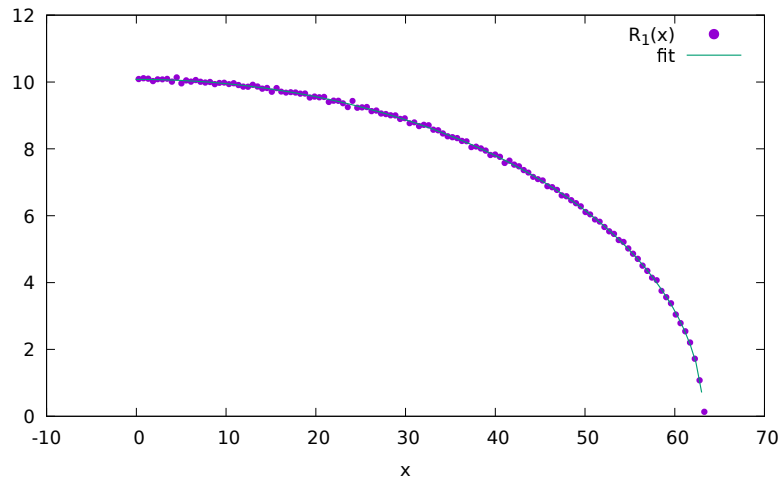

Figure A.9: $R_1(x)$ is fitted with Eq. (A.38)

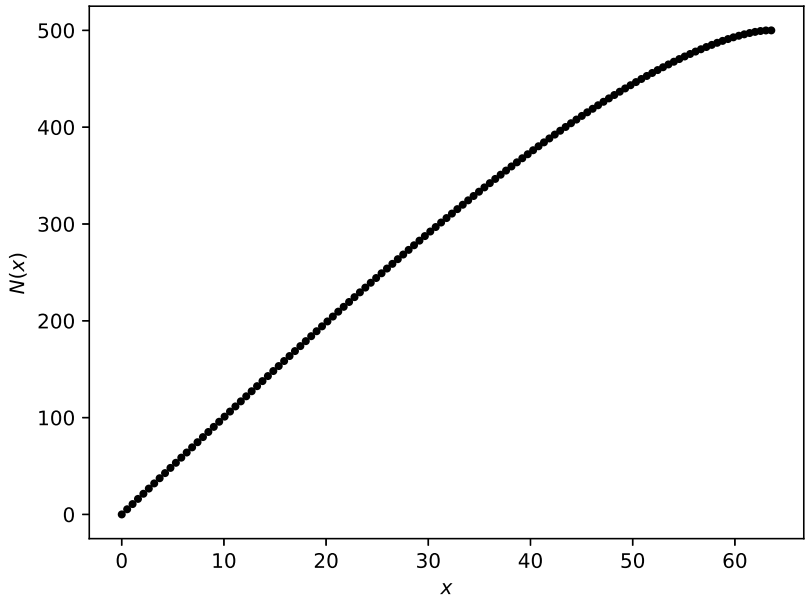

Figure A.10: The staircase function obtained by numerically integrating the function $R_1(x)$.

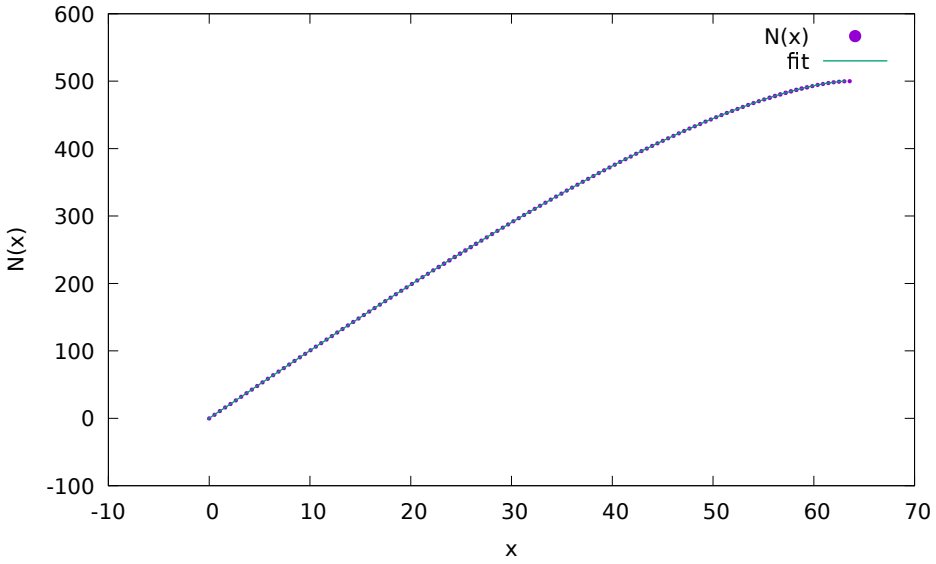

Figure A.11: The staircase function obtained by numerically integrating the function $R_1(x)$ was fitted with Eq. (A.38). This function will be used for unfolding procedure. Note that the range staircase function is same as the dimension of W.

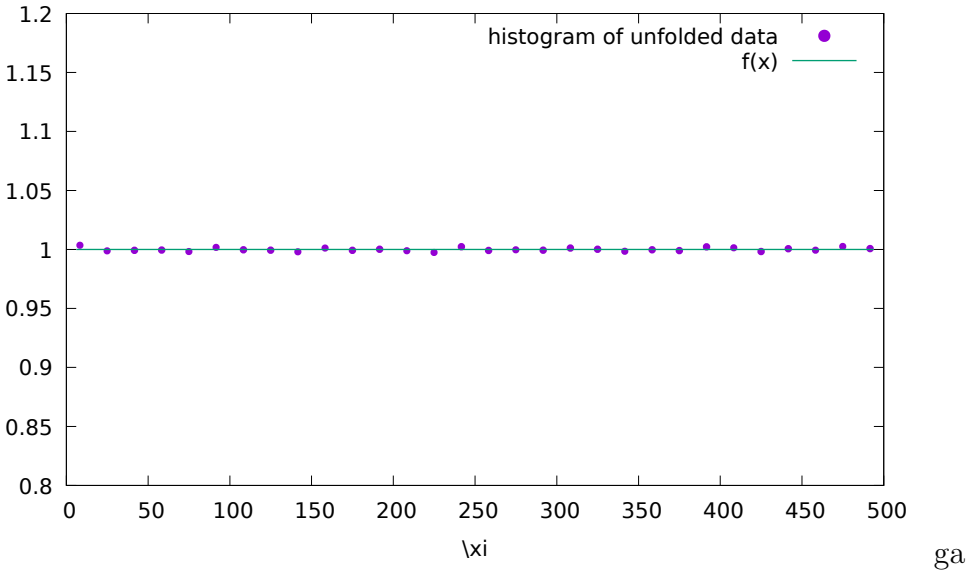

Figure A.12: The histogram of unfolded eigen values of chiral Gaussian Unitary Ensemble.

A.12 Explicit chiral symmetry breaking due to the mass term in QCD lagrangian.

The free QCD lagrangian is

$$L_{QCD}(x) = \bar{\psi}(x)\left(i\gamma^{\mu}D_{\mu} - m\right)\psi(x) \tag{A.39}$$

where the D_μ is the covariant derivative $\partial_\mu - igt^a A^a_\mu$ and $\psi(x)$ is the fermionic field and t_a are the generators of $SU(3)$ group.

The global chiral transformation is

$$\psi(x) \to \exp\left(-i\sum_{b=1}^{8} a_b t_b \gamma^5\right)\psi(x) \tag{A.40}$$

Consider the mass term $m\bar{\psi}\psi = m\psi^\dagger\gamma^0\psi$. Now, under the chiral transformation

$$m\psi^\dagger\gamma^0\psi \to m\psi^\dagger \exp\left(i\sum_{b=1}^{8} a_b t_b \gamma^5\right)\gamma^0 \exp\left(-i\sum_{b=1}^{8} a_b t_b \gamma^5\right)\psi(x)$$

Using the anti-commutation relation $\{\gamma_5, \gamma_\mu\} = 0$, we have

$$\begin{aligned} m\psi^\dagger\gamma^0\psi \to &\quad m\psi^\dagger\gamma^0 \exp\left(-2i\sum_{b=1}^{8} a_b t_b \gamma^5\right)\psi(x) \\ = &\quad m\bar{\psi}\exp\left(-2i\sum_{b=1}^{8} a_b t_b \gamma^5\right)\psi(x) \neq m\bar{\psi}\psi \end{aligned} \tag{A.41}$$